IN VITRO SELECTION OF RNA APTAMERS AGAINST THE DUAL CONFORMATIONS OF A PHOTOCHROMIC COMPOUND, AND CONSTRUCTION OF A LIGHT-SENSITIVE ALLOSTERIC HAMMERHEAD RIBOZYME

by

Hyun-Wu Lee
B.Sc., Simon Fraser University, 2003

THESIS SUBMITTED IN PARTIAL FULFILLMENT OF
THE REQUIREMENTS FOR THE DEGREE OF

MASTER OF SCIENCE

In the Department of
Molecular Biology and Biochemistry

SIMON FRASER UNIVERSITY

Fall 2006

APPROVAL

Name: **Hyun-Wu Lee**

Degree: **Master of Science**

Title of Thesis: ***In vitro* selection of RNA aptamers against the dual conformations of a photochromic compound, and construction of a light-sensitive allosteric hammerhead ribozyme**

Examining Committee:

Chair: **Dr. William Davidson**
Professor of Molecular Biology and Biochemistry, SFU

Dr. Dipankar Sen
Senior Supervisor
Professor of Molecular Biology and Biochemistry, SFU

Dr. Peter Unrau
Committee Member
Assistant Professor of Molecular Biology and Biochemistry, SFU

Dr. Christopher Beh
Committee Member
Assistant Professor of Molecular Biology and Biochemistry, SFU

Dr. Vance Williams
Internal Examiner
Assistant Professor of Chemistry, SFU

Date Defended/Approved: October 26, 2006

ABSTRACT

Using the photochemical properties of the dihydropyrene – cyclophanediene system, *in vitro* selection (SELEX) was carried out to obtain RNA aptamers that bind either closed or open form of a photochromic compound with high affinity and specificity. Among the isolated aptamers, the C8 aptamer, which bound to the closed form of the compound, showed the best affinity and specificity and was able to discriminate the open form of the compound. The C8 aptamer was used successfully to design an allosteric ribozyme by functionally combining the aptamer with a hammerhead ribozyme. This rationally designed allosteric ribozyme demonstrated effective light-dependent switching activity when shown to be catalytically activated by UV light irradiation and inhibited with visible light. In summary, this light-dependent allosteric ribozyme can be potentially used as a photo-regulated molecular switch to create new genetic control systems.

Keywords: Aptamer; In Vitro Selection; Oligonucleotides; RNA; Ribozyme

Subject Terms: Catalytic RNA

DEDICATION

To my family and Angela

for their love, encouragement,

and support through the years

ACKNOWLEDGEMENTS

I would like to express my gratitude and appreciation to Dr. Dipankar Sen for his scientific ideas, support, guidance, inspiration, and encouragement during my graduate career. I thank members of my supervisory committee, Dr. Peter Unrau, and Dr. Christopher Beh for their advice, important suggestions, and time regarding my research project.

I thank Dr. Vance Williams for being the internal examiner of my defense.

I thank Dr. William Davidson for being the chair of my defense.

I like to thank Dr. Reginald Mitchell for allowing me to work on his compound, and Stephen Ribinson for synthesizing the compound for me.

I would also like to thank present members of the Sen lab for their discussions and help during my graduate research: Ed Leung, Gurpreet Sekhon, Yong Liu, Koshiki Sen, Janet Huang, and Nazanin Azrahimi.

Special thanks to Ed Leung and Gurpreet Sekhon for their great friendship and support.

I thank past members of the Sen lab for their guidance and discussions: Dan Chinnapen, Becky Thorne, Carlo Sankar, Yi-Jeng Huang, Kelly Chapple, and Lucien Bergeron.

Special thanks to Dan Chinnapen for his help, guidance, ideas, inspiration, and support. With his guidance on experimental techniques, I was able to establish good laboratory skills and habits.

I thank members of the Unrau lab for their help: Hani Zaher, Sunny Wang, Matthew Lau, and Alex Ebhardt.

I would like to thank friends and staff in the MBB department for their help and support throughout the years.

Special thanks to Hani Zaher and Carrie Simms for their great help, support, and friendship.

I also like to thank the MBB department, the university, NSERC Canada, and CIHR Canada for their financial support throughout the years.

Great thanks to my parents, my brother Joon-Wu, Angela, and Angela's family for their encourgement, support, inspiration, dedication, and love.

TABLE OF CONTENTS

LIST OF FIGURES

LIST OF TABLES

LIST OF ABBREVIATIONS

ATP	Adenosine triphosphate
BCPD	Benzo-cyclophanediene
BCPD-COOH	Carboxylic acid derivative of benzo-cyclophanediene
BCPD-PEG	Polyethylene glycol derivative of benzo-cyclophanediene
BDHP	Benzo-dimethyldihydropyrene
BDHP-COOH	Carboxylic acid derivative of benzo-dimethyldihydropyrene
BDHP-PEG	Polyethylene glycol derivative of benzo-dimethyldihydropyrene
cDNA	Complementary deoxyribonucleic acid
cAMP	Cyclic adenosine monophosphate
cGMP	Cyclic guanosine monophosphate
cNMP	Cyclic nucleotide monophosphate
C. elegans	Caenorhabditis elegans
Co^{2+}	Cobalt
CPD	Cyclophanediene
CTP	Cytidine triphosphate
D. melanogaster	Drosophila melanogaster
DHP	Dimethyldihydropyrene
DMF	Dimethylformamide
DMSO	Dimethyl sulfoxide
DNA	Deoxyribonucleic acid
dNTP	Deoxynucleotide triphosphate
E. Coli	Escherichia Coli
EDTA	Ethylenediaminetetraacetic acid
FMN	Flavin mononucleotide
GlcN6P	Glucosamine-6-phosphate
GTP	Guanosine triphosphate

HDV	Hepatitis delta virus
HIV-RT	Human immunodeficiency virus reverse transcriptase
Mg^{2+}	Magnesium
mRNA	Messenger ribonucleic acid
NMR	Nuclear magnetic resonance
NTP	Nucleotide triphosphate
PAGE	Polyacrylamide gel electrophoresis
PCR	Polymerase chain reaction
RISC	RNA-induced silencing complex
RNA	Ribonucleic acid
RNase	Ribonuclease
RNAi	Ribonucleic acid interference
SELEX	Systematic evolution of ligands by exponential enrichment
siRNA	Small interfering RNA
tRNA	Transfer ribonucleic acid
UTP	Uridine triphosphate
UV	Ultraviolet

CHAPTER 1:
INTRODUCTION TO CATALYTIC RIBOZYMES, *IN VITRO* SELECTION, AND ALLOSTERIC RIBOZYMES

1.1 Introduction

The work described in this thesis covers: 1) *in vitro* selection and characterization of RNA aptamers against the dual transformations of a photochromic compound that reversibly changes its conformation under the specific irradiation wavelength of light between its closed rigid planar form and its open stair shaped form, and, 2) the design and characterization of an allosteric hammerhead ribozyme activated and deactivated by the light-responsive conformational changes of its ligand for its sequence-specific cleavage of RNA phosphodiester bonds.

The introductory chapter will provide readers with sufficient background information to help understand the context of this thesis. The chapter includes introduction to ribozymes and their contribution to the RNA world hypothesis, *in vitro* selection of RNA aptamers, and designing of allosteric ribozymes and their potential use as molecular switches.

1.2 Catalytic Ribozymes

In 1982, Thomas Cech and his co-workers made the first surprising discovery that RNA molecules are capable of catalyzing reactions, even in the absence of any protein component (Kruger *et al.* 1982). These *cis*-splicing group I *Tetrahymena* introns found in the introns of RNA transcripts and removed themselves from the transcripts to catalyze a

transesterification. In other studies, the RNA portion of RNase P was shown to be both necessary and sufficient for the catalysis of the hydrolysis of the phosphodiester bond of its pre-tRNA substrates (Guerrier-Takada *et al.* 1983). These ribonucleic acids with enzyme-like activity were named ribozymes. Since then several classes of ribozymes have been discovered in natural systems, most of which catalyze intramolecular splicing or cleavage reactions. Furthermore, one of the central cellular processes, the peptidyl transfer reaction of newly synthesized proteins, is catalyzed by a ribozyme (Nissen *et al.* 2000), and it was determined that only RNA, but no protein, was located in the vicinity of the catalytic center of the ribosome.

The importance of ribonucleic acids in biochemistry has become more and more evident since the discovery of the ribozymes in 1980s. Over the past decades, RNA has proven itself as a versatile catalyst despite its chemical simplicity. As mentioned previously, RNA catalyzes reactions ranging from phosphodiester cleavage and ligation in small ribozymes to peptide bond formation in the ribosome. However, the ability of RNA to catalyze chemical reactions goes beyond the examples found in nature as demonstrated by *in vitro* selection (SELEX) of novel enzymes that can catalyze a wide variety of chemical reactions. Even though many ribozymes are not as efficient as catalysts as protein enzymes, they achieve the catalysis with a much simpler building blocks and structures. They only use 4 bases instead of 20 amino acids. Despite this apparent simplicity and an increasing amount of structural information about ribozymes, the details of how RNA accomplishes this feat are still the topic of much research and discussion.

1.2.1 Classes of Ribozymes

Catalytic RNAs are broadly grouped into two classes based on their size and reaction mechanisms. Large ribozymes consists of the self-splicing group I and group II introns, the RNA component of RNase P and ribosomes, whereas small ribozymes includes hammerhead, hairpin, hepatitis delta ribozymes, varkud satellite RNAs, and Glucosamine-6-phosphate (GlcN6P) riboswitch ribozymes as well as artificially selected nucleic acids. Large ribozymes consists of several hundreds up to 3000 nucleotides, and they generate reaction products with a 3′-hydroxyl and 5′-phosphate group, a 2′-3′-cyclic phosphate and a 5′-hydroxyl group or a polypeptide chain. Small catalytically active nucleic acids, which range from 30 to 150 nucleotides in length, generate products with a 2′-3′-cyclic phosphate and a 5′-hydroxyl group (Tanner 1999; Doudna and Cech 2000).

1.2.1.1 Group I Introns

Group I intron ribozymes were the first RNA molecules discovered to possess catalytic activity (Kruger *et al.* 1982). Group I introns are found in lower eukaryotes and some bacteria, and perform a splicing reaction by a two-step transesterification mechanism (Figure 1-1a). The reaction is initiated by a nucleophilic attack of the 3′-hydroxyl group of an exogenous guanosine cofactor on the 5′-splice site. Subsequently, the free 3′-hydroxyl of the upstream exon initiates a second nucleophilic attack on the 3′-splice site to ligate both exons and release the intron (Cech 1990). Essential to this catalysis is presence of target binding site or internal guide sequence on the 5′-end of the group I intron for base-pairing with the target RNA. A uridine at position –1 relative to the cleavage site is highly conserved and forms a functionally important G·U wobble base-pair with the internal guide sequence.

The catalytically active site for the transesterification reaction residues in the intron can be engineered to catalyze reactions in *trans* to cleave a separate substrate (Sullenger and Cech 1994). It has been demonstrated that modified group I introns are suitable to fix mutant mRNAs. The genetic basis of sickle cell disease is A to T conversion of in the sixth codon of the β-globin gene (Ingram 1957). People who are homozygous for this mutational conversion make long polymers of sickle hemoglobin in their erthrocytes to cause a tissue damage, and chronic anemia (Ingram 1957). A trans-active group I intron was used to demonstrate the conversion of sickle β-globin transcripts to RNA transcripts encoding γ-globin because γ-globin in fetal hemoglobin has been demonstrated to inhibit polymerization of sickle hemoglobin (Sunshine *et al.* 1978). Therefore, design of group I introns that encode wild-type exon sequences enable gene repair at the mRNA level.

1.2.1.2 Group II Introns

Like group I introns, group II introns are found in bacteria and lower eukaryotic organelles, but they are less widely distributed than group I introns. They catalyze a self-splicing reaction in a similar manner as group I introns, except group II introns do not require a guanosine cofactor. Instead, the 2′-hydroxyl of a specific adenosine at the branch site of the intron initiates the reaction by a nucleophilic attack on the splice site to form a lariat-type structure as shown in Figure 1-1b (Michel and Ferat 1995). In addition, group II introns have ability to insert into double-stranded DNA and to incorporate into genomic DNA upon reverse transcription by an intron-encoded protein (Zimmerly and Lambowitz 2004). The intron-encoded protein is a multifunctional protein with reverse transcriptase, RNA splicing, and endonuclease activities. Upon translation, the intron-

encoded protein facilitates splicing of the group II intron into its catalytically active form and remains associated with it forming a ribonucleoprotein complex (Zimmerly *et al.* 1995). Group II introns use both their RNA and protein subunits for target site recognition (Guo *et al.* 1997). The intron reverse splices into double-stranded DNA and uses a nascent leading or lagging strand at a DNA replication fork as the primer for reverse transcripting the inserted intron RNA (Zhong and Lambowitz 2003). Much less is known about group II introns than about group I introns, and their applications are still very limited. However, the improved group II intron technology can be used to insert new genomic information specifically into target genes for gene repair.

1.2.1.3 RNase P

RNase P is a ribonucleoprotein complex responsible for tRNA processing and cleavage of 5′-end of tRNA precursors to produce mature tRNAs as shown in Figure 1-1c (Frank and Pace 1998). While the prokaryotic RNase P is composed of protein and RNA subunits in a 1:1 ratio, the eukaryotic RNase P is more complex, consisted of an RNA subunit and several protein subunits (Vioque *et al.* 1988; Fang *et al.* 2001). The RNA component of the enzyme alone possesses full catalytic activity *in vitro* providing the first example of a true naturally occurring *trans*-cleaving RNA ribozyme (Guerrier-Takada *et al.* 1983). However, for full enzymatic activity under *in vivo* conditions, the protein component is required. In human cells, RNase P contains multiple protein components and in the absence of protein the RNA moiety is thought to be catalytically inactive.

An interesting feature of RNase P ribozymes is their ability to recognize structures instead of specific sequences as their target substrates such as pre-tRNA

(Kirsebom 2002). This feature is manipulated for therapeutic applications by covalently linking the RNase P ribozyme to an external guide sequence. The external guide sequence base pairs in a complementary manner with the substrate target site while also mimicking the structure of the 5′-terminus of pre-tRNAs that contains the acceptor stem, T-stem, 3′-CCA sequence, and 5′-leader sequence (Forster and Altman 1990). The complex, that consists of the external guide sequence and substrate, is similar in structure to the portion of tRNA that the RNase P ribozymes recognizes, enables sequence-specific recognition and cleavage of the target substrate. Therefore, RNA can be targeted *in vitro* or *in vivo* by a specifically designed external guide sequence for specific cleavage by RNase P.

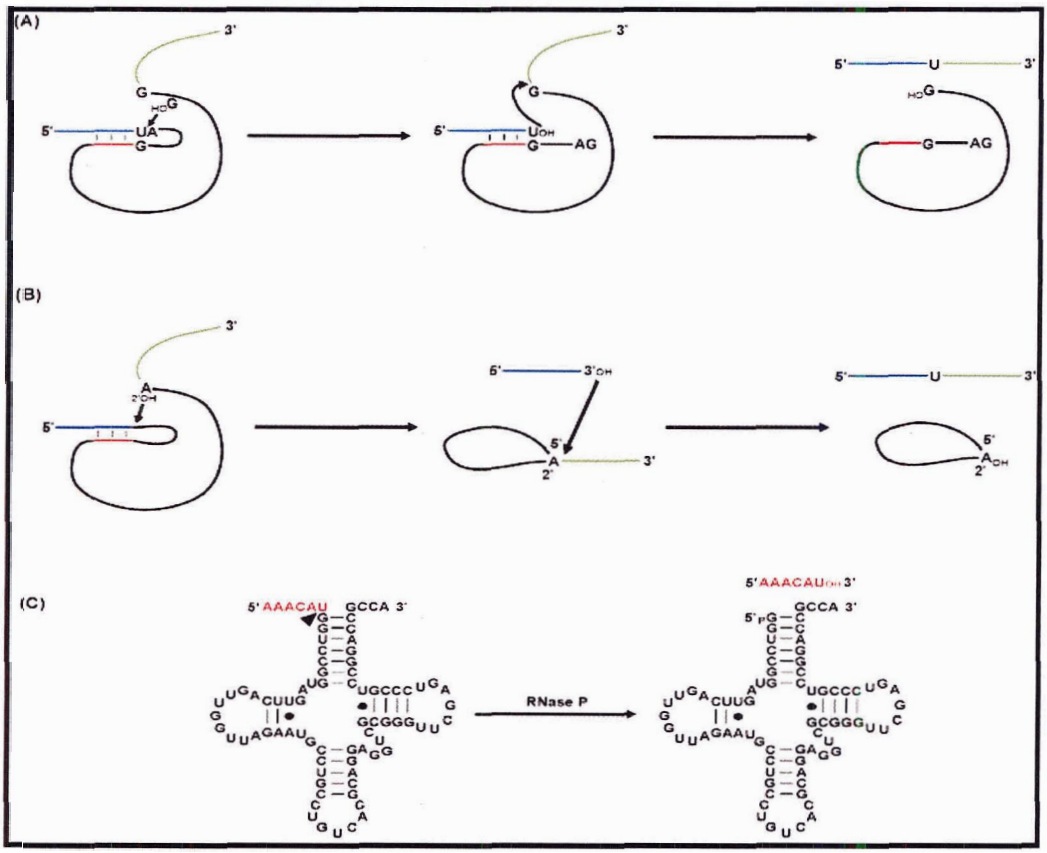

Figure 1-1 **Reaction mechanisms of large ribozymes. (A) Schematic representation of cis-splicing reaction of group I introns. Red: internal guide sequence; Blue: 5'-exon; Green: 3'-exon. (B) Schematic representation of cis-splicing reaction of group II introns. Red: internal guide sequence; Blue: 5'-exon; Green: 3'-exon. (C) Nuclear tRNA hydrolysis catalyzed by RNase P ribozyme. Red: precursor sequence. Arrow indicates the site of hydrolysis.**

1.2.1.4 Hammerhead Ribozyme

The hammerhead ribozyme is the most intensively studied and applied ribozyme to date. It has been found in several plant virus satellite RNAs, viroids, and transcripts of a nuclear satellite DNA (Forster and Symons 1987). In 1992, a naturally occurring *cis*-cleaving hammerhead ribozyme structure was resolved into separate substrate and catalytic moieties, enabling its modification for *trans*-cleaving activity (Haseloff and Gerlach 1992). This discovery and identification of minimal sequences required for

hammerhead *trans*-cleavage (Uhlenbeck 1987) allowed its use in applications to down-regulate the expression of potentially any gene.

As shown in Figure 1-2a, the hammerhead ribozyme is about 30 nucleotides in size and is the smallest known ribozyme. It consists of three stems that intersect at a conserved catalytic core, as it was determined by crystal structure studies (Symons 1992). Stem II contains the conserved catalytic core that is responsible for the cleavage reaction. Stem I and III enable substrate recognition, binding, and sequence-specific cleavage. Stem II is linked to stem III through the catalytic site that cleaves NHH target sequences, where N can be any nucleotide, and H can be A, U, or C (Kore *et al.* 1998). The hammerhead ribozyme promotes the sequence-specific cleavage of RNA phosphodiester bonds with a rate of about 1 min^{-1} at 25°C and neutral pH. This demonstrates a 10^6-fold rate enhancement compared to the non-catalyzed reaction of RNA (Doudna and Cech 2002; Blount and Uhlenbeck 2002). Using Watson-Crick base pairing, the hammerhead ribozyme has been engineered to cleave a variety of different RNA substrates (Breaker 2004), and numerous studies have shown that *trans*-acting ribozymes can be successfully employed inside living cells as functional genomic tools to knock down expression of specific genes. (Akashi *et al.* 2005).

1.2.1.5 Hairpin Ribozyme

Another catalytic RNA found in pathogenic plant virus satellite RNAs is the hairpin ribozyme. The second smallest ribozyme, ranging from 50-70 nucleotides in size, with a secondary structure consisting of two domains, each containing two helical regions separated by an internal loop, connected by a hinge region (Figure 1-2b). The hairpin targets a 14-nucleotide RNA sequence as its substrate, with a BNGUC sequence

requirement, where B can be any nucleotide but adenosine (Lewin and Hauswirth 2001). Like other small ribozymes, hairpin ribozymes cleave a RNA phosphodiester backbone to yield a 5′-hydroxyl and 2′, 3′-cyclic termini. However, unlike most other ribozymes, the hairpin does not require divalent metal cations as a catalytic cofactor or transition state stabilizer (Ferre-D'Amaré and Rupert 2002). Instead, its mechanism of catalysis requires major structural rearrangement of its catalytic core, which is comprised of two irregular double helices, and this rearrangement causes a distortion in the substrate structure and ultimately induces a reactive conformation in the substrate (Ferre-D'Amaré and Rupert 2002). The reaction is thought to be driven by the binding energy of the two helices comprising the catalytic core with stabilization of the transition state through the formation of complex hydrogen bond network (Rupert *et al.* 2002).

1.2.1.6 Hepatitis Delta Virus Ribozyme

The hepatitis delta virus ribozyme was found in a satellite virus of hepatitis B virus, a major human pathogen (Wu *et al.* 1989). Both the genomic and antigenomic strands express *cis*-cleaving ribozymes of about 85 nucleotides that differ in sequence but fold into similar secondary structures. A crystal structure of the ribozyme has been determined (Ferre-D'Amaré *et al.* 1998), in which five helical regions are organized by two pseudoknot structures with a P1 stem comprised of a G·U wobble base pair and six non-specific Watson-Crick base pairs. These base pairs are involved in substrate binding and recognition (Figure 1-2c). Although the nucleotides at positions –1 to –4 from the cleavage site are not directly involved in substrate recognition, they greatly influence the ribozyme catalysis with certain sequences severely reducing its cleavage efficiency (Roy *et al.* 1999; Ananvoranich *et al.* 1999). This characteristic has been successfully applied

to developing specific target sites within the hepatitis B viral genome to develop useful gene-inactivation systems based on the hapatitis delta virus ribozyme (Bergeron and Perreault 2002). Like other small ribozymes, the hepatitis delta virus ribozyme also catalyzes a self-cleavage reaction that generates products with 5′-hydroxyl and 2′, 3′-cyclic termini.

1.2.1.7 Varkud Satellite Ribozyme

The Varkud satellite ribozyme is the largest of the small ribozymes, originally discovered in mitochondria of certain strains of *Neurospora* (Collins and Saville 1990). This ribozyme is capable of both the cleavage and reverse ligation reactions (Saville and Collins 1991; Jones *et al.* 2001), and is a metalloenzyme requiring divalent metal cations for catalysis (Jones *et al.* 2001). Unlike other small ribozymes, the *trans*-cleaving Varkud satellite ribozyme does not use long stretches of complementary base-pairing to interact with its substrate and does not have any sequence requirements upstream of its cleavage site (Collins and Olive 1993; Guo and Collins 1995). The secondary structure of the ribozyme is shown in Figure 1-2d.

1.2.1.8 Glucosamine-6-phosphate riboswitch ribozyme

A riboswitch is a part of mRNA molecule that can directily bind a small target molecule, and this binding of the target molecule affects the gene's expression (Winkler and Breaker 2003a). Riboswitches consists of two parts, which are an aptamer and expression platform. The aptamer directly binds the small molecule, and undergoes structural changes upon binding of the small molecule. These structural changes affect expression platform, and gene expression is subsequently regulated (Mandal and Breaker

2004b). Expression platforms typically turn off gene expression in response to the small molecule by the formation of transcription termination hairpins, sequestering ribosome-binding site to block translation, and self-cleavage (Winkler and Breaker 2003a; Mandal and Breaker 2004b). Glucosamine-6-phosphate (GlcN6P) riboswitch (Figure 1-2e) is the only known natural riboswitch that inhibit gene expression by self-cleavage (Mandal and Breaker 2004b). The *GlmS* gene encodes an enzyme that produces GlcN6P. The GlcN6P riboswitch contains a ribozyme that cleaves the mRNA of *GlmS* gene in Gram-positive bacteria. The ribozyme is activated to repress the *GlmS* gene in response to rising GlcN6P concentrations by catalyzing a self-cleavage reaction that generates products with 5′-hydroxyl and 2′, 3′-cyclic termini (Winkler *et al.* 2004). Therefore, the ribozyme acts as metabolite-sensing genetic switch to downregulate the production of GlcN6P.

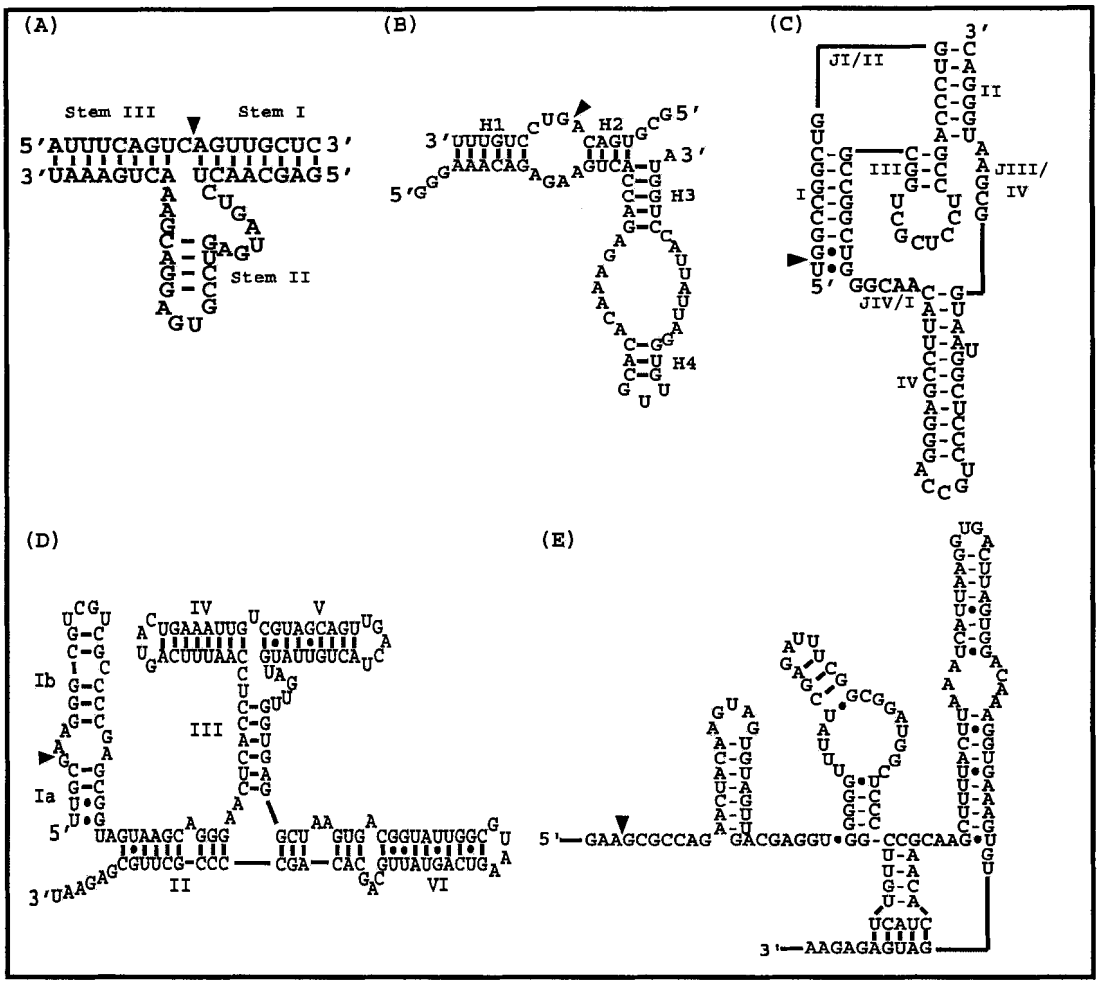

Figure 1-2 **Representation of small self-cleaving ribozymes. Cleavage sites are indicated by solid arrows. (A) Hammerhead ribozyme. (B) Hairpin ribozyme. (C) HDV ribozyme. (D) VS ribozyme (E) GlcN6P riboswitch ribozyme.**

1.3 The RNA World Hypothesis

Prior to the discovery of catalytic RNAs, proteins were considered the only organic molecules in living organisms that could function as catalysts. DNA carries the genetic information required for the synthesis of proteins. The replication and transcription of DNA require a complex set of enzymes and other proteins. How then could the first living cells with DNA-based central dogma have originated by spontaneous chemical processes on the prebiotic earth? Primordial DNA synthesis would have required the presence of specific enzymes, but how could these enzymes be

synthesized without the genetic information in DNA and without RNA for translating that information into the amino acid sequence of the protein enzymes? In other words, proteins are required for DNA synthesis, and DNA is required for protein synthesis.

This classic "chicken-and-egg" problem made it immensely difficult to think of any realistic pre-biotic pathway to the molecular biological system. Certainly, no such pathway had been demonstrated experimentally by the late 1970s. Therefore, the suggestion that RNA molecules might have formed the first self-replicating chemical systems on the primitive earth seemed a natural one, given the unique properties of these substances (Gilbert 1986). RNA carries genetic information and occurs primarily as single-stranded molecules that can assume a great variety of tertiary structures, and might therefore be capable of catalysis, in a manner similar to that of proteins. Self-replicating RNA-based systems would have arisen first, and DNA and proteins would have been added later. However, in the absence of any direct demonstration of RNA catalysis, this suggestion remained only an interesting possibility.

In the early 1980s, the discovery of self-splicing catalytic RNA molecules in the ciliated protozoan *Tetrahymena thermophila* (Kruger *et al.* 1982) was consistant with the RNA initiated molecular biological system. These catalytic RNA molecules have subsequently been named ribozymes. Then, the phrase "The RNA World" was first introduced by Walter Gilbert in 1986 in a commentary on the observations of the catalytic properties of various RNAs (Gilbert 1986). The RNA World referred to an hypothetical stage in the origin of life on Earth. During this stage, proteins were not yet participated in biochemical reactions, and RNA carried out both the information storage task of genetic information and the full range of catalytic roles necessary in a very

primitive self-replicating system. Gilbert pointed out that neither DNA nor protein were required in such a primitive system, if RNA could perform as a catalyst.

Further evidence to the RNA world hypothesis came from the series of technical innovations now known generally as ribozyme engineering. Naturally occuring RNA catalytic activities are actually restricted to a small set of highly specialized reactions such as the processing of RNA transcripts primarily in eukaryotic cells. However, ribozyme engineering, made possible by techniques such as DNA sequencing, *in vitro* transcription, and polymerase chain reaction, allowed molecular biologists to manipulate RNA to whatever extent the molecule will permit.

The catalytic repertoire of RNA can be expanded beyond the naturally occurring activities by two major strategies of ribozyme engineering. One strategy involves the direct modification of existing species of ribozymes to produce better or even novel catalysts. This has been called the rational design approach (Tang and Breaker 1997a). The other strategy employs pools of short randomized RNA molecules, which are subjected repeatedly to a selection process designed to enhance the concentration of RNA molecules with the desired functional activity (Soukup *et al.* 2000).

The RNA world hypothesis has been widely accepted, since many examples of ribozymes have been found in nature, and they have been effectively demonstrated to catalyze phosphodiester bond cleavage and RNA splicing reactions. However, it remains to discover a ribozyme with self-replicating activity to demonstrate how RNA survived a harsh environment of the primitive earth (Joyce 1996).

1.4 *In Vitro* Selection

As shown in Figure 1-3a, *in vitro* selection or SELEX (**S**ystematic **E**volution of **L**igands by **Ex**ponential enrichment) is an approach to isolate a molecule with a specific property and has been used to engineer RNA molecules with various functions (Ellignton and Szostak 1990; Tuerk and Gold 1990). In *in vitro* selection, three important processes must be carried out. First, it requires introduction of a large pool of mutated or random nucleotide sequences. Second, it requires selection of functional sequences best suited for a particular process and lastly, the selected sequences must be amplified.

The general procedure for *in vitro* selection of RNA is shown in Figure 1-3b. The process starts with a population of DNA templates. The starting DNA templates are chemically synthesized with a region of random sequence flanked on each end by constant sequence. For primer binding and PCR amplication, the template contains a T7 RNA polymerase promoter at the 5′ end. The DNA templates are transcribed into RNAs by T7 RNA polymerase. From a pool of RNA molecules, a fraction of RNA molecules are selected based on their ability to carry out specific function. The selected RNA molecules are copied into cDNAs by reverse transcriptase. PCR is used to amplify the cDNAs, and then the entire cycle is repeated. After successful rounds of selection, the resulting population of RNAs must be able to carry out a specific function more efficiently than the starting pool of RNAs. This resulting population of selected RNAs are cloned and sequenced. In the end, a representative number of sequences is tested for the desired function.

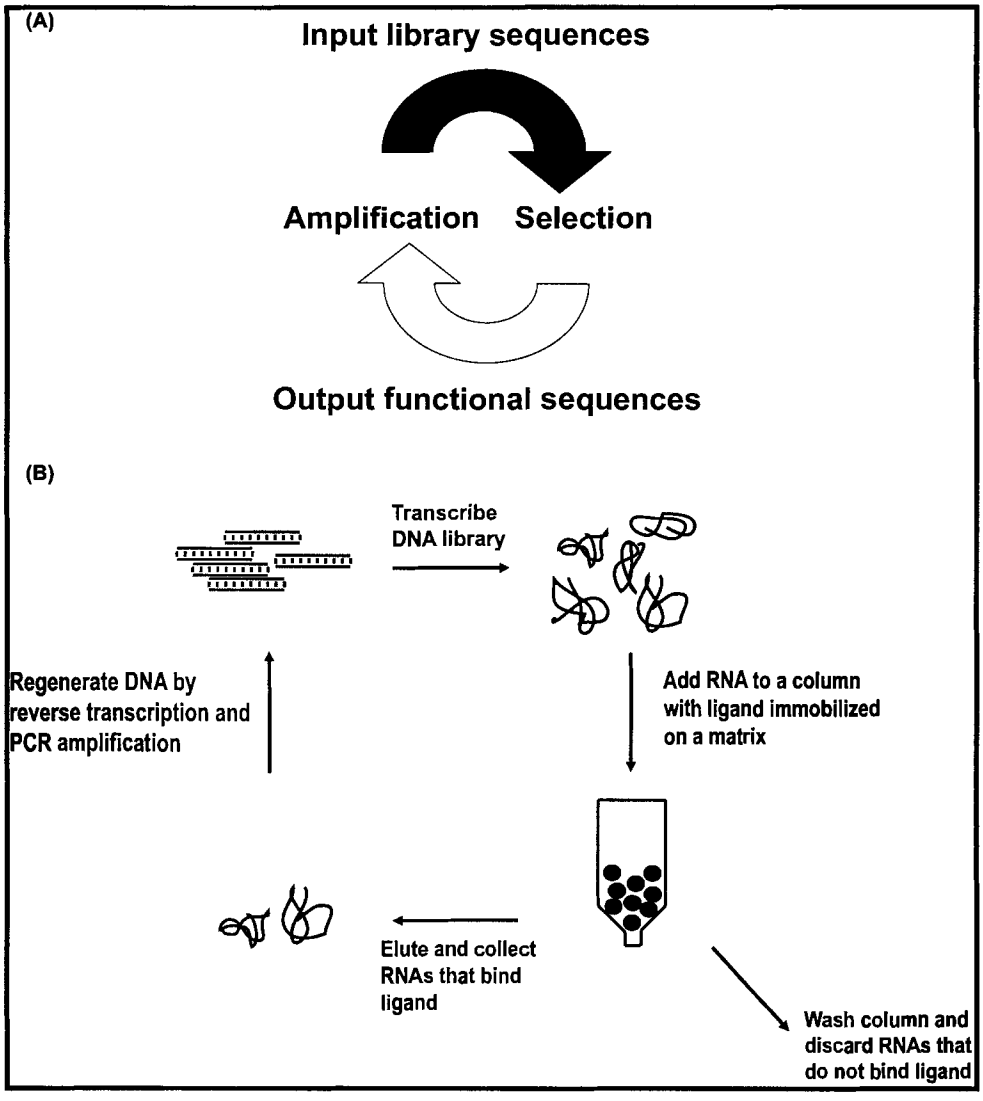

Figure 1-3 **(A) General scheme for in vitro selection. (B) General scheme for RNA aptamer selection.**

The important factor for successful *in vitro* selection is the degree of diversity in the initial random library (Osborne and Ellington 1997). The total possible number of unique sequences that can be generated from the random library depends on the number of nucleotides (n) in a random sequence region and it is given by 4^n. Depending on desired functional diversity, the size of a random sequence region should be decided for a given selection. If a large random sequence region (e.g. 4^{80}) is used, only a very small fraction of the total possible sequences can be generated. Also, it is not practical to

synthesize oligonucleotides beyond 150 nucleotides in length by using an automated DNA synthesizer. On the other hand, if a small random sequence region is used (e.g. 4^{20}), it will limit the complexity of each sequence. Therefore, a 40-nucleotide random sequence region, which has about 10^{24} total possible sequences, is typically used, and 10^{14}~10^{15} unique sequences are typically generated to start a given selection (Osborne and Ellington 1997).

Another key feature of all *in vitro* selection procedures is the selective replication of active molecules. This is accomplished in either of two ways. Active molecules are physically separated from inactive molecules before replication. Self-cleaving catalytic RNA molecules become smaller and are readily separated from larger inactive molecules by gel electrophoresis. In other case, the reaction catalyzed by the active molecules can result in the covalent addition of a sequence required for replication, typically a primer-binding site, and therefore, enable the replication of active molecules without requiring physical separation from inactive sequences. RNA molecules with binding activities are separated from those that do not bind by using immobilized ligands in a procedure analogous to affinity chromatography. RNA molecules with binding activity are eluted and then replicated.

There are several applications for *in vitro* selection including engineering an enzyme with a novel function, investigating the RNA hypotheses, and designing molecules for clinical applications. RNA molecules that bind specific ligands, known as aptamers can be designed and manipulated for clinical or diagnostic purposes (Breaker 2004). Ribozymes can be modified to cleave infectious viral or bacterial components. According to the RNA world hypothesis as described previously, the primitive self-

replicating system was composed of ribonucleic acids, and processes that are carried out by protein enzymes today must have been carried out by RNAs. *In vitro* selection has been used investigate the theory, and its ultimate goal is to create a RNA replicase that is composed entirely of RNA.

1.4.1 Nucleic Acid Aptamers

In vitro selection procedures can isolate nucleic acid molecules, known as aptamers, which bind ligands with a high affinity and selectivity comparable to highly evolved protein molecules (Ellingtion and Szostak 1990). *In vitro* selection has been used to discover aptamers to target a wide variety of ligands with a wide range of size including small ion (Ciesiolka and Yarus 1996), small molecules (Ellington and Szostak 1990), peptides (Nieuwlandt *et al.* 1995), single proteins (Tuerk and Gold 1990), organelles (Ringquist *et al.* 1995), viruses (Pan *et al.* 1995), and even entire cells (Morris *et al.* 1998). Proteins possess extensive surfaces with grooves, ridges, projections, and depressions with numerous hydrogen bond acceptors and donors that can be bound by nucleic acids. Therefore, it suggests that proteins are excellent targets for aptamer selection. Bock and co-workers made the first discovery of an aptamer to a protein that does not normally interact with RNA or DNA (Bock *et al.* 1992). They isolated single-stranded DNA aptamers that bind and and inhibit thrombin, a protease essential for blood clotting. Starting from a pool of 60-nucleotide random sequences flanked by primer-binding sites, sequences were amplified by PCR. One PCR primer was biotinylated, and single stranded sequences from the unmodified strand were isolated by alkaline denaturation of PCR products bound to avidin-agarose. Active and inactive DNA molecules were separated by binding to human thrombin immobilized on concanavalin

A. After five rounds of selection, individual sequences were cloned for sequencing and assays to measure thrombin binding and inhibition of clotting activity. 28 clones that were sequenced had a consensus sequence of GGNTGGN_{2-5} GGNTGG. Inhibition of thrombin activity was determined by a standard clotting time assay. A specific 96 nucleotide aptamer derived by selection resulted in a three-fold increase in clotting time, whereas the 15 nucleotide aptamer representing just the consensus sequence, GGTTGGTGTGGTTGG, increased the clotting time about a seven-fold. The three-dimensional structure of the aptamer in solution was determined by NMR (Macaya *et al.* 1993; Wang *et al.* 1993), and the aptamer-thrombin complex was determined by X-ray crystallography (Padmanabhan *et al.* 1993). These data illustrated that the aptamer forms a G-quartet structure, but details of how the aptamer interacts with thrombin are still not determined.

Gold and co-workers (Tuerk *et al.* 1992) used selection methods to isolate RNA aptamers that bind to HIV reverse transcriptase (HIV-RT). HIV-RT participates in two known interactions with RNA. It binds a $tRNA^{Lys}$ primer and a RNA template for initiation of cDNA synthesis. Selection was begun with a pool of 32-nucleotide random sequences flanked by primer-binding sites. Two populations were used with one containing $tRNA^{Lys}$ sequences in the fixed sequence region, and another containing sequences unrelated to sequences normally recognized by HIV-RT. Nine rounds of selection were performed, and 153 clones were isolated and sequenced. A majority of these clones showed structural similarities and folded into RNA pseudoknot containing one stem of three to five bases, where the sequence as well as secondary structure was conserved, and a second stem conserved in structure but not in sequence. Some sequence

similarity was also observed in the single-stranded regions that span the helices. Binding studies with purified HIV-RT showed that RNA molecules containing the pseudoknot motif specifically bound to the protein, some with dissociation constants at about 50 nM. The dissocation constant is an equilibrium constant that measures the propensity of a receptor-ligand complex to dissociate reversibly into a receptor and a ligand (Mathews *et al.* 2000). In other words, the dissociation constant indicates the strength of the binding between receptors and their ligands in terms of how easy it is to separate the receptor-ligand complexes. The dissociation constant, K_d, is expressed as [receptor][ligand] / [receptor ·ligand] (Mathews *et al.* 2000). Therefore, if the K_d is high, it indicates that the strength of binding is weak. If the K_d is low, it indicates that the strength of binding is strong. The consensus pseudoknot structure was used to design a subsequent selection experiment to find sequence preferences in the more highly variable regions of the pseudoknot consensus structure. After eight rounds of selection, selected sequences were cloned and sequenced. There were no obvious preferred sequences in the region, but one aptamer was identified that inhibited reverse transcriptase activity with an inhibitory constant approximately equal to its dissociation constant. Therefore, the inhibition of HIV reverse transcriptase activity by this aptamer was achieved without losing its binding affinity. In addition, the inhibition was demonstrated to be selective, because reverse transcriptase from avian myeloblastosis virus and Moloney murine leukemia virus were not inhibited. These results are significant because they demonstrate that single-stranded DNA as well as RNA can form structures capable of specific protein recognition and that proteins do not bind nucleic acids in nature are suitable targets for selection of aptamers.

Some naturally occurring RNA molecules have well-characterized abilities to specifically bind small organic molecules. For example, group I introns bind guanosine (Bass and Cech 1984), and L-arginine (Hicke *et al.* 1989), and the TAR RNA element of HIV forms a specific complex with L-arginine (Puglisi *et al.* 1992). Therefore, it was predicted that RNA aptamers should be capable of specifically recognizing and binding small molecules. Ellingtion and Szostak (Ellington and Szostak 1990) selected RNA aptamers by binding to a variety of organic dye molecules covalently coupled to agarose. Five rounds of separate selection experiments were carried out on each of seven different dye-agarose columns with an initial pool of 100-nucleotide random sequences for each selection. These dyes such as Cibacron Blue 3G-A and Reactive Blue 4 contained planar aromatic molecules, various hydrogen bond acceptors and donors, and an overall negative charge. The dye binding activity for pools of selected sequences showed a significant increase in binding activity as rounds of selection progressed, and analysis of cross-binding ability of selected pools of aptamers demonstrated selective binding, even though binding of more than one dye was observed in some cases. Consensus sequences were obtained from sequencing data and specific structural folding was thought to be responsible for selective dye-binding activity. Ellington and Szostak (Ellington and Szostak 1992) also showed DNA aptamers against similar immobilized dyes could be selected. Also, Szostak group (Famulok and Szostak 1992) showed stereo-specific aptamer binding of D-tryptophan by using the same procedure. The dissociation constant of the aptamer to D-tryptophan was about 18 μM, whereas the dissociation constant of the aptamer to L-tryptophan was about 12 mM, which demonstrated much less tight binding.

The first RNA aptamer against a small biomolecule was an ATP aptamer (Sassanfar and Szostak 1993). This aptamer was selected by passing a large random RNA pool through an ATP immobilized column, washing away unbound RNAs and eluting bound RNAs with free ATP. Six rounds of selection were performed, and selected sequences were cloned and sequenced. 11-nucleotide consensus sequence was found with a secondary structure containing a hairpin loop with an internal, asymmetric purine-rich bulge. The dissociation constant of the aptamer to ATP was about 1 μM. Szostak and co-workers (Huizenga and Szostak 1995) also selected DNA aptamers against ATP, and the dissociation constant was about 6 μM.

Jenison and co-workers (Jenison *et al.* 1994) isolated RNA molecules that can bind to immobilized theophylline, which is a therapeutic alkaloid, from a pool of 40-nucleotide random sequences. After eight rounds of selection, a majority of RNA population was specifically eluted from the column by free theophylline. Three more rounds of selection were performed known as counter-SELEX to isolate RNA molecules that were capable of discriminating against caffeine, which is different from theophylline by having one additional methyl group. The counter-SELEX was performed by first eluting the theophylline column with caffeine. The selected aptamers were cloned and sequenced, and a hairpin with two small conserved internal loops, one symmetric and one asymmetric was determined. Impressively, the theophylline aptamer had a dissociation constant of 0.1 μM, and was able to discriminate against caffeine by over 10000-fold.

According to examples described above, general features that make ligands most optimal for aptamers to recognize and bind to their ligands are planarity, presence of hydrogen bond acceptors and donors, and positively charged groups (Wilson and Szostak

1999). On the other hand, it is difficult for aptamers to recognize ligands that are non-planar with a neutral to negative overall charge. Also, simple aptamer structures tend to, but not always, have purine-rich loops to recognize ligands, because these bases participate in noncanonical base-pairing interactions to form a properly folded structure for ligand interaction (Wilson and Szostak 1999). Lastly, most DNA aptamers do not bind to their ligands, if they are converted into RNA and vise versa. This is most likely due to the presence of the 2′-hydroxyl group in determining helix stability and overall tertiary structure stability of aptamers (Wilson and Szostak 1999).

Many aptamers have functional characteristics that are similar to antibodies (Jayasena 1999), because aptamers can specifically recognize and bind to proteins and small molecules at target concentrations of micromolar, nanomolar, or even picomolar range. Also, aptamers can be delivered into organisms or expressed in cells, and are immobilized on solid matrix for *in vitro* use. Therefore, just like antibodies, the potential application of aptamers is enormously wide and significant (Figure 1-4). Aptamers can be immobilized on solid matrix to be used as chromatographic agents (Romig *et al.* 1999). After the integration of fluorescence tags with aptamers immobilized on surfaces, they can be used as biosensor elements to detect specific proteins (Hamaguchi *et al.* 2001) or small molecules (Jhaveri *et al.* 2000) by detecting the change in fluorescence that occurs upon ligand binding, since aptamers undergo a structural change upon ligand binding. Aptamers can also be used as therapeutic agents by blocking protein synthesis (gene switches) (Suess *et al.* 2003), and turning allosteric ribozymes on and off (Mandal and Breaker 2004).

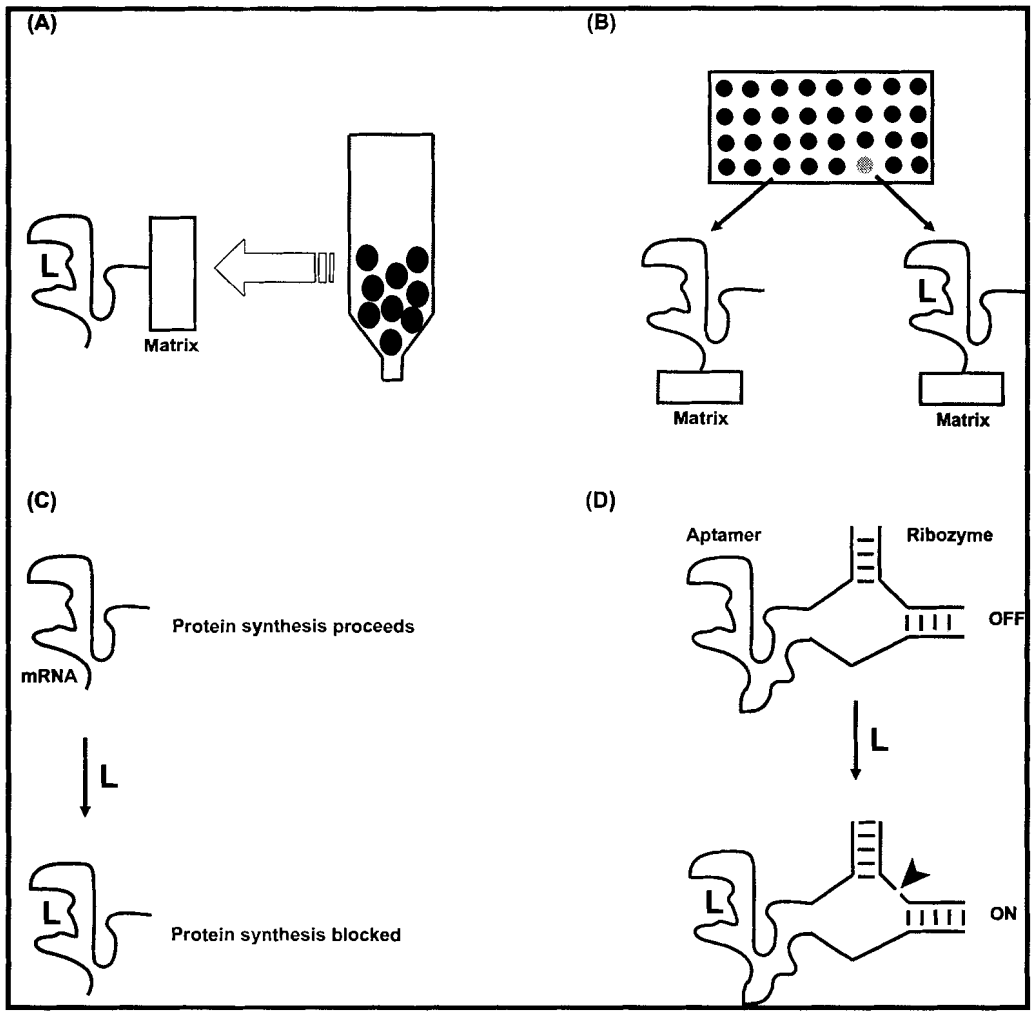

Figure 1-4 **Potential applications of aptamers. (A) Affinity chromatography. (B) Molecular biosensor. (C) Genetic switches. (D) Allosteric ribozymes.**

1.5 Natural Allosteric Riboswitches

Expression of many genes in a cell is maintained in appropriate levels at all times by upregulating or downregulating the production of RNAs and proteins according to their needs and environmental changes (Mandal and Breaker 2004b). This genetic control mechanism must be maintained in a temporal and spatial control and should be able to respond rapidly and selectively to dynamic changes in a cell. In recent studies, it has been demonstrated that mRNAs are capable of controlling gene expression according to chemical and physical condition changes in a cell (Winkler *et al.* 2002a; Winkler *et al.*

2002b; Winkler *et al.* 2003b; Winkler *et al.* 2004). A riboswitch is a part of mRNA molecule that can sense the concentrations of a specific target molecule by directly binding the target molecule, and this binding of the target molecule affects the gene's expression (Winkler and Breaker 2003a). Riboswitches consists of two parts, which are an aptamer and expression platform. The aptamer directly binds the small molecule, and undergoes structural changes upon binding of the small molecule. These structural changes affect expression platform, and gene expression is subsequently regulated (Mandal and Breaker 2004b). Expression platforms typically turn off gene expression in response to the small molecule by the formation of transcription termination hairpins, sequestering ribosome-binding site to block translation, and self-cleavage (Winkler and Breaker 2003a; Mandal and Breaker 2004b). There are several natural riboswitches that have been discovered including thiamine pyrophosphate (TPP) (Winkler *et al.* 2002a), coenzyme B_{12} (Nahvi *et al.* 2002), S-adenosylmethionine (SAM) (Winkler *et al.* 2003b), flavin mononucleotide (FMN) (Winkler *et al.* 2002b), Glucoseamine-6-phosphate (GlcN6P) (Winkler *et al.* 2004), adenine (Mandal and Breaker 2004a), guanine (Mandal *et al.* 2004c), and lysine (Sudarsan *et al.* 2003). Understanding of the riboswitch mechanisms has guided to the development of engineered riboswitches that can be used as therapeutic agents, since numerous artificial RNA aptamer sequences against a wide variety of small organic molecules have been identified (Famulok 1999). In a recent study, conditional gene expression by controlling translation with tetracycline-binding aptamers has been demonstrated (Suess *et al.* 2003). Therefore, engineered riboswitches can be developed further to be used as novel therapeutic genetic control systems.

1.6 Allosteric Ribozymes

The potential of RNA to form specific structures has been utilized in ribozyme engineering to develop allosteric ribozymes or molecular switches. Unlike other enzyme activation or inactivation mechanisms, an allosteric ribozyme possesses an effector-binding site that is separate and distinct from the active site of the catalytic allosteric ribozyme. Ligand binding to this effector-binding site induces conformational changes in its structure, and subsequently, the conformational changes activate or inhibit catalytic function of the allosteric ribozyme. Therefore, the specificity of the effector-binding site is crucial for ligand-mediated folding of an allosteric ribozyme into an active or inactive conformation. To carry out this mechanism, RNA needs to have two important properties. First, RNA needs to carry out precise molecular recognition, and RNA aptamers are very efficient at forming binding sites with high affinity for specific ligands such as small organic molecules (Famulok 1999). Second, RNA should be able to form dynamic structures upon ligand binding, and RNA aptamers are usually able to undergo adaptive binding, which a conformational change in the aptamer allows ligand interaction (Patel *et al.* 1997). The ligand-binding aptamers, therefore, can be used to allosterically regulate the catalytic activity of artificial ribozymes (Breaker 1997). These engineered allosteric ribozymes can be used as therapeutic agents or biosensors for a variety of target compounds, or as artificial molecular switches to control RNA function in biological mixtures.

1.6.1 Engineering Allosteric Ribozymes

Initial attempts to engineer ribozymes were done by using modular rational design approaches. By combining the structural and catalytic components to build allosteric

ribozymes, the allosteric ribozymes were constructed accordingly by combining pre-determined ligand binding aptamers and catalytic ribozymes. For example, the hammerhead ribozyme, the most widely used small catalytic motif for the generation of allosteric ribozymes, cleaves RNA by a transesterification reaction, as it was discussed before (Forster and Symons 1987; Haseloff and Gerlach 1988), and has been engineered into an allosteric ribozyme by appending an aptamer domain that specifically binds ATP (Sassanfar and Szostak 1997; Tang and Breaker 1997a; Tang and Breaker 1997b). This allosteric ribozyme inhibits its catalytic cleavage in response to ATP binding. For this ATP-dependent inhibition of the ribozyme, proper folding of both the aptamer and the ribozyme domains is independent, and a steric clash between folded aptamer and ribozyme domains was responsible for the inhibition of the ribozyme according to the proposed model (Tang and Breaker 1998).

In other cases, modular rational design has been used to construct allosteric hammerhead ribozymes that are activated by ligand binding (Tang and Breaker 1997a; Araki *et al.* 1998; Soukup and Breaker 1999a). In these cases, proper folding of the aptamer and ribozyme domains is interdependent. A communication module, a stem informing the ligand binding of an appended aptamer domain to the adjacent ribozyme domain, contains GC and G·U base pairs, and these base pairs are required for optimal cleavage activity. Ligand binding to the ATP-binding aptamer stabilizes the communication module and initiates the catalytic cleavage activity of the ribozyme. In other words, by appending aptamer and ribozyme domains through communication modules, the proper folding of both domains can be achieved upon ligand binding. Therefore, allosteric hammerhead ribozymes that are activated by ATP (Figure 1-5a)

(Tang and Breaker 1997a), FMN (Figure 1-5b) (Araki *et al.* 1998; Soukup and Breaker 1999a; Fan *et al.* 1996), or theophylline (Figure 1-5c) (Soukup and Breaker 1999a; Jenison *et al.* 1994; Zimmermann *et al.* 1997) have been generated by using modular rational design approaches.

The folding and function of catalytic allosteric ribozymes can also be affected by antisense interactions with complementary oligonucleotide sequences. An allosteric ribozyme has been constructed that is activated by an oligonucleotide effector that binds and occupies an oligonucleotide-binding domain of the hammerhead RNA (Porta and Lizardi 1995). Without the presence of the oligonucleotide effector, the oligonucleotide-binding domain causes disruption and misfolding of the catalytic core. Another example (Figure 1-5d) of an oligonucleotide-dependent hammerhead ribozyme has a ribozyme domain composed of two RNAs binds to the mRNA sequence of a BCR-ABL gene fusion (Kuwabara *et al.* 1998). In this case, the mRNA serves as both allosteric effector and substrate for the allosteric ribozyme. Also, in a recent study, an oligonucleotide-dependent allosteric ligase ribozyme was selected from an *in vitro* selection experiment (Robertson and Ellington 1999). In the absence of DNA oligonucleotides, the ribozyme is proposed to adopt an inactive conformation with the oligonucleotide-binding domain disrupting the function of the ligase ribozyme, whereas, in the presence of the complementary oligonucleotide, this ribozyme ligates between the substrate and ribozyme (Figure 1-5e). Furthermore, this RNA ligase has been engineered to respond to both an oligonucleotide and ATP as effector molecules (Figure 1-5f) (Robertson and Ellington 1999).

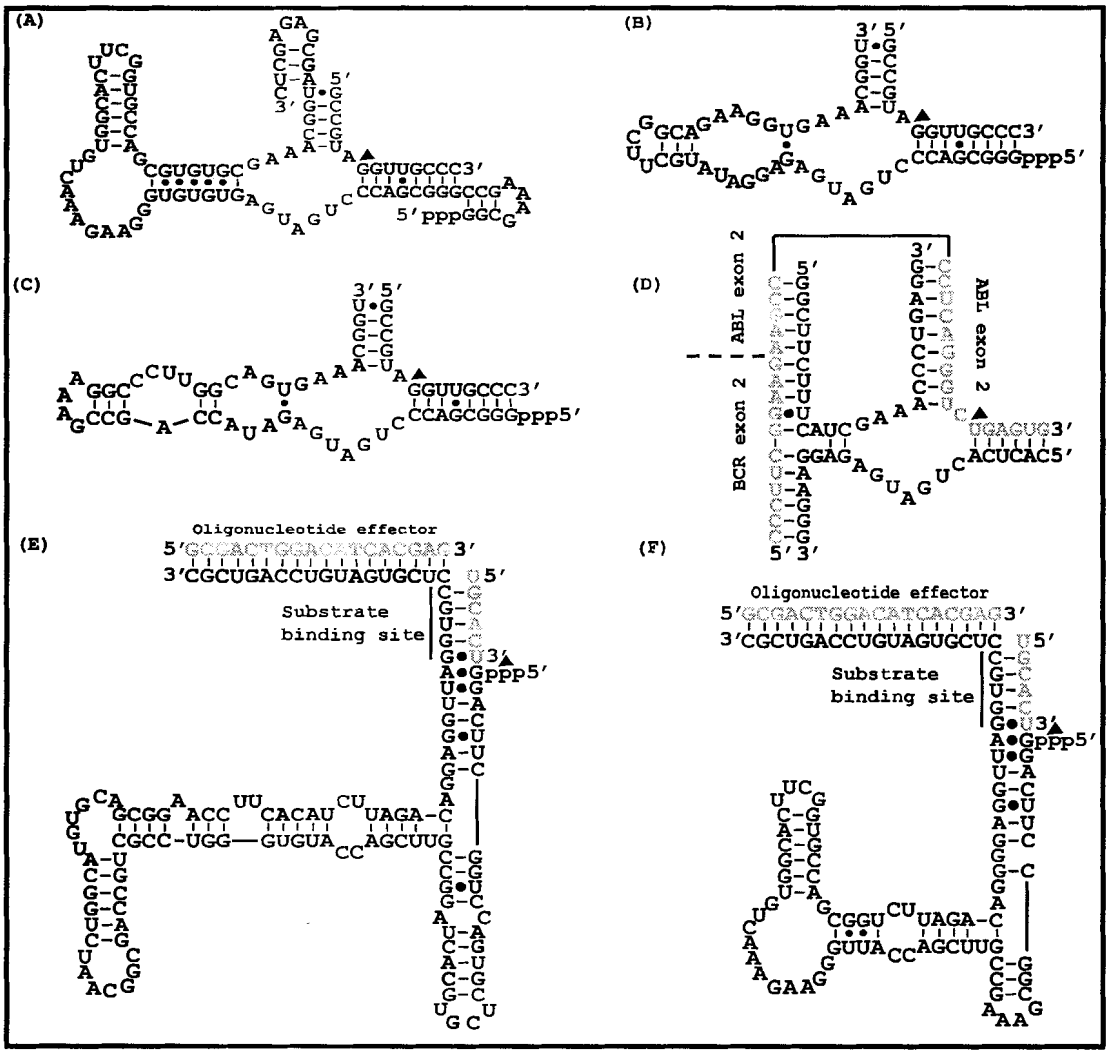

Figure 1-5 **Modular rational design of allosteric ribozymes. (A) ATP-activated allosteric hammerhead ribozyme. (B) FMN-activated allosteric hammerhead ribozyme. (C) Theophylline-activated allosteric hammerhead ribozyme. (D) An oligonucleotide-dependent hammerhead ribozyme. (E) Allosteric ligase ribozyme – L1 ligase. (F) allosteric ligase ribozyme – L1.dB2-ATPm1. Cleavage or ligation sites are indicated by solid arrows.**

Although modular rational design strategies are important approaches for engineering new allosteric ribozymes, it is impossible to test an infinite number of structural and functional motifs by constructing new allosteric ribozymes one at a time (Breaker and Joyce 1994). For this reason, combinatorial strategies are the most productive strategies for allosteric ribozyme engineering, and they are the combined use of modular rational design and *in vitro* selection. For example, if the appropriate aptamer

and ribozyme domains are available, the two domains can be joined via a communication module. *In vitro* selection can then be used to isolate allosteric ribozymes from the enormous number of possible communication module sequences (Williams and Bartel 1996; Osborne Ellington 1997). By using pre-determined domains, the difficulty of creating allosteric ribozymes becomes considerably simplified. As shown in Figure 1-6a, this combinatorial strategy has been used to select allosteric hammerhead ribozymes that are either activated or inhibited by binding of flavin mononucleotide (FMN) (Soukup and Breaker 1999b). The communication modules of the allosteric hammerhead ribozymes are proposed to function by a slip-strucuture mechanism of allosteric regulation. Ligand-binding affects localized base-pairing changes that are responsible for modulating ribozyme activity. Furthermore, certain slip-structure communication module can be versatile, because they retain their allosteric function after attachment to aptamer domains for other ligands. For example, one such communication module was demonstrated to activate an allosteric hammerhead ribozyme with a theophylline (Figure 1-6b), or ATP (Figure 1-6c) aptamer domain appended (Soukup and Breaker 1999b). Therefore, the ligand specificity of an allosteric ribozyme can be changed by merely replacing one aptamer domain for another.

A more challenging usage of the combinatorial strategy is to isolate allosteric ribozymes that are modulated by effectors that have no pre-determined aptamers. For example, allosteric hammerhead ribozymes contain novel effector-binding sites for three different cyclic nucleotide monophosphate compounds (cNMPs) have been identified (Koizumi *et al.* 1999), and each cNMP-dependent allosteric ribozyme is able to

distinguish its cognate ligands (Figure 1-6d, e, f). Therefore, novel effector-dependent allosteric ribozymes can be identified by using the combinatorial strategies.

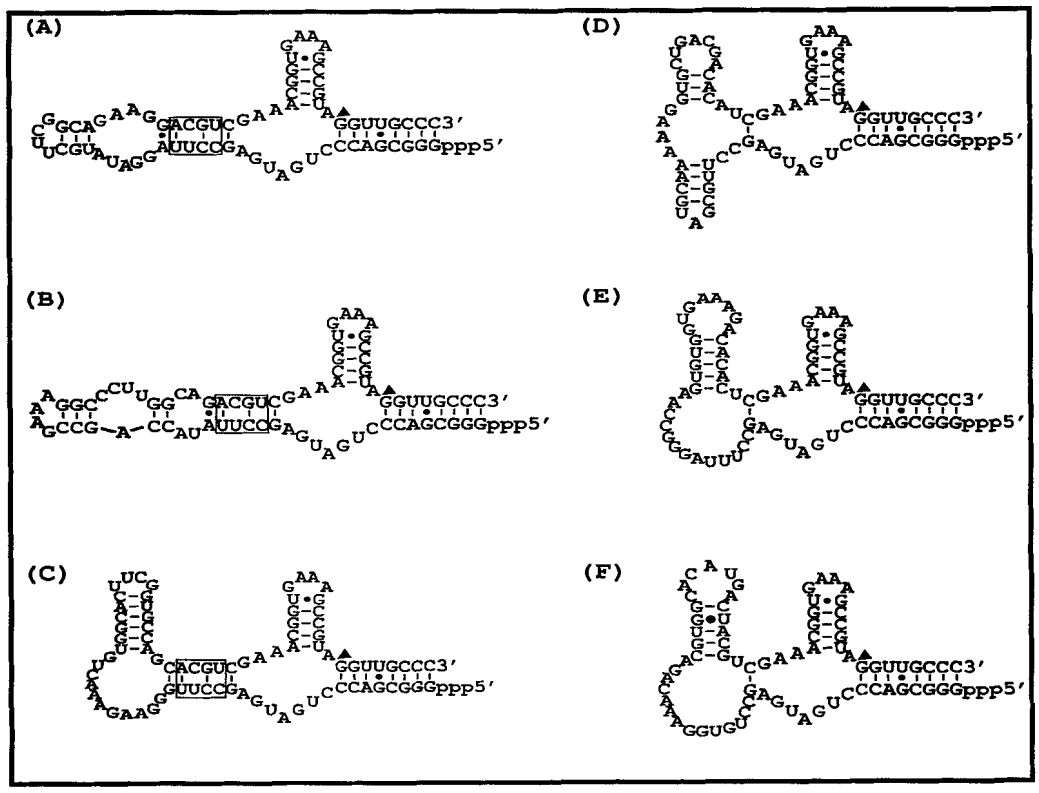

Figure 1-6 **Combinatorial selection strategies for generating allosteric ribozymes. (A) FMN-activated allosteric ribozyme by communication module selection. (B) Theophylline- and (C) ATP-activated allosteric ribozyme respectively by aptamer domain swapping. (D) cGMP-, (E) cCMP-, and (F) cAMP-activated allosteric ribozyme respectively by allosteric selection. Cleavage sites are indicated by solid arrows. The selected FMN communication modules are indicated by boxes.**

1.6.2 Allosteric Ribozymes as Potential Molecular Switches

Allosteric ribozymes can be used as molecular switches for the control of RNA function in cells. The ability of oligonucleotide-dependent hammerhead ribozymes to control gene expression *in vivo* by targeting the destruction of a specific mRNA that serves as both effector and substrate has been demonstrated (Kuwabara *et al.* 1998). From this example, it is quiet favorable that allosteric ribozymes that respond to small molecules have potential to be used in controlling gene expression. Recently, Green and

co-workers indeed demonstrated *in vivo* binding of exogenous ligands by endogenously expressed aptamers (Werstuck and Green 1998). Allosteric self-splicing ribozymes, therefore, may be used to process mRNA precursors to produce mature mRNAs in response to the presence or absence of ligands. Furthermore, allosteric self-cleaving ribozymes can be used for ligand-induced destruction or stabilization of mRNAs.

1.7 Thesis Overview

In a recent study (Liu and Sen 2004), the light-controlled RNA-cleaving 8-17 deoxyribozyme was demonstrated by chemically incorporating small compounds, azobenzene, into DNA sequences via covalent modifications demonstrated in a previous study (Asanuma *et al.* 1998). Azobenzene has been chosen to design the light-responsive RNA-cleaving deoxyribozyme, because it undergoes light-responsive reversible transformations between its *cis* and *trans* forms, and a short double-stranded DNA, that has an incorporated azobenzene in its *trans* form favors base-stacking, whereas its *cis* form disrupts base-stacking (Liang *et al.* 2003). The catalytic activity of the ribozyme was approximately five fold greater, when incorporated azobenzene residues were in its *trans* form compared to its *cis* form (Liu and Sen 2004). However, the change in the catalytic rates was very moderate, because the light-dependent transformations of azobenzene in the context of the ribozyme caused only moderate structural perturbation. The higher rate enhancements can be obtained if aptamers against one of the two light-responsive forms of a small compound are appended to enzymes. Furthermore, the advantage of appending aptamers is that it is not necessary to chemically incorporate a small light-responsive compound into the backbones of DNA oligonucleotides using automated synthesis.

RNA structures can exhibit conformational changes in response to ligand binding. When these ligand-dependent conformational changes are combined with the function of RNAs, allosteric ribozymes that respond to the ligand can be developed, and the distinct ligand-binding and catalytic RNA domains interact dynamically to control catalysis. All aspects of the function of these allosteric ribozymes, such as ligand specificity and affinity, can be engineered for desired purposes. Therefore, allosteric ribozymes can be used as molecular switches to set up new genetic control systems.

My thesis covers the *in vitro* selection of RNA aptamers against dual transformations of a light responsive compound, and designing and testing of a light-responsive allosteric *trans*-acting hammerhead ribozyme. Chapter 2 describes the *in vitro* selection and characterization of RNA aptamers that bound one of the two light-responsive isomers of the compound. Crude binding assays and spectroscopic measurements were used to determine specificity and affinity of the aptamers and to determine if the aptamers were able to discriminate between different isomers of the compound. Boundary analysis and truncation experiments were performed to determine a minimal ligand-binding domain. Chapter 3 describes the modular rational design of the *trans*-acting allosteric hammerhead ribozyme and its characterization including the determination of rate constants, magnesium dependence, ligand dependence, and real-time light-responsive activation and inhibition of the allosteric ribozyme by a change in the irradiation wavelength of light. Chapter 4 summarizes all the significant findings of my research, and potential implications of the allosteic ribozyme in controlling gene expression.

CHAPTER 2:
IN VITRO SELECTION OF RNA APTAMERS AGAINST DUAL CONFORMATIONS OF A PHOTOCHROMIC COMPOUND

2.1 Introduction

Photochromism is defined simply as a light-induced reversible change of color and defined more precisely as a reversibly switching chemical species between different structural states induced in one or both directions by absorption of different wavelengths of light between two forms, which have different absorption spectra (Bouas-Laurent and Dürr 2001). In photochromism, the thermodynamically stable form A is transformed by irradiation into form B. The back reaction can occur thermally or photochemically. In positive photochromism, photochromic molecules have a colorless thermodynamically form A and a colored form B. In negative photochromism, photochromic molecules have a colored thermodynamically stable form A and a colorless form B.

The dihydropyrene (DHP)-cyclophanediene (CPD) system is a negative photochromic compound, which thermally stable form is colored and becomes colorless by irradiation. The thermally stable green dimethyldihydropyrene (Figure 2-1) has a closed rigid planar π-system and has absorption to about 600 nm. The colorless dimethyldihydrocyclophanediene (Figure 2-1) is also rigid, but is an open step-shaped compound, and shows absorption with an extended tail (Blattmann *et al.* 1965; Mitchell *et al.* 2003). The typical absorption spectra of DHP-CPD system is shown in Figure 2-2. Because of this transformation, the number of interacting π-orbitals changes from

continuous 14π orbitals to two isolated 6π orbitals. The green dimethyldihydropyrene partially changes its planar form and color to its colorless step-shaped cyclophanediene form by irradiation with visible light. However, unfortunately, the reverse reaction occurs by irradiation with UV light as well as by heat (Mitchell *et al.* 1982). Since this thermal back reaction and light-dependent back reaction are much more favorable than the forward reaction, it is difficult to sustain the cyclophanediene form at room temperature, and therefore, this photochromic compound is not ideal as a potential photoswitch (Mitchell *et al.* 2003).

The disadvantages mentioned above are vastly improved by appending another benzene group to create benzo-dimethyldihydropyrene (BDHP) (Figure 2-3). This derivative of the compound still maintains above-mentioned essential light-dependent properties. However, the thermal back reaction is sufficiently reduced by changing the thermal rate constant at 30°C from $10x10^{-4}$ min^{-1} to less than $4x10^{-4}$ min^{-1}. Consequently, the cyclophanediene form (BCPD) (Figure 2-3) maintains high thermal stability. (Mitchell *et al.* 1982). In addition, the light-dependent forward reaction is much more favorable than that of the parent compound, because there is complete bleaching to the colorless BCPD instead of the partial color change by irradiation with visible light. As it is expected, the transformation of BCPD brings even larger change in the interacting π-orbitals from continuous 18π orbitals to two isolated 6π orbitals. Therefore, the fusion of the benzene ring makes this photochromic compound desirable to be used as a photoswitch, because it has a reasonably slow thermal back return with relatively fast photo-opening and closing (Mitchell *et al.* 2003).

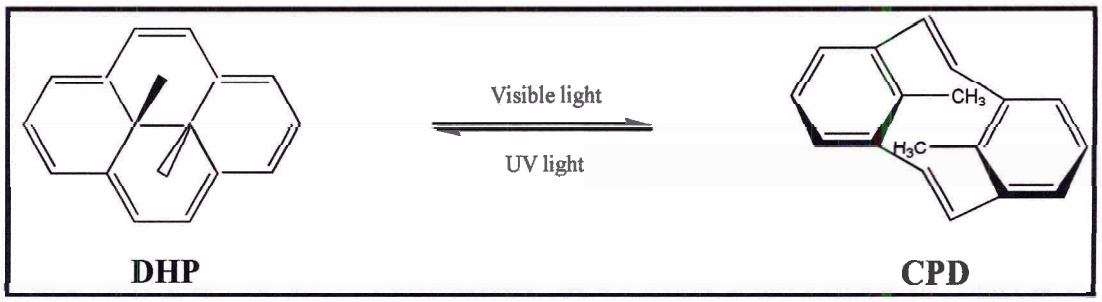

Figure 2-1 Schematic representation of DHP-CPD system.

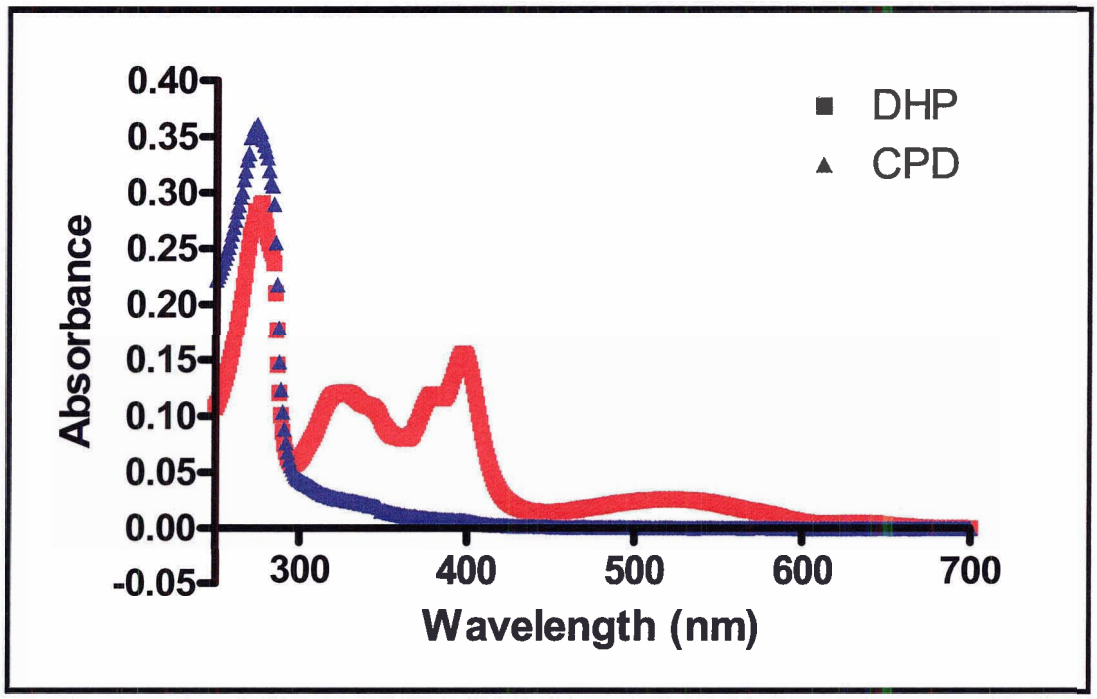

Figure 2-2 UV-Vis spectrum of CPD (blue) and DHP (red).

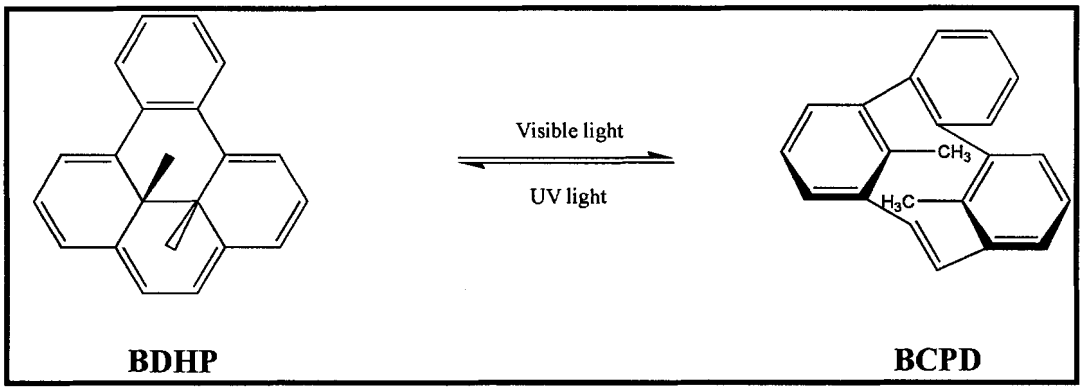

Figure 2-3 Schematic representation of BDHP-BCPD system.

The actual compound that was used for *in vitro* selection of RNA aptamers was a carboxylic group attached BDHP (BDHP-COOH) (Figure 2-4), because the compound needed to be immobilized on oxirane acrylic beads by the formation of a covalent bond between the compound and beads under acidic condition. Since the compound consisted of five aromatic rings and no hydrophilic groups, it was insoluble and extremely difficult to use it for any characterization experiments in aqueous solution. To resolve this problem, polyethylene glycol group attached BDHP (BDHP-PEG), which has several additional oxygen groups, was synthesized (Figure 2-5). It was used for characterization experiments of RNA aptamers and other aqueous based reactions.

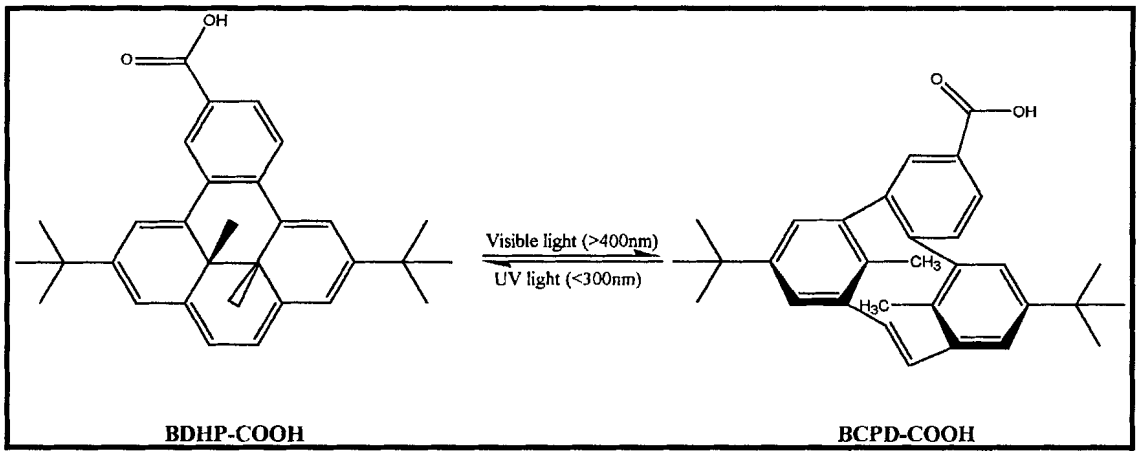

Figure 2-4 Schematic representation of BDHP-COOH - BCPD-COOH system.

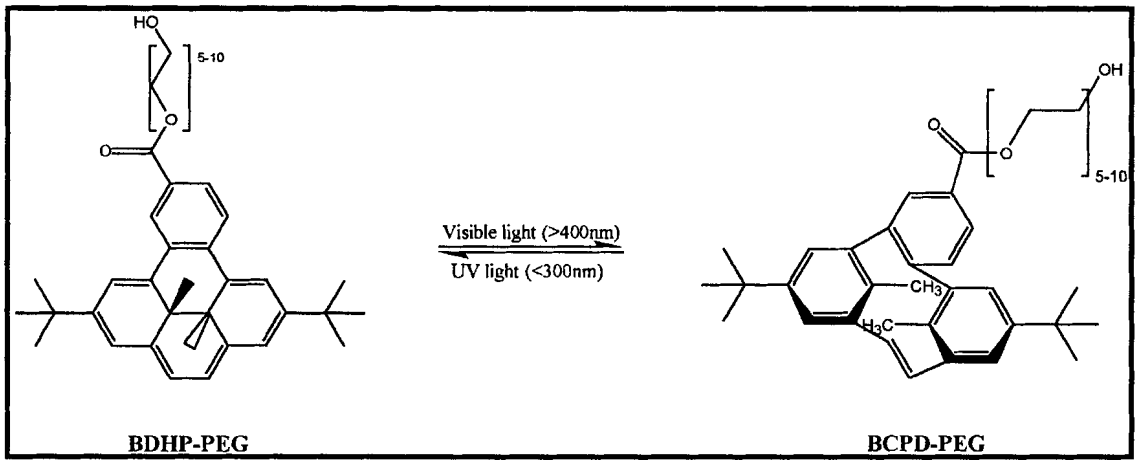

Figure 2-5 Schematic representation of BDHP-PEG – BCPD-PEG system.

To create a light-responsive allosteric hammerhead ribozyme for its potential use in the regulation of gene expression, RNA aptamers that recognize only one of the dual forms of the BDHP-BCPD system with high affinity and specificity need to be isolated. As it was mentioned previously, *in vitro* selection procedures can isolate aptamers, and these selected aptamers can specifically recognize and bind to their ligands at target concentrations of micromolar, nanomolar, or even picomolar range. The large, planar aromatic ring structures of the BDHP-BCPD system should make it attractive targets for binding by specific RNA aptamer structures, since Ellingtion and Szostak (Ellington and

Szostak 1990; Ellington and Szostak 1992) selected RNA and DNA aptamers by binding to a variety of polycyclic organic dye molecules. Also, it is absolutely required that the selected RNA aptamers discriminate light-reponsive transformations of the BDHP-BCPD system and have high affinity for the closed form and weak affinity for the open form or vice versa. This kind of extremely specific discrimination and recognition of RNA aptamers has been demonstrated by Jenison and co-workers (Jenison *et al.* 1994) by isolating theophylline-binding RNA molecules that were capable of discriminating against caffeine, which is different from theophylline by having one additional methyl group.

This chapter describes the *in vitro* selection and characterization of RNA aptamers that bind closed or open form of the photochromic compound. Crude binding assays and spectroscopic measurements were used to determine specificity and affinity of the aptamer against the closed form of the compound and to determine if the aptamer was able to discriminate between different isomers of the compound. Boundary analysis and truncation experiments were performed to determine a minimal ligand-binding domain.

2.2 Materials and Methods

2.2.1 Materials

Mono-carboxylic acid derivative of benzo-dimethyldihydropyrene (BDHP-COOH) and polymethylene glycol derivative of benzo-dimethyldihydropyrene (BDHP-PEG) were synthesized by Stephen Robinson from Dr. Mitchell's lab at the University of Victoria. Oxirane-acrylic beads and nucleotide triphosphates (NTPs) were purchased from Sigma. Deoxynucleotide triphosphates (dNTPs) were purchased from Pharmacia. T4 kinase was purchased from Invitrogen. T7 RNA polymerase and Taq DNA polymerase were made from Dr. Sen's lab. Superscript II reverse transcriptase was purchased from Invitrogen. Calf intestinal alkaline phosphatase was purchased from New England Biolabs and Roche. T1 ribonucleases were purchased from Fermentas. Cytidine phosphate (Cp) and T4 RNA Ligase were obtained from Hani Zaher in Dr. Unrau's lab at Simon Fraser University. [α-^{32}P]-UTP and [γ-^{32}P]-ATP were purchased from Perkin Elmer. TA cloning kit was purchased from Invitrogen. Thermo-Sequenase dideoxy kit was purchased from USB. A portable lamp (10 W) with a UV filter was obtained from Dr. Unrau's lab at Simon Fraser University and was used as a source of visible light (> 400nm). UVGL-58 hand-held lamp (6W) was purchased from UVP and was used as a source of UV light (<300 nm).

2.2.2 DNA Oligonucleotides

All DNA oligomers were purchased from University of Calgary Core DNA Services. All oligonucleotides were purified by denaturing polyacrylamide gel electrophoresis (PAGE), visualized by UV shadowing and eluted from the gel by crush-

soaking in a buffer containing 10 mM Tris-HCl (pH 8.0 at 23°C) and 0.1 mM EDTA followed by precipitation with ethanol.

2.2.3 BDHP-COOH Coupling to Oxirane Acrylic Beads

BDHP-COOH was coupled to oxirane-acrylic beads in 0.1 M sodium phosphate buffer (pH 4.0), and 50% DMF. The mixture was incubated on a rotating shaker for 72 hours at room temperature. After the completion of the coupling reaction, the beads were washed several times with water and incubated for another 48 hours with 4% β-mercaptoethanol to block unreacted oxirane groups. These blocked beads were washed with water and stored at 4°C in the presence of the sodium phosphate buffer. At each round of selection, the beads were washed several times with water and selection buffer (100 mM Tris acetate, 100 mM sodium acetate, 25 mM potassium acetate, 10 mM magnesium acetate, 0.05% Triton X-100, 1% DMSO, and pH 7.0), and pre-equilibriated with the selection buffer before use. Figure 2-6 shows the general reaction mechanism of the coupling between oxirane group of the beads and carboxylic group of the compound under acidic condition.

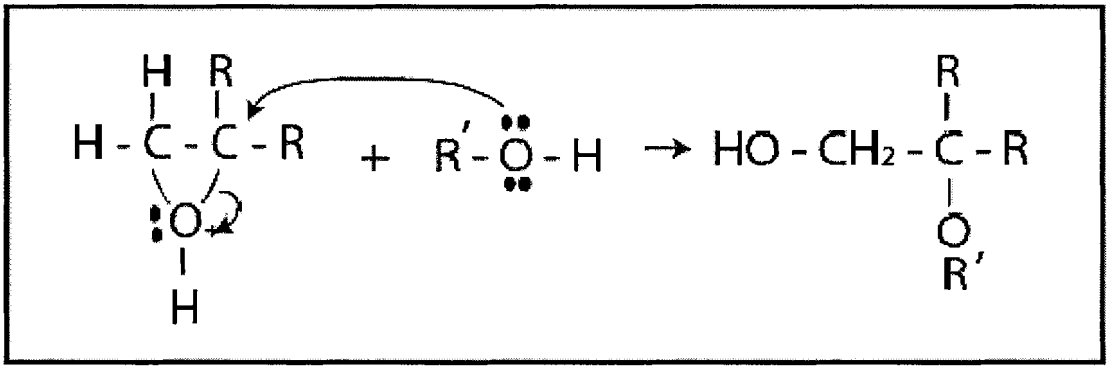

Figure 2-6 The mechanism of a covalent bond formation between BDHP-COOH and an oxirane group of the beads under acidic condition.

2.2.4 Selection Protocol

An initial population of RNA transcripts (5′-pppGGTGTGCGTACGAGTATATGG[N_{40}]GTCTCAATCGGTCTGTATC-3′) was prepared by *in vitro* transcription using PCR amplified double-stranded DNA template that carries the T7 RNA polymerase promoter. 150 PCR reactions were performed to generate approximately 10^{14} unique double-stranded DNA templates. Each PCR reaction (100 µl) containing 4 pmoles of DNA template, 100 pmol of 5′ primer (DP1), and 100 pmol of 3′ primer (LT2) were performed in 2.5 mM $MgCl_2$, 10 mM Tris-HCl (pH 8.0 at 23°C), 50mM KCl, 200 µM dATP, 200 µM dCTP, 200 µM dGTP, 200 µM dTTP, and 5 units of *Taq* polymerase. 30 *in vitro* transcription reactions were performed to generate the initial population of RNA transcripts. Each *in vitro* transcription reaction (50 µl) containing 20 pmoles of double-stranded DNA template was incubated in 40 mM Tris-HCl (pH 7.9 at 23°C), 26 mM $MgCl_2$, 10 mM DTT, 2.5 mM spermidine, 0.01% Triton X-100, 8 mM GTP, 4 mM ATP, 4 mM CTP, 2 mM UTP, 20 µCi of [α-^{32}P]-UTP, 150 units of T7 RNA polymerase for 3 hours at 37°C. Following transcription, the internally radiolabeled RNA were purified by a 10% denaturing PAGE, visualized by autoradiography, and eluted from the gel by crush-soaking in a buffer containing 10 mM Tris-HCl (pH 8 at 23°C) and 0.1 mM EDTA followed by precipitation with ethanol. This provided approximately 10 copies of each 10^{14} RNA sequence variants. This initial population of internally radiolabeled 10^{15} RNA transcripts were incubated at 90°C for 1 minute and allowed cool to 23°C slowly for approximately 90 minutes. The RNA population was incubated for 15 minutes with a selection buffer containing 100 mM Tris-acetate, 100 mM sodium acetate, 25 mM potassium acetate, 10 mM magnesium acetate,

0.05% Triton X-100, 1% DMSO, and pH 7.0 at 23°C. The folded RNA population was loaded onto an eppendorf tube containing BDHP-COOH or BCPD-COOH coupled oxirane acrylic beads and incubated for 20 minutes to allow the RNA to bind. In the case of selecting for BCPD-COOH binding aptamers, the state of the compound was changed from its closed form to open form by irradiation with greater than 400 nm of visible light until the color of the compound was completely bleached, before the RNA pool was added to the BCPD-COOH beads, since BDHP-COOH was the original state of the compound. After the incubation, unbound supernatants were removed from the tube, and the beads were washed with the selection buffer until almost no more radioactive counts were detected in washes. The beads with BDHP-COOH or BCPD-COOH bound RNAs were transferred to an elisa plate and irradiated with either visible (> 400 nm) or UV light (< 300 nm) until the color of the compound bound to the beads was changed. Because of the conformational changes of the compound, the closed form and open form aptamers bound to the corresponding compound coupled beads became unbound. The mixture was transferred back to a new eppendorf tube and supernatant was removed and transferred to a new eppendorf tube. The beads were then continuously washed with the selection buffer until almost no more radioactive counts were detected in washes. The washes were transferred to the eppendorf tube containing the initial supernatant and ethanol precipitated. The fraction of RNA that bound to a given column in each cycle (% RNA retained per cycle) was measured by scintillation counting and calculated by dividing the number of counts eluted by the number of counts originally loaded. (Scintillation counting was performed from round 6.) The eluted RNA was then reverse transcribed from a 3′ primer with Superscript II (Invitrogen), and the cDNA was amplified by PCR

with *Taq* DNA polymerase using both 5′ and 3′ primers. The resulting double-stranded DNA was used in an *in vitro* transcription reaction to prepare the RNA population for the subsequent round of selection. For round 12 and 13, negative selection was performed by adding the folded RNA pool to the beads coupled to β-mercaptoethanol, before the pool was added to the compound coupled beads. The overall *in vitro* selection scheme and detailed selection step scheme are shown in Figure 2-7 and Figure 2-8.

Figure 2-7 Overall schematic representation of in vitro selection.

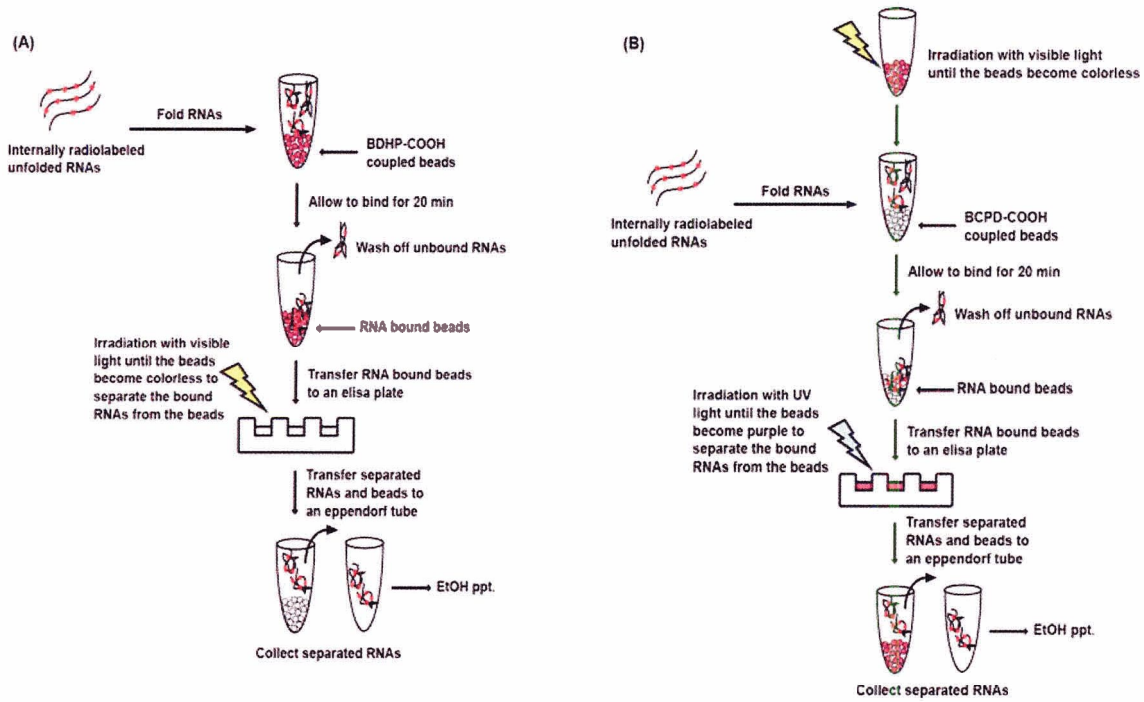

Figure 2-8 Detailed selection step representations for (A) BDHP-COOH binding aptamers and (B) BCPD-COOH binding aptamers.

2.2.5 Crude Binding Assays

Crude binding assays were performed in a very similar fashion as the selection process described above. The only difference was to test specificity and affinity of selected individual aptamers or each pool against both closed and open isomers of the compound. For instance, closed form aptamers were tested against the closed form coupled beads to determine its affinity and against the open form coupled beads to determine its specificity. The fraction of RNA that bound to a given column was measured by scintillation counting and calculated by dividing the number of counts eluted by the number of counts originally loaded.

2.2.6 Cloning and Sequencing

Following 13 rounds of *in vitro* selection, the pools were cloned using standard protocols. The amplified double-stranded DNA was purified by a 8% denaturing PAGE and ligated into the pCR2.1 plasmid using a TA cloning kit (Invitrogen). The plasmid was then transformed InVαF' competent *E. coli* cells (Invitrogen). 20 recombinant clones from each pool were picked and the plasmids were purified by a QIAprep Spin Miniprep kit (Qiagen). Finally, these clones were sequenced by using a Thermo-sequenase dideoxy kit (USB).

2.2.7 Dissociation Constant Determinations

The binding affinities of closed form C8 aptamers against BDHP-PEG or BCPD-PEG were determined spectroscopically by monitoring hyperchromicity of either BDHP-PEG or BCPD-PEG. All electronic absorption spectra were obtained in a dual-beam Cary 300-Bio UV-Visible Spectrophotometer at 23°C. The changes in absorbance at 398 nm for BDHP-PEG and at 310 nm for BCPD-PEG were determined at increasing concentrations of RNA (0-15 μM) titrated to a fixed concentration (2 μM) of either BDHP-PEG or BCPD-PEG in selection buffer. Because the absorbance peak of BCPD-PEG was overlapping with RNA absorbance peak at 260 nm, absorbance spectra of the aptamer alone at various concentrations were measured before taking absorbance spectra of the C8 aptamer in the presence of the open BCPD-PEG in order to determine the binding affinity of the C8 aptamer against BCPD-PEG. Then, the absorbance sepectra of the C8 aptamer alone were subtracted from the absorbance spectra of the C8 aptamer in the presence of the open BCPD-PEG. The data obtained were analyzed by GraphPad Prism 4 software.

2.2.8 Boundary Analysis Experiments

Closed form C8 aptamers were ^{32}P labeled either at their 5′ terminus with T4 polynucleotide kinase (Invitrogen) and [γ-^{32}P]-ATP or at their 3′ terminus with T4 RNA ligase and [5′-^{32}P] pCp, followed by purification using a 8% denaturing PAGE. Purified radiolabeled RNAs were cleaved randomly in the presence of 50 mM sodium carbonate (pH 9.0) by heating to 90°C for 5 min, precipitated with ethanol, and resuspended in TE buffer (10 mM Tris, pH 8.0, 0.1 mM EDTA). The partially digested radiolabeled RNAs were then heated for 1 min at 90°C to denature any folded structures and cooled down slowly. Following cooling to 23°C, the RNAs were added to an eppendorf tube containing BDHP-PEG coupled, BCPD-PEG coupled, or β-mercaptoethanol coupled oxirane acrylic beads and incubated for 30 min. After the incubation, the beads were washed with selection buffer to get rid of unbound RNAs until almost no more counts were detected in washes and bound RNAs were eluted with TE buffer after the washes. Samples from these fractions were separated by a 8% denaturing PAGE, visualized, and quantitated using a Phosphoimager and ImageQuant software (Molecular Dynamics). G-specific cleavage ladders were generated by incubating RNA in 10 μl containing 7 M urea, tRNA, and RNase T1 (Fermentas) for 2 min at 23°C.

2.2.9 Truncation Experiments

Truncation experiments were performed in a very similar way as the selection process as described above. Only difference was the collection of bound RNA fractions. The bound RNA fractions were eluted in TE buffer (10 mM Tris, pH 8.0, 0.1 mM EDTA) instead of using UV or visible light to let the bound RNAs to come off. The fraction of RNA that bound to a given column was measured by scintillation counting and calculated

by dividing the number of counts eluted by the number of counts originally loaded. Figure 2-9 shows the set of designed truncated constructs that have been tested.

Figure 2-9 **The set of truncated constructs that have been used for truncation experiments to determine a minimal ligand binding domain. Underlined regions represent 5′ and 3′ constant regions. The nucleotides in red are the minimal ligand binding domain that was determined by boundary analysis experiments.**

2.3 Results and Discussion

2.3.1 *In Vitro* Selection of BDHP-COOH or BCPD-COOH Specific Aptamers

RNA aptamers for closed or open form of the photochromic compound were isolated by *in vitro* selection from a population of 80-nucleotide RNA transcripts, each containing a region of 40 randomized nucleotides flanked by constant regions. Each selection experiment was initiated with an RNA pool containing 1 x 10^{15} different sequences. Aptamers were isolated by incubating the RNA pool in a BDHP-COOH or BCPD-COOH coupled beads, washing extensively to remove unbound and weakly bound RNAs, and then eluting specifically bound molecules by irradiating visible (> 400 nm) or UV (< 300 nm) light to isolate closed or open form binding aptamers respectively. The

different wavelengths of light were used in order to select aptamers that were able to discriminate between different conformational forms of the photochromic compound.

Figure 2-10 shows the percentage of RNA retained per round. The fraction of RNA that bound to a given column in each round was calculated by dividing the number of counts eluted by the number of counts originally loaded. Data from round 1 to 5 was not presented due to no scintillation counting measurements. As shown in the figure, there was no significant increase in the percentage of RNA bound until round 9. In round 10, there were moderate increases in the binding percentages for both forms of aptamers, and in round 11, the binding percentages for both close and open form aptamers were noticeably increased up to 13 and 14% respectively. Round 12 and 13 were performed with negative selection by adding the folded RNA pool to a column containing the beads coupled only with β-mercaptoethanol before adding the RNA pool to a column containing compound coupled beads. Therefore, only those RNA molecules not binding to the column in the absence of the compound were allowed to continue through the selection. In this way, sequences that bound to β-mercaptoethanol, that was used to block unreacted oxirane groups, were eliminated. About 8% of the RNA pool was bound to the negative selection column for each form of aptamers in round 12 and 13. After thirteen rounds, there was no further enrichment.

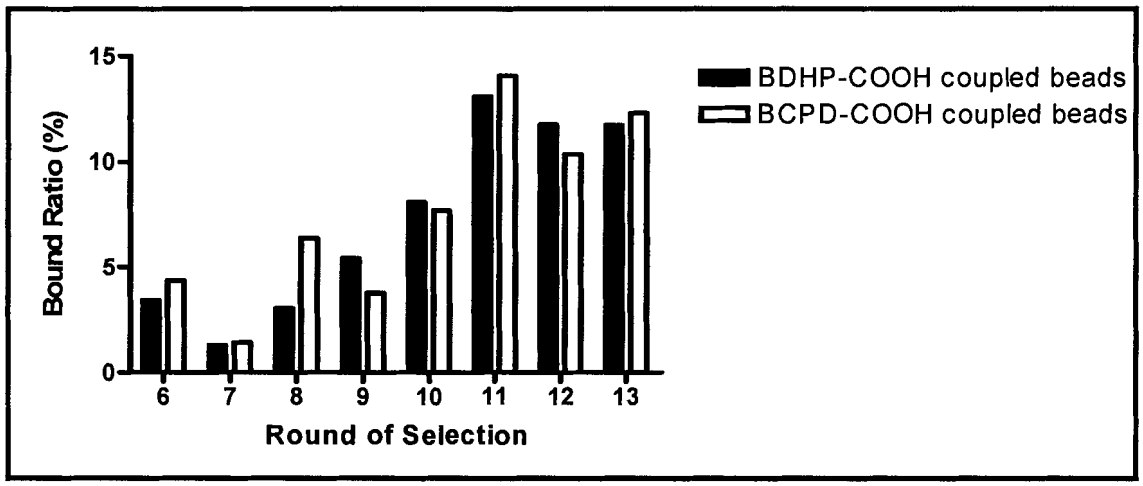

Figure 2-10 A fraction of each form of aptamers bound to a given column in each round. Black bars represent bound ratios of closed form binding aptamers, while white bars represent bound ratios of open form binding aptamers.

Before cloning and sequencing, crude binding assays of individual pools were carried out to determine how each pool was specifically responding to light-responsive transformations by measuring the binding of each pool against both columns (Figure 2-11). For the closed form binding aptamer pool, approximately 17% bound to closed BDHP-COOH coupled beads, and less than 3% bound to open BCPD-COOH coupled beads. For the open form binding aptamer pool, approximately 29% bound to open BCPD-COOH coupled beads and less than 3% bound to closed BDHP-COOH coupled beads. Therefore, the isolated aptamers were able to discriminate the different conformational forms of the compound by a change of irradiation with different wavelengths of light.

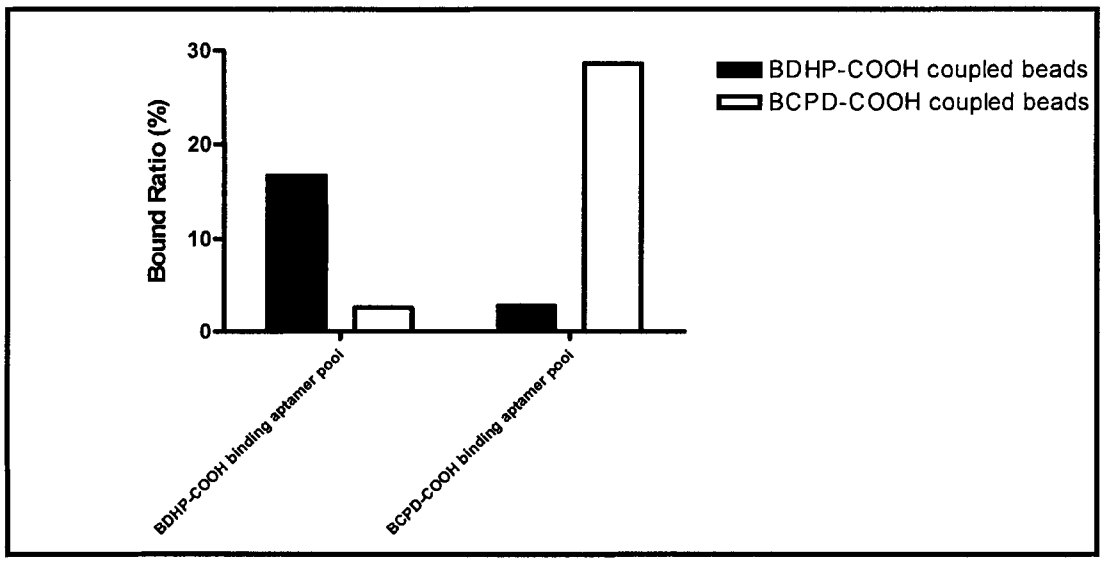

Figure 2-11 Crude binding assays of individual pools against both columns. Black bars represent closed form bound ratios of the individual pools, while white bars represent open form bound ratios of the individual pools.

2.3.2 Comparison of Aptamer Sequences

20 clones from closed form binding aptamer pool and 20 clones from open form binding aptamer pool were sequenced. Their random region sequences in a given pool were compared in search for sequence similarities that might be important for the binding of different isomers of the compound. Careful sequence comparison revealed short regions of similarity between clones in each pool, suggesting that these regions might be involved in binding. For the closed form binding aptamers, C3 and C8, and C6 and C18 pairs had short regions of similarity. For the open form binding aptamers, O4 and O19 pair showed the best sequence similarity (Figure 2-12). The binding of the aptamers to the compound might rely on base stacking of the compound in a helical region of the folded aptamer structure instead of specific hydrogen bond formations between the compound and the aptamers, since there is the absence of hydrogen bond donor or acceptor groups on the compound. Therefore, these similar regions in each family of a given pool could be important and necessary aptamer binding regions.

Figure 2-12 **The random region sequences of clones from each pool with the best similarity are shown. The top two pairs are from the closed form binding aptamer pool, while the bottom pair is from the open form binding aptamer pool. Black letter nucleotides represent the short regions of similarity between a given pair.**

2.3.3 Crude Binding Assays of Individual Clones

To roughly determine binding affinities of six individual clones mentioned in the previous section, crude binding assays of these six aptamers were performed as described previously. The assays were performed to determine a fraction of each aptamer bound to either BDHP-COOH or BCPD-COOH coupled beads to determine how specific each clone was against the corresponding form of the compound (Figure 2-13). Among the closed form binding aptamers, C8 showed the best affinity and specificity, since less than 1% of the C8 aptamers bound to the open BCPD-COOH, and approximately 27% bound to the closed BDHP-COOH. C3 showed moderately good affinity and specificity. Among the open form binding aptamers, O4 showed better affinity, whereas O19 showed better specificity between the two clones. Since C8 showed the best discriminating ability of light-responsive transformations of the compound, this aptamer was chosen for further characterization and investigation.

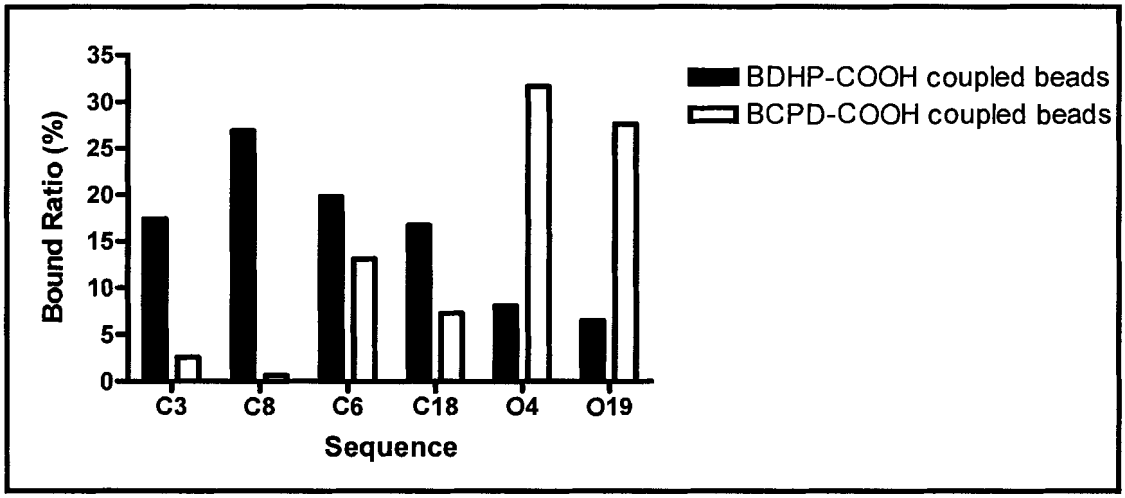

Figure 2-13 Crude binding assays of individual clones against both conformational forms of the comopound. Black bars represent closed form bound ratios of the individual clones, while white bars represent open form bound ratios of the individual clones.

2.3.4 Spectroscopy of BDHP-PEG or BCPD-PEG Binding to C8 Aptamer

The dissociation constants (K_d) of the C8 aptamer for BDHP-PEG or BCPD-PEG were measured by UV-Vis spectroscopy as described previously (Travascio *et al.* 1998). BDHP-PEG and BCPD-PEG were used to replace BDHP-COOH and BCPD-COOH respectively, since BDHP-COOH or BCPD-COOH, which consisted of five hydrophobic aromatic rings and only one hydrophilic carboxylic group, were insoluble and not suitable to use in aqueous reactions. BDHP-PEG and BCPD-PEG had a polyethylene glycol group instead of a carboxylic group in order to have five to ten additional oxygen groups for increased solubility. It was predicted that replacing a carboxylic group to a polyethylene glycol group would not cause a problem for the aptamer binding to the compound, because the carboxylic group attached side of the compound was occupied for the formation of a covalent bond with an oxirane group of the beads. Consequently, the aptamer might interact with the polycyclic-ring side of the compound, and this was in fact the case.

Figure 2-14a shows that the C8 aptamer binding to closed BDHP-PEG resulted in a hyperchromicity in the BDHP-PEG absorbance. This hyperchromicity was probably resulted from the C8 aptamer offering a binding site for closed BDHP-PEG by shifting the monomerization and oligomerization equilibria of the closed BDHP-PEG in the aqueous selection buffer containing trition X-100 towards the monomeric form (Travascio *et al.* 1998). Triton X-100 was added to the buffer to disaggregate the closed BDHP-PEG, which likely has tendency to aggregate because of poor solubility and high hydrophobicity of the closed BDHP-PEG. In addition, the hyperchromicity perhaps was an indication of the binding site for the closed BDHP-PEG being hydrophobic because of the base stacking of the compound in a helical region of the folded aptamer structure. Similarly, it was demonstrated in a previous study that the interaction between hemin and the hydrophobic surface of the guanine quartet of the CH6A DNA aptamer gave rise to the hyperchromicity in the hemin absorption spectra (Chinnapen and Sen 2002). The change in absorbance at 398 nm as a function of the C8 aptamer concentration was used to determine the dissociation constant by fitting the data to a one site binding hyperbola equation of GraphPad Prism 4 software. The dissociation constant of the C8 aptamer against the closed BDHP-PEG was 2.7 ± 0.4 μM (Figure 2-14b, Table 2-1). The closed form of the compound was sustained for duration of the experiment, since there was no indication of forming an extended tail above 300 nm, which is the main characteristic of open form compound absorption spectra as shown in Figure 2-2.

The dissociation constant of the C8 aptamer against open BCPD-PEG was also measured to determine how much weaker the binding was against open conformation of the compound. However, there was a problem of determining the dissociation constant of

the C8 aptamer against the open BCPD-PEG spectroscopically, because the absorbance peak of BCPD-PEG was at 250 nm, which was overlapping with RNA absorbance peak at 260 nm. To solve this problem, absorbance spectra of the aptamer alone at various concentrations were measured before taking absorbance spectra of the C8 aptamer in the presence of the open BCPD-PEG, and then the absorbance sepectra of the C8 aptamer alone were subtracted from the absorbance spectra of the C8 aptamer in the presence of the open BCPD-PEG (Figure 2-15a). Since the absorbance at 250 nm was significantly affected by the absorbance of the C8 RNAs, the absorbance values at 250 nm was not reliable even after the subtraction. Figure 2-15b shows the 300 nm to 325 nm region of the absorption spectra, and gradual absorption increase was observed in this tail region of the spectra. The change in absorbance at 310 nm as a function of C8 aptamer concentration was used to determine the dissociation constant by fitting the data to the same equation mentioned above. The dissociation constant of the C8 aptamer against open BCPD-PEG was inconclusive, since it was unable to reach a saturating plateau even at 15 μM (Figure 2-15c, Table 2-1). Therefore, the only conclusion that could be illustrated from this experiment was that the dissociation constant of the C8 aptamer against open BCPD-PEG was probably greater than 15 μM. However, this result was indicative enough to show less tight binding of the C8 aptamer for open form of the compound. The open form of the compound was sustained for duration of the experiment, since there was no indication of forming several absorption peaks above 300 nm, which is the main characteristic of closed form compound absorption spectra as shown in Figure 2-2. In summary, the C8 aptamer showed a good binding affinity to closed BDHP-PEG

with the low micromolar K_d, and a good discriminating ability against open BCPD-PEG with approximately a seven-fold difference in the dissociation constants.

Table 2-1 Summary of dissociation constants.

	K_d (μM)
C8 aptamer against BDHP-PEG	2.7 ± 0.4
C8 aptamer against BCPD-PEG	> 15

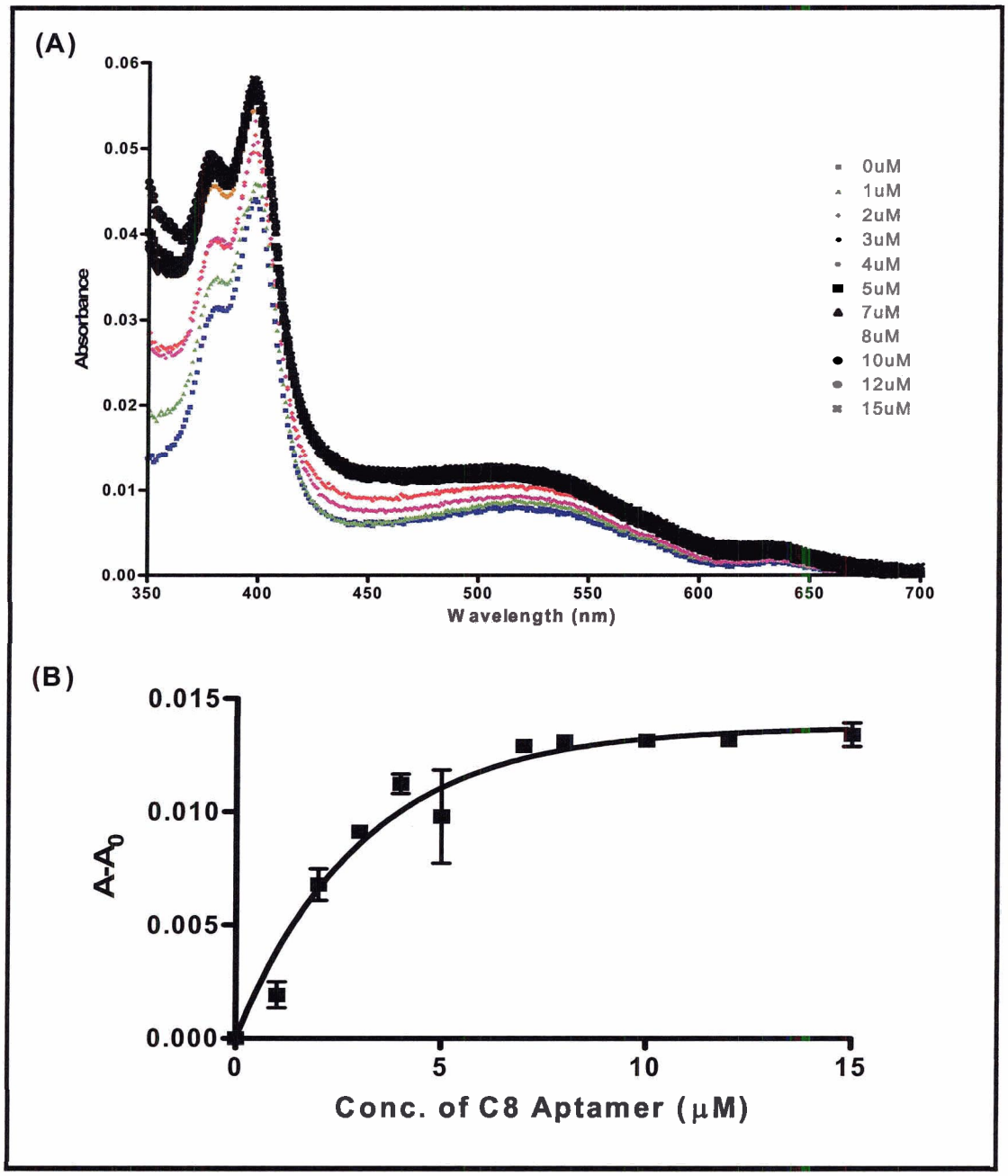

Figure 2-14 **Spectroscopical determination of the binding affinity of C8 aptamer against closed BDHP-PEG. (A) Absorption titration of BDHP-PEG (2μM of BDHP-PEG, in the presence of 0.05% Triton X-100, and 1% DMSO) with increasing concentrations of the C8 aptamers in the range of 350-700 nm. C8 aptamer concentrations were indicated on the right side of the graph. (B) The binding curve of the C8 aptamer against BDHP-PEG at 398 nm. A-A_0 on the Y-axis of the graph represents absorbance of BDHP-PEG in the presence of different concentrations of the C8 aptamers at 398 nm subtracted by absorbance of BDHP-PEG in the absence of the C8 aptamers at 398 nm.**

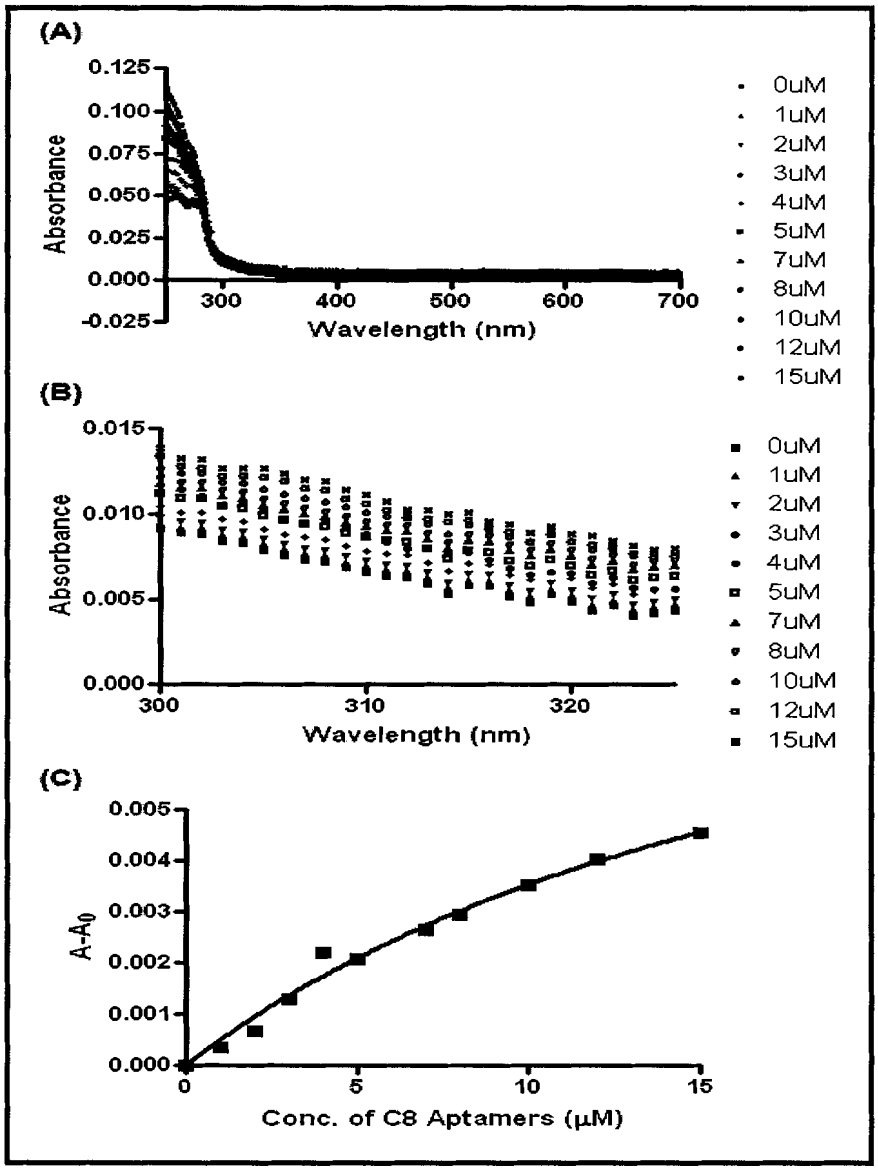

Figure 2-15 **Spectroscopical determination of the binding affinity of C8 aptamer against open BCPD-PEG. (A) Absorption titration of BCPD-PEG (2μM of BCPD-PEG, in the presence of 0.05% Triton X-100, and 1% DMSO) with increasing concentrations of the C8 aptamers in the range of 350-700 nm. C8 aptamer concentrations were indicated on the right side of the graph. The absorbance spectra were obtained by subtracting the absorbance spectra of the C8 aptamers in the presence of BCPD-PEG from the absorbance spectra of the C8 aptamers alone. (B) Absorption titration of BCPD-PEG with increasing concentrations of the C8 aptamer in the range of 300-325 nm. (C) The binding curve of the C8 aptamers against BCPD-PEG at 310 nm. $A-A_0$ on the Y-axis of the graph represents absorbance of BCPD-PEG in the presence of different concentrations of the C8 aptamers at 310 nm subtracted by absorbance of BDHP-PEG in the absence of the C8 aptamers at 310 nm.**

2.3.5 Determination of Minimal Ligand Binding Domains via Boundary Analysis Experiments

The minimum sequence requirements for the C8 aptamer were determined by boundary analysis experiments. RNAs representing the C8 aptamers were radiolabeled with ^{32}P either at their 5′ or at their 3′ termini and subjected to partial alkaline-mediated phosphodiester bond cleavage. The resulting truncated RNAs were transferred to an eppendorf tube containing closed BDHP-COOH coupled beads (positive column), which selectively complexed with the truncated RNAs that retained closed BDHP-COOH binding function and to an eppendorf tube containing β-mercaptoethanol coupled beads (negative column). The truncated RNAs that did not bind to the closed BDHP-COOH were collected in the wash, while the truncated RNAs that bound to the closed BDHP-COOH were retained by the beads and eluted with TE buffer. PAGE analysis of the distribution of RNAs derived from 5′ ^{32}P-labeled C8 transcripts was used to establish the shortest C8 RNA that binds to the closed BDHP-COOH and to establish the importance of flanking constant sequences on the function of the minimal RNA aptamer. Since it was difficult to determine exact nucleotide position visually from the gel (Figure 2-16), ratio analysis at each nucleotide position was performed. Each nucleotide position was quantitated by densitometry, and a ratio of eluate to wash for each nucleotide position was determined by dividing a fraction of eluate by a fraction of wash for a given column. If there is an increase in the ratio trend of the positive column as compared to negative column, the point where the increase in the ratio trend starts, is likely to be the boundary position.

In the case of 3′ boundary analysis, the RNA aptamer could be truncated to nucleotide position C43 with full retention of the closed form binding function (Figure 2-

17). Likewise, an analysis conducted with 3′ ^{32}P-labeled C8 aptamer revealed that the RNA aptamer could be truncated to nucleotide position G14 towards the 5′-terminus (Figure 2-18). In both cases, a few additional nucleotide positions away from the exact nucleotide positions where the increase in the ratio trend started, were chosen as the 5′ and 3′ boundary nucleotides to make sure the minimal ligand-binding domain was included. As a result, the smallest C8 aptamer was 30 nucleotides in length, which included a part of the 5′ primer binding site.

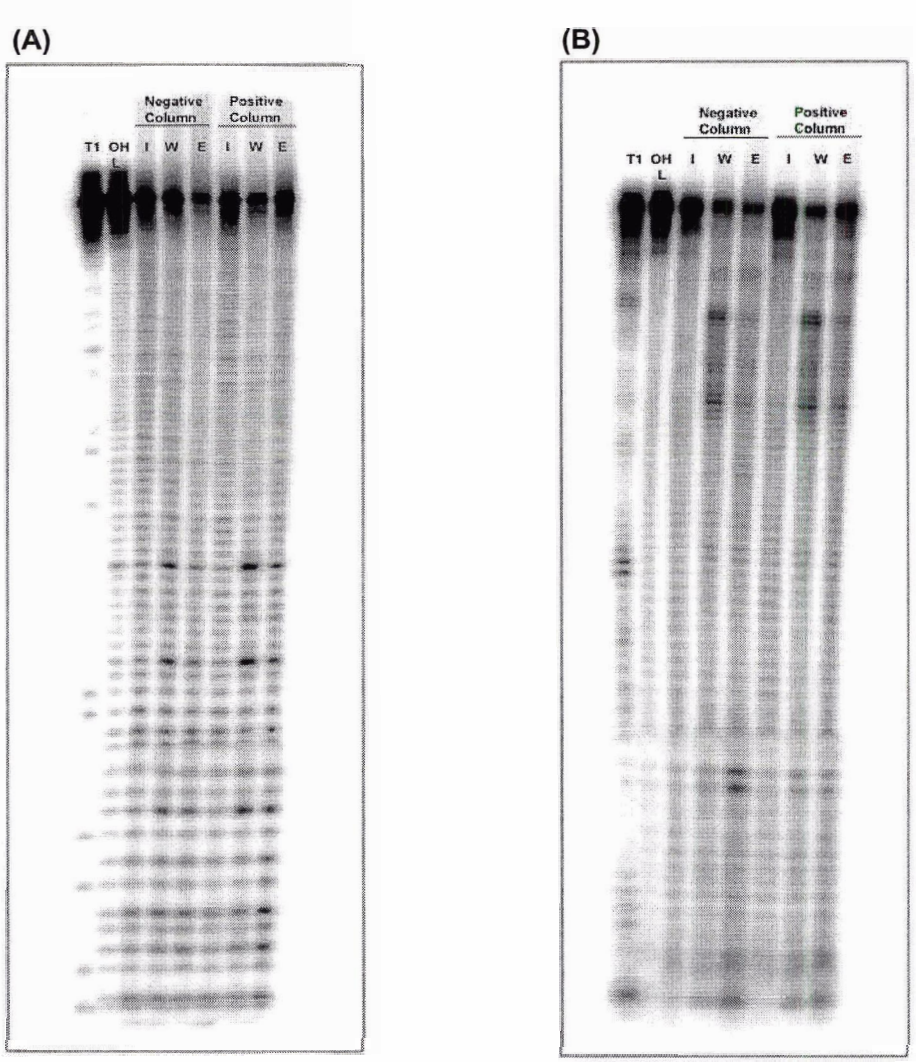

Figure 2-16 **Boundary analysis experiment for determining the 5′ and 3′ terminus of the functional BDHP-COOH binding domain of C8 aptamer. (A) 3′ boundary analysis. (B) 5′ boundary analysis. "T1" represents ribonuclease T1 treatment of the RNA to generate RNA products that are cleaved on the 3′ side of G residues. "OH ladder" represents partial alkaline-mediated degradation of C8 aptamer. "I" represents truncated RNAs before adding to the indicated column. "W" represents unbound truncated RNAs that were collected in the wash. "E" represents bound truncated RNAs eluted with TE buffer.**

5′ GGUGUGCGUACGAGUAUAUGGUCAUCCUACAUCUGCUUUGAGCAUCUCGACGAAGAGUUUGUCUCAAUCGGUCUGUAUC 3′

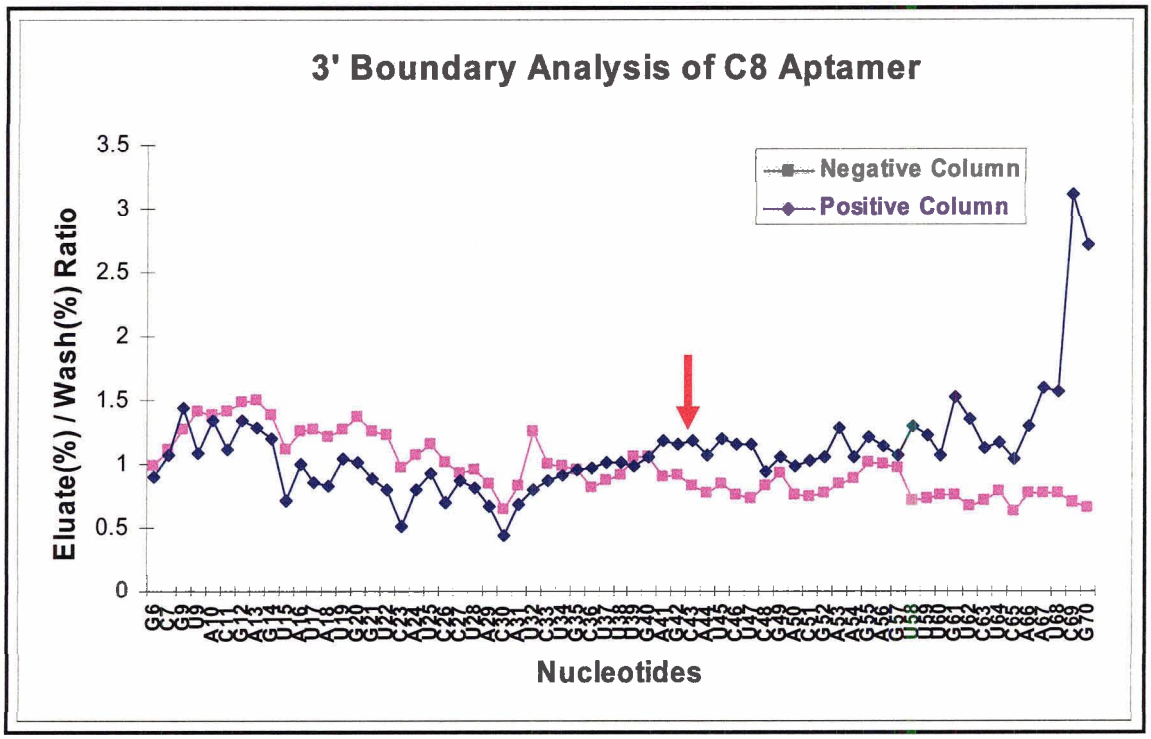

Figure 2-17 **3′ boundary analysis of C8 Aptamer. Red arrow in the graph and red letter in the above sequence indicate 3′ end of a minimal aptamer domain. Underlined nucleotides in the above sequence represent 5′ and 3′ primer binding sites.**

5′ GGUGUGCGUACGAGUAUAUGGUCAUCCUACAUCUGCUUUGAGCAUCUCGACGAAGAGUUUGUCUCAAUCGGUCUGUAUC 3′

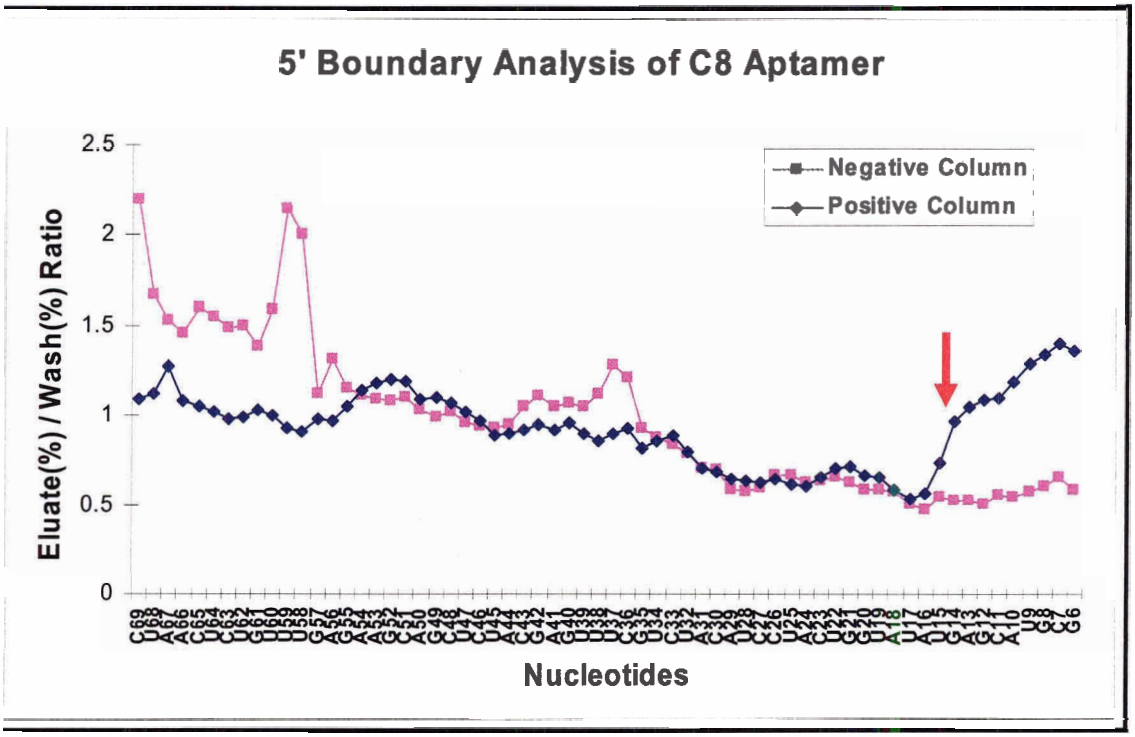

Figure 2-18 **5′-boundary analysis of C8 Aptamer. Red arrow in the graph and red letter in the above sequence indicate 3′ end of a minimal aptamer domain. Underlined nucleotides in the above sequence represent 5′ and 3′ primer binding sites.**

2.3.6 Determination of Minimal Ligand Binding Domains via Truncation Experiments

To prove the results obtained from the boundary analysis experiments, a series of deletion mutant constructs were designed to eliminate stretches of nucleotides from 5′ and 3′ ends based on the minimal C8 aptamer determined from the boundary analysis experiments. These are summarized in Figure 2-19 with a fraction of each construct bound to a given closed BDHP-COOH coupled beads containing column. The wild-type C8 aptamer showed 34% binding to the column. The 5TR1 construct, which thirteen primer-binding nucleotides from 5′ end were removed from the wild-type aptamer, showed relatively the same binding affinity. However, if six additional nucleotides,

which formed base-pairs in a stem region or an internal bulge loop according to the predicted secondary structures of the minimal C8 aptamer from the RNA mfold program (Figure 2-20a, b), were removed from 5′end of the 5TR1 construct (5TR2), the binding affinity of the construct was significantly decreased from 30% to 20%. Using the same approach, deletion constructs for the 3′ ends were tested as well. The 3TR1 construct, which all nineteen primer-binding nucleotides from 3′ end were removed from the wild-type aptamer, showed retained closed form binding function with 29% binding compared to 34% binding of the wild-type construct. If nucleotides up to 3′ end of the minimal C8 aptamer were removed in the case of the 3TR2 construct, the aptamer function was still retained with 32% binding to the column. The binding of the minimal C8 aptamer (MA) itself to a given closed BDHP-COOH coupled beads containing column showed increase in the binding affinity probably suggesting that secondary or tertiary structures formed using the nucleotides 5′ and 3′ of the minimum aptamer domain can modulate ligand binding. Seven nucleotides at the 3′end of the minimal C8 aptamer could be removed without disrupting the aptamer binding, as it was shown in the 3TRMA1 construct, because those nucleotides were not involved in forming any structures or base pairs according to secondary structures predicted by the RNA mfold program (Figure 2-20a, b). However, the deletion of nine more nucleotides from 3′ end of the 3TRMA1 construct resulted in almost complete loss of the aptamer function suggesting that the loop region shown in Figure 2-20a, or the internal bulge region shown in Figure 2-20b provided crucial interactions with the ligand. Among the two predicted structures, the structure shown in Figure 2-20a probably was the secondary structure of the minimal C8 aptamer, because the binding affinity was lost even further to 4%, when the loop region of the

Figure 2-20a structure was disrupted in the 3TRMA2 construct, while the retained loop region in 5TR2 construct showed 20% binding affinity. In addition, crude binding assays of 3TRMA1 construct against closed, open, or β-mercaptoethanol coupled beads showed that this minimum aptamer binding construct was able to discriminate effectively between different forms of the compound (Table 2-2). Therefore, the minimal C8 aptamer determined from the boundary analysis experiments included the minimal ligand-binding domain. Seven more nucleotides from 3′ end of the aptamer could be removed to form an even shorter aptamer domain.

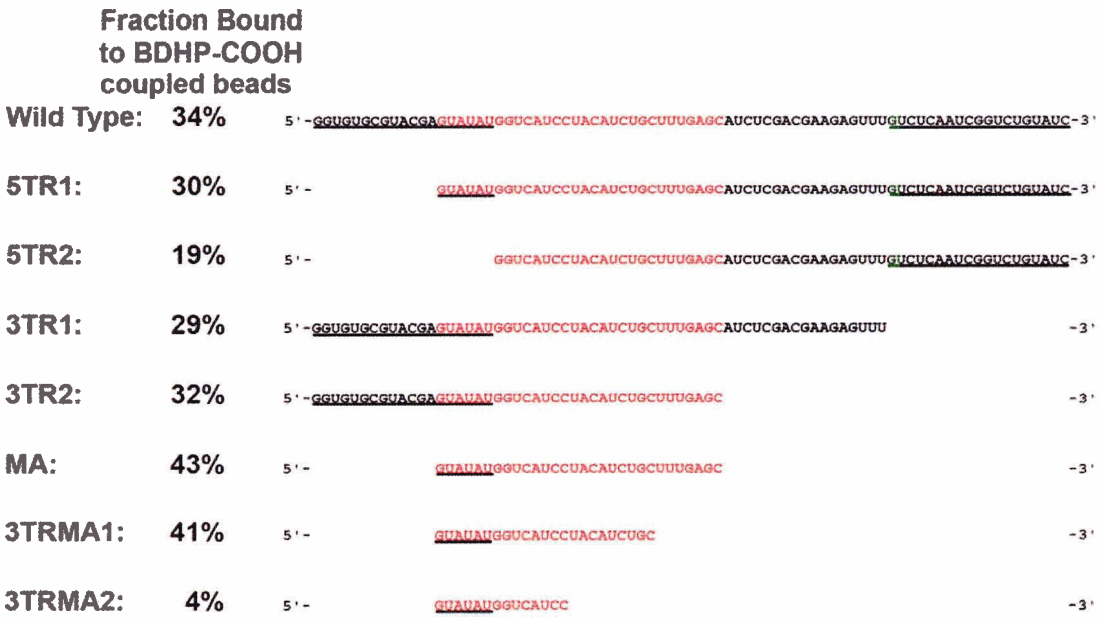

Figure 2-19 Summary of truncation experiments of C8 aptamer. Fraction of each truncated construct bound to a given column was shown. Underlined regions represent 5′ and 3′ constant regions. The nucleotides in red are the minimal ligand binding domain that was determined by the boundary analysis experiments.

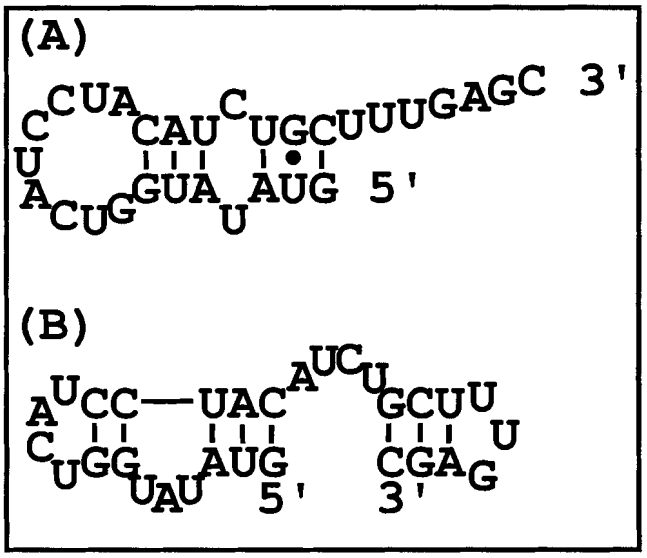

Figure 2-20 **Two secondary structure models of the minimal C8 aptamer predicted by the RNA mfold program.**

Table 2-2 **Crude binding assays of 3TRMA1 to a given column.**

	BDHP-COOH Coupled Beads	BCPD-COOH Coupled Beads	β-Mercaptoethanol Coupled Beads
Fraction of 3TRMA1 Bound	44.98%	4.34%	8.91%

2.4 Conclusion

In vitro selection and characterization of RNA aptamers that recognized and bound to closed dimethyldihydropyrene or its isomeric open cyclophanediene were described in this chapter. These aptamers were able to discriminate between different forms of the compound by irradiation of different wavelengths of light. Among these aptamers, the C8 aptamer, which bound to closed form of the compound, showed the best affinity and specificity with the low micromolar K_d and was able to discriminate its isomeric open form of the compound with approximately a seven-fold lower binding affinity. In our knowledge, the C8 aptamer is the only aptamer that recognizes light-responsive transformations of a photochromic compound to date and perhaps employs only base-stacking hydrophobic interactions to specifically recognize a polycyclic portion

of the compound instead of recognizing its ligand by usual hydrogen bonding. The minimum ligand-binding domain of C8 aptamer was determined by boundary analysis and truncation experiments. The minimum C8 aptamer domain itself was able to discriminate two different isomers of the compound by showing high binding affinity to closed form of the compound and low binding affinity to open form of the compound.

This aptamer that recognizes different forms of the photochromic compound will allow us to construct an allosteric ribozyme by combining the aptamer and a catalytic hammerhead ribozyme that cleaves its RNA substrate by a transesterification reaction. This allosteric hammerhead ribozyme can be potentially used as a photo-regulated molecular switch to create a new genetic control system. The next chapter describes the modular rational design of an allosteric *trans*-acting hammerhead ribozyme and its characterization including the determination of rate constants, magnesium dependence, ligand dependence, and real-time photo-regulated activation and inhibition of the allosteric ribozyme by a change in the irradiation wavelength.

CHAPTER 3:
RATIONAL DESIGN OF ALLOSTERIC HAMMERHEAD RIBOZYMES

3.1 Introduction

The *de novo* design of new ribozymes using a purely rational approach remains problematic until precise control over nucleic acid folding can be achieved (Breaker and Joyce 1994). However, new ribozymes and ligand-binding RNAs can be created relatively easily by using *in vitro* selection, which uses iterative selection and amplification processes (Breaker 1997; Williams and Bartel 1996). The success of this process relies on the probability that a rare and active molecule can be isolated from a large population of randomized or mutagenized RNAs. An intermediate approach to RNA engineering, called 'modular rational design' makes use of pre-existing RNA structures that retain their structure and function, even when removed from their original system and setting in an entirely different context. This method eliminates the need for inventing new enzyme active sites and ligand-binding RNAs and can be used to create new functional nucleic acids.

Recently, modular rational design was successfully employed to engineer artificial ribozymes that act as allosteric ribozymes (Tang and Breaker 1997a; Tang and Breaker 1997b; Tang and Breaker 1998). Modular rational design seeks to achieve a ribozyme engineering objective through the careful integration of pre-existing RNA structures. Pre-existing RNA domains that function independently either as a receptor for ATP or as an RNA-cleaving ribozyme were fused to create a series of allosteric

ribozymes with catalytic rates that respond either positively or negatively to the presence of ATP (Tang and Breaker 1997a). Independently, the ATP-binding aptamer binds ATP with a K_d of approximately 10 μM (Sassanfar and Szostak 1993), and the hammerhead ribozyme cleaves its RNA substrate with a rate constant of 1 min^{-1} in the presence of saturating concentrations of magnesium ions and substrates (Forster and Symons 1987; Fedor and Uhlenbeck 1992). When they are joined, specific arrangements of the aptamer-ribozyme constructs display ATP-dependent activation and inactivation of the catalytic cleavage. Rate modulation of the ATP-dependent allosteric ribozyme is caused by ATP-induced conformational changes that occur in the aptamer domain upon ATP-binding. The resulting conformational rearrangement creates either up- or down-regulating interactions between the two domains, therefore, creating the ligand-dependent ribozyme responses (Tang and Breaker 1997a). By appending aptamer and ribozyme domains through communication modules, the proper folding of both domains can be engineered to be dependent upon ligand binding. In this manner, allosteric hammerhead ribozyme that are activated by FMN (Araki *et al.* 1998; Soukup and Breaker 1999a; Fan *et al.* 1996) or theophylline (Soukup and Breaker 1999a; Jenison *et al.* 1994; Zimmermann *et al.* 1997) have been generated by modular rational design.

Many aptamers that bind small ligands have adaptive binding (Hermann and Patel 2000; Patel *et al.* 1997). The ligand-binding pocket sites of these aptamers undergo substantial structural reorganization in the presence of the ligand. Probably, the dynamic motions of the aptamer's binding pocket occasionally take the optimal conformation that is ideal for its corresponding ligand docking. This complex formation stabilizes the RNA conformation that is bound to the ligand. The modular nature of RNA and its ability to

undergo substantial ligand-mediated structural rearrangements are ideal characteristics to have allosteric control.

As previously demonstrated using certain other communication module sequences, effector specificity of an allosteric ribozyme can be altered simply by exchanging the ligand-binding domain (Soukup and Breaker 1999b; Soukup *et al.* 2000). The unique stem sequences of FMN-activated ribozymes have been demonstrated to function as 'communication modules', which inform the binding status of an appended aptamer domain to the adjoining ribozyme domain. One such communication module mediates ligand-dependent activation of the hammerhead ribozyme, when the FMN-binding domain is replaced with either an aptamer domain that binds ATP or an aptamer domain that binds theophylline (Soukup and Breaker 1999b). Therefore, ribozymes with new effector specificities can be created simply by aptamer domain swapping.

This chapter describes the modular rational design of an allosteric *trans*-acting hammerhead ribozyme by appending the C8 aptamer via previously reported communication modules, and its characterization including the determination of rate constants, magnesium dependence, ligand dependence, and light-responsive activation and inhibition of the allosteric ribozyme by a change in the irradiation wavelength.

3.2 Materials and Methods

3.2.1 DNA Oligonucleotides

All DNA oligomers and the 14-nucleotide RNA substrate for the hammerhead ribozymes were purchased from University of Calgary Core DNA Services. All oligonucleotides were purified by denaturing polyacrylamide gel electrophoresis (PAGE), visualized by UV shadowing and eluted from the gel by crush-soaking in a buffer containing 10 mM Tris-HCl (pH 8.0 at 23°C) and 0.1 mM EDTA followed by precipitation with ethanol. The purified RNA substrate was 5′-end labeled with [γ-^{32}P]-ATP (Perkin Elmer) using standard phosphorylation protocols of T4 Kinase kit (Invitrogen) and then re-purified by a 14% denaturing PAGE. A portable lamp (10 W) with a UV filter was obtained from Dr. Unrau's lab at Simon Fraser University and was used as a source of visible light (> 400nm). A hand-held UV lamp (6W) was purchased from Spectroline and was used as a source of UV light (<300 nm).

3.2.2 Ribozyme Synthesis

The double-stranded DNA template for each ribozyme construct was generated by primer extension of the oligonucleotide 5′ CTAATACGACTCACTATAGG 3′ on a DNA template that is complementary to the desired RNA construct used. Primer extension reactions (100 µl) contain 200 pmol template, 300 pmol primer, 10 mM Tris-HCl (pH 8 at 23°C), 2.5 mM $MgCl_2$, 50 mM KCl, 200 µM of each dNTP, and 1 U/µl Taq DNA polymerase, and were incubated at 94°C for 45 seconds, at 50°C for 1 minute, and at 72°C for 5 minutes for one cycle. Extension products were precipitated with ethanol and resuspended in a buffer containing 10 mM Tris-HCl (pH 8 at 23°C) and 0.1 mM EDTA. *In vitro* transcription reactions (50 µl) containing 20 pmole of double-stranded

DNA template were incubated in 40 mM Tris-HCl (pH 7.9 at 23°C), 26 mM $MgCl_2$, 10 mM DTT, 2.5 mM spermidine, 0.01% triton X-100, 8 mM GTP, 4 mM ATP, 4 mM CTP, 2 mM UTP, 150 units of T7 RNA polymerase for 2 hours at 37°C. Following transcription, the RNA were purified by a 12% denaturing PAGE, visualized by autoradiography and eluted from the gel by crush-soaking in a buffer containing 10 mM Tris-HCl (pH 8 at 23°C) and 0.1 mM EDTA followed by precipitation with ethanol.

3.2.3 Ribozyme Catalysis Assays

Ribozyme assays for all constructs were conducted under single-turnover conditions with ribozyme (400 nM) in excess over trace amounts (~2 nM) of [5′-^{32}P]-labeled substrate. Under these conditions the concentration of ribozyme exceeds the dissociation constant (K_d) for the enzyme-substrate complex, thereby saturating substrate with enzyme. Ribozyme and substrate RNA solutions in water were heated, separately, for 1 min at 90°C to disrupt folded structures that may have formed during storage. Following cooling to 23°C slowly, the ribozyme and substrate RNAs were preincubated separately for 15 min at 23°C in buffer containing 50 mM Tris-HCl (pH 7.5 at 23°C) and 20 mM $MgCl_2$ (except for Mg^{2+}-dependence and ligand-dependence studies) in the absence or presence of BDHP-PEG or BCPD-PEG. Ribozyme reactions were initiated by combing the preincubated mixtures. Several experiments were performed under irradiation of corresponding light (visible light for closed BDHP-PEG and UV light for open BCPD-PEG). Aliquots (4 μl) were removed at appropriate time intervals and quenched by the addition of a denaturing gel loading buffer (0.05% bromophenol blue, 0.05% xylene cyanol, 95% formamide, and 40 mM EDTA). Reaction products separated

by a 14% denaturing PAGE were visualized and quantitated using a PhosphoImager and ImageQuant software (Molecular Dynamics).

3.2.4 Kinetic Analysis

Initial observed rate constants (initial k_{obs}) for reactions were derived by plotting the fraction of cleaved RNA plotted against time. The initial k_{obs} was derived by determining the positive slope of the resulting line through the early stages of the reaction. Apparent dissociation constants (K_d) were established as the concentrations of ligand required to produce half maximum k_{obs}.

3.3 Results and Discussion

3.3.1 Design of Ribozyme Constructs

The hammerhead ribozyme consists of three stems that intersect at a conserved core and positions scissile phosphodiester linkage near the central core of conserved nucleotides (Figure 3-1) (Fedor and Uhlenbeck 1992). When correctly folded, the hammerhead ribozyme in the presence of divalent ions such as magnesium stimulates nearly complete cleavage of the phosphodiester chain at a defined internal site to give 2′, 3′-cyclic and 5′-hydroxy termini (Figure 3-2).

Figure 3-1 The secondary structure of the hammerhead ribozyme.

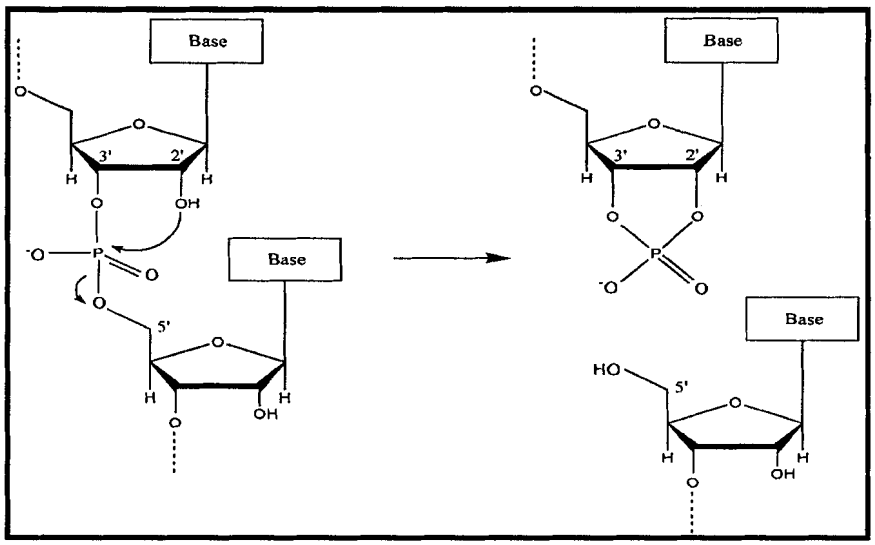

Figure 3-2 Mechanism of RNA cleavage of the hammerhead ribozyme by promoting an internal phosphorester transfer reaction.

For the sake of simplicity, all of the hammerhead ribozyme constructs designed in this study were derived from the structure shown in Figure 3-1, and therefore, it provided a comparison for the interpretation of the effects of added ligand. All our ribozyme constructs had the same catalytic domain that comprises stem I and III as the substrate recognition sites and the conserved central core of the hammerhead ribozyme. Stem II was replaced by an aptamer motif to function as the allosteric domain (Tang and Breaker 1997a), in this case, replaced by the C8 aptamer sequence and connected to the catalytic domain via previously reported communication modules. The placement of the allosteric domain on stem II was logical, because it was known that destabilization of stem II could dramatically reduce the catalytic rate of the ribozyme (Tuschl and Eckstein 1993; Long and Uhlenbeck 1994), and successful examples of allosteric hammerhead ribozymes reported to date had stem II modifications (Tang and Breaker 1997a; Soukup and Breaker 1999b). The incorporated C8 aptamer sequence was composed of either eleven or thirteen nucleotides and modified from the original aptamer structures by removing nucleotides

up to a loop or bulge region of the aptamer assuming the loop or bulge region in each secondary structure predicted by the RNA mfold program is essential for ligand-binding (Figure 3-3).

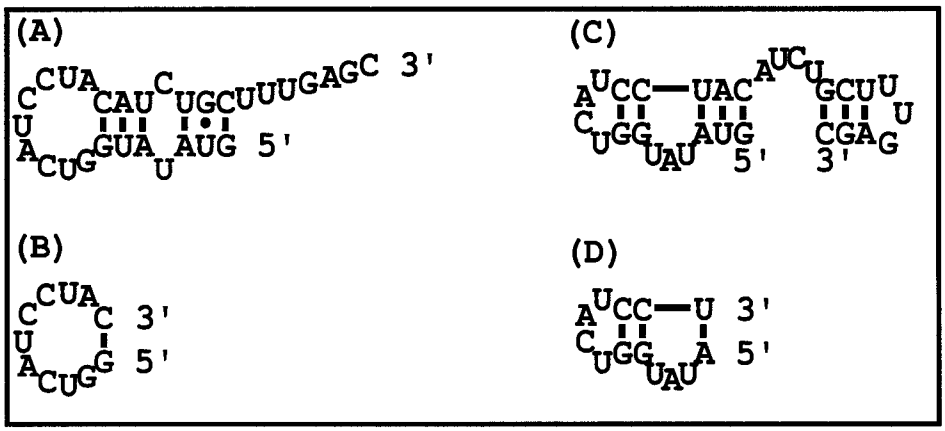

Figure 3-3 **Sequence and secondary structure models for minimum C8 aptamer. (A and C) The minimum C8 aptamer structures determined from the *in vitro* selection. (B and D) The modified minimum C8 aptamer structures incorporated in designing allosteric hammerhead ribozymes.**

The critical aspect in the modular rational design of allosteric ribozymes is that the correct functional folding of the ribozyme and the allosteric domain must be interdependent, and this interdependence can be achieved by incorporating a communication module as a stem II sequence between the two domains. Upon ligand binding, the aptamer should undergo adaptive binding to stabilize the weakened stem II region. Three different previously reported communication module sequences were incorporated for designing an allosteric hammerhead ribozyme. The first of these sequences involved the disabling of the stem II region in the absence of ligand by utilizing a single G·U wobble base pair as the bridging sequence between the catalytic and allosteric domains (Figure 3-4a, b). As full catalytic activity of hammerhead ribozymes is dependent on a structurally stable stem II as mentioned previously, this design anticipates that ligand binding will stabilize the weakened stem II element and

initiate catalytic activity of the ribozyme. A second class of ribozyme constructs involved the slip-structure mechanism of FMN-activated allosteric hammerhead ribozymes (Soukup and Breaker 1999b), in which ligand binding affects localized base-pairing changes that are untimately responsible for modulating ribozyme activity. Furthermore, this slip-strucuture element was demonstrated to act in a modular designing to convey occupation status of an adjacent aptamer domain regardless of its sequence or ligand specificity by simply swapping an FMN aptamer domain with an ATP or theophylline aptamer domain (Soukup and Breaker 1999b). This second class of ribozyme constructs is shown in Figure 3-4c, and 3-4d. The third class of ribozyme constructs involved a 'cm^{+}theo6' communication module (Kertsburg and Soukup 2002) of theophylline activated allosteric HDV ribozymes as their bridging sequences (Figure 3-4e, f). This communication module requires certain base-pair identities flanking the unpaired nucleotide, and consequently, base stacking interactions play a crucial role in communication module structure and function. As previously mentioned using the slip-structure element, cm^{+}theo6 demonstrated an ability to deliver effector-dependent function to the HDV ribozyme, when the theophylline-binding domain is replaced with a domain that binds FMN or ATP. Also, surprisingly, cm^{+}theo6 functioned similarly to deliver theophylline-, FMN-, or ATP- dependent function upon to hammerhead ribozymes. The function of the FMN- and ATP-dependent hammerhead ribozyme demonstrated interdependent structural organization of the communication module, as the module was effective in contexts totally different from that of the theophylline-dependent HDV ribozme. In the next section, these constructs were tested for BDHP-PEG dependent catalytic activity of the hammerhead ribozymes.

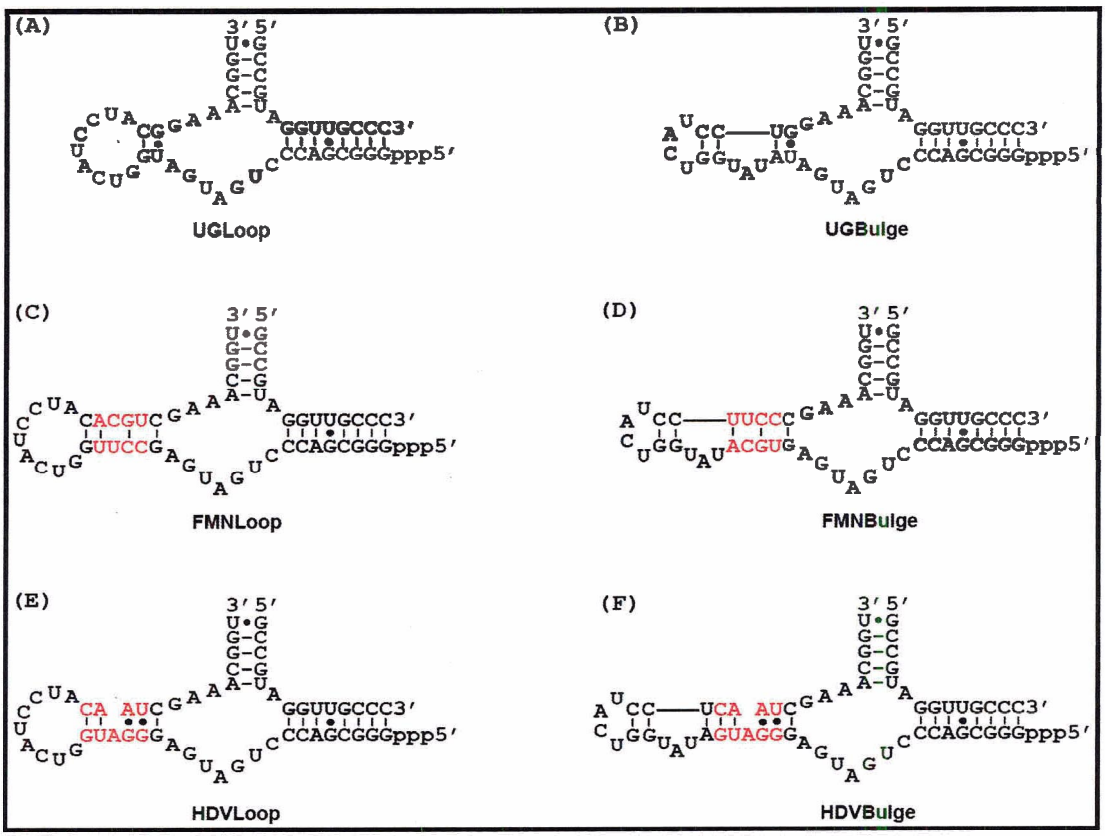

Figure 3-4 **Sequence design of ribozyme constructs. The nucleotides in red are three previously determined communication module sequences incorporated into the ribozyme constructs.**

3.3.2 Testing Ribozyme Constructs

Each designed allosteric ribozyme construct was tested under single-turnover conditions for overnight (16 hrs) at room temperature in the absence of closed BDHP-PEG and magnesium, which were necessary component for the ribozyme to catalyze its substrate cleavage reaction, and in the absence or presence of closed BDHP-PEG with the presence of 20 mM Mg^{2+} in order to identify the construct that showed ligand-responsive modulation of the ribozyme cleavage activity (Figure 3-5).

As predicted, in the absence of both closed BDHP-PEG and magnesium, none of the constructs showed substrate cleavage activity. The FMNLoop and FMNBulge constructs carrying the communication module from FMN-dependent allosteric

hammerhead ribozymes showed no ligand-dependent modulation of the ribozyme cleavage activity. This might be due to having too many stable Watson-Crick base pairs that might create a pre-stablized stem II region in the absence of the ligand. The FMNBulge construct showed higher cleavage activity than that of the FMNLoop construct, perhaps due to carrying an additional C-G base pair (Figure 3-6). This result suggested that even small increases in the stability could dramatically improve catalytic function.

The HDVLoop and HDVBulge constructs carrying the communication module derived from theophylline-dependent allosteric HDV ribozymes also showed no ligand-dependent modulation of the ribozyme cleavage activity. The cleavage activity was approximately 2% in both constructs, and these values were considerably lower than other constructs (Figure 3-6). The possible reason for the low cleavage activity was incorrect base stacking interactions of the unpaired adenosine, since this unpaired nucleotide plays crucial role in stabilizing communication module in the presence of ligand and in maximizing the ligand-mediated rate enhancement (Kertsburg and Soukup 2002).

The UGLoop and UGBulge constructs carried a single G·U wobble base pair as a bridging element. Constructing the constructs with a single G·U wobble base pair as the bridging element was based on an important assumption. Weakening of stem II should slow the rate of uninduced RNA cleavage compared to carrying additional Watson-Crick base pairs. G·U wobble base pairing is thermodynamically less stable than the G-C pair (Serra and Turner 1995), and therefore, is expected to be more dependent upon neighboring structural elements for its formation and ribozyme catalysis. The UGLoop

construct showed closed BDHP-PEG-dependent modulation of the ribozyme cleavage activity with approximately 40% cleavage activity in the presence of closed BDHP-PEG and 3% cleavage activity in the absence of closed BDHP-PEG (Figure 3-6). Therefore, the UGLoop construct demonstrated significant closed BDHP-PEG induced substrate cleavage with approximately a 13-fold increase in activity and demonstrated that the loop structure was the correct aptamer-folding pattern. The UGBulge construct did not show ligand-dependent modulation of the ribozyme cleavage activity (Figure 3-6). This meant that the folded structure with the internal bulge was the incorrect aptamer folding pattern, and consequently, two C-G base pairs in the aptamer domain simply acted as additional base pairs to stabilize the stem II region.

The UGLoop construct was used for further characterization of the rationally designed allosteric ribozyme. To make sure that the closed form of the compound was sustained for the duration of overnight reaction, absorbance changes of closed BDHP-PEG at 0 and 16 hours were measured. As Figure 3-7 shows, the absorbance at 0 and 16 hours were virtually the same, and the compound maintained its stable closed state during the reaction.

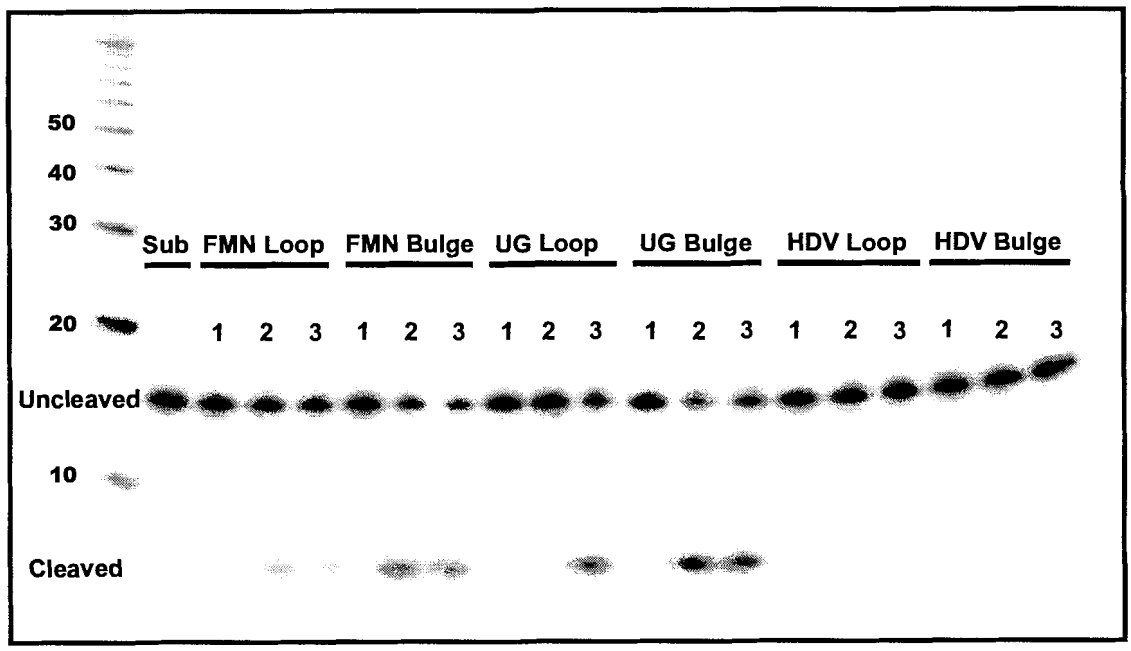

Figure 3-5 Testing the six rationally designed allosteric hammerhead ribozyme constructs for ligand-dependent modulation of ribozyme activity under single turnover reactions at room temperature. 'Sub' represents the reaction containing only substrate and no ribozymes. In each construct, lane 1 represents the absence of Mg^{2+} in the reaction, lane 2 represents the absence of BDHP-PEG and the presence of 20 mM Mg^{2+} in the reaction, and lane 3 represents the presence of 1mM BDHP-PEG and 20 mM Mg^{2+} in the reaction.

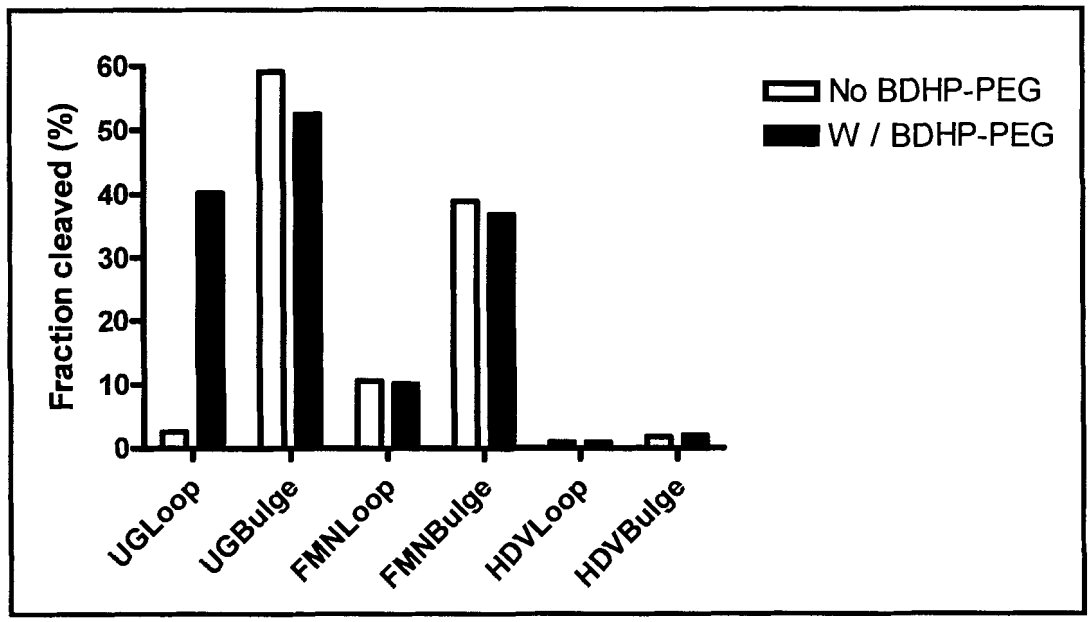

Figure 3-6 The fraction of RNA substrate cleaved in the absence and presence of 1mM BDHP-PEG for each construct tested.

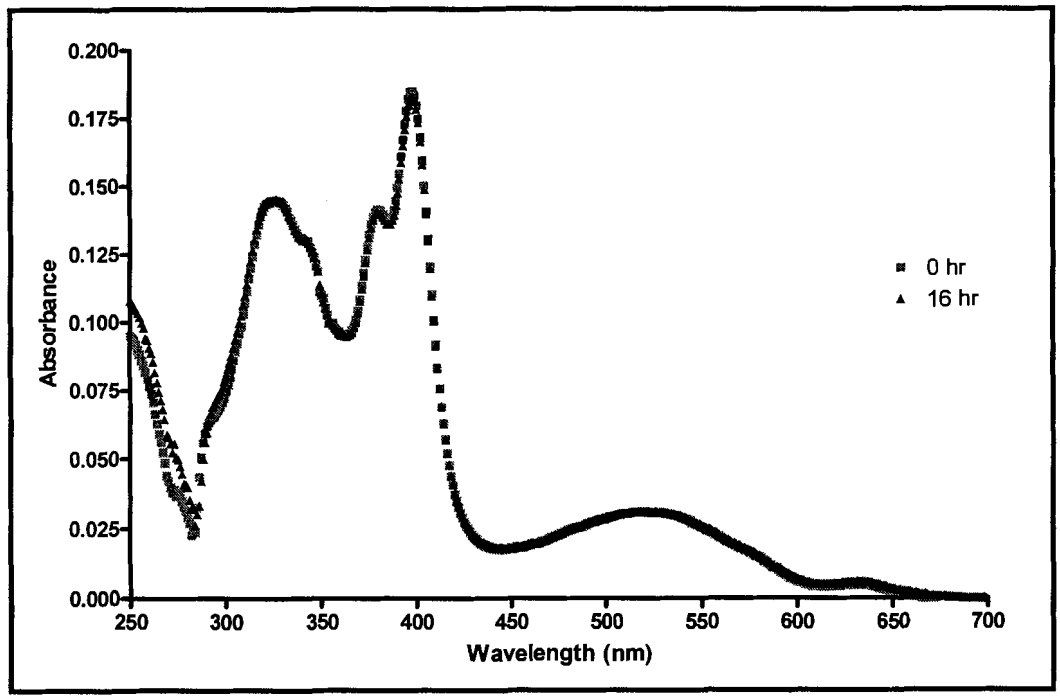

Figure 3-7 Spectroscopic monitoring of ligand at closed state by measuring absorbance changes of BDHP-PEG at 0 (grey) and 16 (black) hours.

3.3.3 Ligand binding and Allosteric Performance

In previous allosteric ribozyme studies, it was demonstrated that effector concentrations are important on the activities of allosteric ribozymes (Tang and Breaker 1997a; Soukup *et al.* 2000). From those studies, it was discovered that the functional dissociation constants (K_d) for their cognate ligands determined by various engineered hammerhead ribozymes were usually larger than the K_d values for those ligands determined by only the aptamer motifs. The reduction in affinity of aptamer against its ligand in the context of the engineered allosteric ribozymes is perhaps due to the lack of structural pre-organization of the aptamer domain in the engineered allosteric ribozymes (Soukup and Breaker 1999a; Soukup *et al.* 2000).

The functional dissociation constant for closed BDHP-PEG or open BCPD-PEG binding to the allosteric ribozyme was determined using UGLoop construct under single-

turnover reactions at room temperature for 8 hrs. In order to determine how active the ribozyme is in a physiological condition, 1 mM Mg^{2+} was included in the reaction. Figure 3-8 shows the activity curve obtained with each concentration of closed BDHP-PEG or open BCPD-PEG in the presence of 1 mM physiological Mg^{2+} concentration by plotting a semi-log plot of the initial observed rate constants (0-90 min) for the allosteric ribozyme obtained in the presence of various concentrations of the ligand. Sigmoidal curves were formed in both cases, although it was not possible to determine the saturated initial k_{obs} for the BCPD-PEG dependence, because 1 mM of closed BCPD-PEG was the highest concentration tested. Activation of the ribozyme by closed BDHP-PEG or open BCPD-PEG reached a maximum as the added ligand concentration increased indicating that the ligand saturated its binding site, and specific ligand binding enhanced the catalytic activity of the ribozyme. The functional K_d values were estimated by determining the ligand concentration that produced a half maximal rate constant (½ k_{max}), and these concentrations were determined to be 12 μM for closed BDHP-PEG and 160 μM for open BCPD-PEG according to EC_{50} values, which are the concentrations required to get a response halfway between the minimum and maximum (obtained using GraphPad Prism 4 software). As expected, these binding constants were approximately four- and eight-fold higher than the binding constants previously estabilished for the C8 aptamer alone against closed BDHP-PEG and open BCPD-PEG respectively, because both the ribozyme and aptamer domains shared the weakened G·U wobble stem II. For further characterization of the UGLoop ribozyme, 10 μM of closed BDHP-PEG or open BCPD-PEG was used in further experiments to activate the ribozyme only in the presence of closed BDHP-PEG and remain inactive in the presence of open BCPD-PEG.

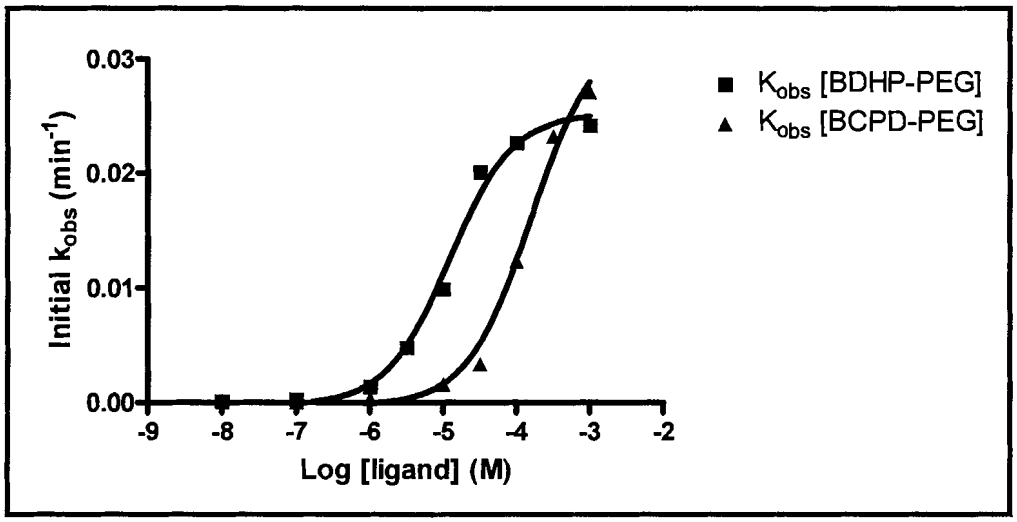

Figure 3-8 **Dependence of the initial observed rate constants of UGLoop ribozyme activity on ligand concentration. Single turnover reactions were performed in the presence of 1 mM Mg^{2+} at room temperature.**

3.3.4 Catalytic Rate Constants for On and Off States of UGLoop Allosteric Ribozyme

The RNA-cleaving activities of UGLoop allosteric hammerhead ribozyme were measured in the presence of either 10 μM closed BDHP-PEG or open BCPD-PEG for 8 hrs under single-turnover conditions including 20 mM Mg^{2+} and room temperature. As shown in Figure 3-9 and Table 3-1, initial k_{obs} (0-45 min) for the ribozyme in the presence of closed BDHP-PEG was determined to be 0.53 min^{-1}, whereas k_{obs} for the ribozyme in the presence of open BCPD-PEG was determined to be 0.00059 min^{-1}. This represents a rate enhancement of about 900-fold upon the addition of closed BDHP-PEG.

This high initial k_{obs} in the presence of closed form of the compound was very surprising because other similarly designed allosteric hammerhead ribozymes that had a U·G wobble base pair as a bridging sequence (H10, H12, H13, H14, and Hstab2 in Table 3-2) previously showed relatively low initial catalytic rate constants and low rate enhancements upon addition of effector molecules. It is difficult to obtain very high

catalytic rate constants of allosteric ribozymes by only using modular rational design (Soukup *et al.* 2000). Several recent studies demonstrated that allosteric ribozymes could be made to approach their maximum rate enhancement when allosterically activated. For example, the hammerhead ribozyme has been made to respond with maximum possible k_{obs} values (~1 min^{-1}) to Co^{2+} (Seetharaman *et al.* 2001), theophylline (Soukup *et al.* 2000), and cGMP and cAMP (Koizumi *et al.* 1999). However, these results were obtained by the combination of modular rational design and *in vitro* selection for the creation of the allosteric ribozymes that exhibited maximum catalytic activity for application purposes.

Last two allosteric ribozymes listed in Table 3-1 were theophylline-activated allosteric hammerhead ribozymes isolated from a population of 10^6 RNA molecules, each of which carried the theophylline aptamer and hammerhead ribozyme motifs adjoining through a random sequence region (Soukup *et al.* 2000). Populations of theophylline-dependent ribozymes were isolated by selection against self-cleavage in the absence of effector and selection for self-cleavage in the presence of effector. These two ribozymes were particularly interesting, because the communication module in each ribozyme included a single G·U wobble base pair, two Watson-Crick base pairs, and two mismatched base pairs, and each ribozyme was activated 1300 or 3300-fold by theophylline binding under *in vitro* selection conditions, where k_{obs} in the presence of effector was approximately 1 min^{-1}. The UGLoop ribozyme also had a single G·U wobble base pair, but only one Watson-Crick base pair as the bridging sequence. Therefore, the three ribozymes were roughly comparable to each other according to the number of base pairs formed in each communication module region. The 900-fold rate enhancement and

active rate constant of 0.53 min^{-1} were certainly achievable only via modular rational design as demonstrated in this study if the stabilization of the weakened bridging sequence was effectively modulated by adaptive binding of ligand to its binding site.

To avoid false-positive activation of allosteric ribozymes, the rate constant for catalytic activity in the absence of effector must be significantly lower than the active k_{obs} value. It is unlikely for allosteric constructs to exhibit an inactive k_{obs} value that is less than the rate constant for the uncatalyzed reaction. Allosteric hammerhead ribozymes typically have an inactive k_{obs} value that is not lower than approximately 10^{-8} min^{-1} under normal assay conditions, which corresponds to the uncatalyzed rate of RNA transesterification at neutral pH and 23°C (Li and Breaker 1999). The values for inactive k_{obs} of many allosteric hammerhead ribozymes range from approximately 10^{-2} min^{-1} to 10^{-4} min^{-1} (Koizumi *et al.* 1999; Soukup *et al.* 2000). Therefore, the inactive rate constant of 5.9×10^{-4} min^{-1} for the UGLoop ribozyme in the presence of open BCPD-PEG fell into this category.

Several control experiments have been performed in various conditions for 8 hrs under single-turnover conditions at room temperature to further investigate the activation and inactivation of the UGLoop ribozyme (Figure 3-10). In the absence of Mg^{2+}, light, and compound (lane 1), the catalytic activity of the ribozyme was inactivated because magnesium ions were needed for the hammerhead ribozyme catalytic activity, and closed form of the compound was needed to allosterically activate the ribozyme. In the absence of light and compound and in the presence of Mg^{2+} (lane 2), the ribozyme was still inactive, since closed form of the compound was absent to activate the ribozyme. In the absence of compound and in the presence of Mg^{2+} and light (lane 3 and 4), the ribozyme

remained inactive because closed form of the compound was absent to activate the ribozyme. When finally closed form of the compound was present, the catalytic activity of the ribozyme was activated (lane 6 and 8). However, if open form of the compound was present, the ribozyme remained inactive (lane 5 and 7). The irradiation of either UV for closed form or visible light for open form of the compound did not influence the catalytic activity of the ribozyme as long as closed form of the compound was maintained to activate the ribozyme, and open form of the compound was maintained to inactivate the ribozyme (lane 5 to 8). These results indicated that closed and open form of the compound sustained their forms for duration of the experiment. In addition, a derivative of the UGLoop ribozyme, UGBulge, which acted like a wild-type hammerhead ribozyme with the incorrect aptamer domain for closed form of the compound (Figure 3-4, and 3-5), was used to determine if open form of the compound acted as an inhibitor against the catalytic activity of the UGLoop ribozyme. As shown in Figure 3-5, the UGBulge ribozyme was active both in the absence and presence of closed form compound. If open form of the compound acted as the inhibitor, the UGBulge ribozyme should be inactivated in the presence of open form of the compound. However, the UGBulge ribozyme remained active even in the presence of open form of the compound (lane 10). This ribozyme was only inactive without the presence of Mg^{2+}. Therefore, open form of the compound did not act as an inhibitor of the UGLoop ribozyme.

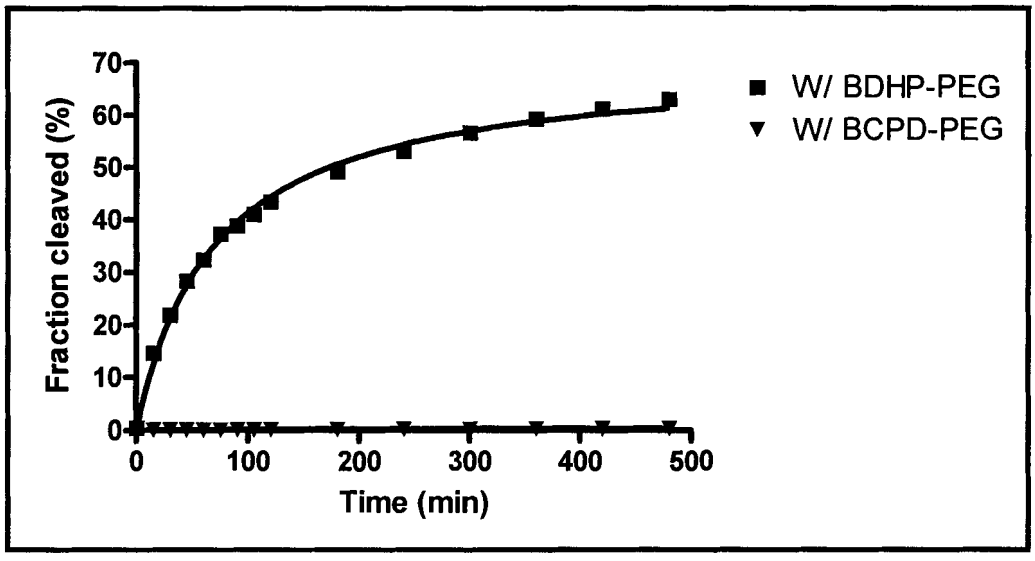

Figure 3-9 Time course of RNA cleavage activity of UGLoop construct in the presence of 10 μM BDHP-PEG or BCPD-PEG to determine catalytic rate constants for on and off states of the UGLoop allosteric ribozyme. Single turnover reactions were performed in the presence of 20 mM Mg^{2+} at room temperature.

Table 3-1 Active and inactive catalytic rate constants of UGLoop and previously studied allosteric hammerhead ribozymes. k_{obs} of active states of the ribozymes were initial k_{obs} for catalytic cleavage in the presence of corresponding ligand. k_{obs} of inactive states of the ribozymes were determined in the absence of corresponding ligand. k_{obs} of active state of the UGLoop ribozyme was initial k_{obs} for catalytic cleavage in the presence of 10 μM BDHP-PEG. k_{obs} of inactive state of the UGLoop ribozyme was determined in the presence of 10 μM BCPD-PEG. Fold activation is calculated by dividing k_{obs} of active states by k_{obs} of inactive states.

	k_{obs} (min^{-1})				
Construct Name	On	Off	Fold activation	Effector specificity	References
UGLoop	5.3×10^{-1}	5.9×10^{-4}	898	BDHP-PEG	
H10	3.0×10^{-3}	9.2×10^{-5}	33	FMN	Soukup et al. 1999a
H12	2.0×10^{-2}	2.0×10^{-2}	0	FMN	Soukup et al. 1999a
H13	3.0×10^{-2}	1.5×10^{-3}	20	FMN	Soukup et al. 1999a
H14	2.0×10^{-2}	5.0×10^{-4}	40	Theophylline	Soukup et al. 1999a
Hstab2	1.1×10^{-2}	3.6×10^{-3}	3	Argininamide	Wang et al. 2002
cm+theo3	5.2×10^{-1}	4.1×10^{-4}	1300	Theophylline	Soukup et al. 2000
cm+theo4	9.0×10^{-1}	2.7×10^{-4}	3300	FMN	Soukup et al. 2000

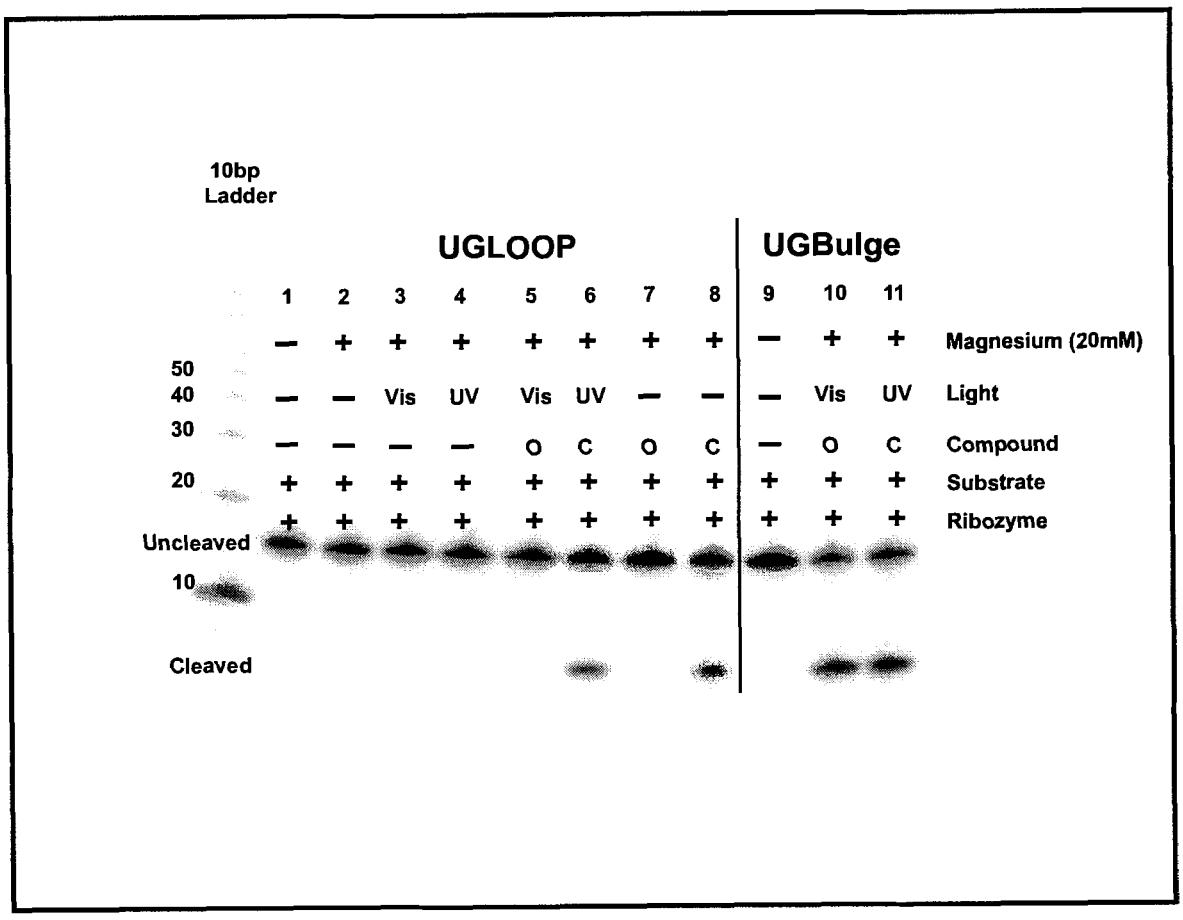

Figure 3-10 Control experiments of UGLoop and UGBulge ribozymes in various single-turnover conditions. Vis represents visible light. UV represents UV light. O represents open form of the compound. C represents closed form of the compound.

3.3.5 Magnesium Dependence on Allosteric Response

The rate constant for catalytic activity of an enzyme may change significantly under different experimental conditions, and it is possible that a change in the degree of allosteric response may also change with different experimental conditions. Here, the effect of magnesium concentration on UGLoop allosteric hammerhead ribozymes was studied. The RNA-cleaving activities of UGLoop allosteric hammerhead ribozyme were measured in the presence of either 10 μM closed BDHP-PEG or open BCPD-PEG for 8 hrs under single-turnover conditions at room temperature with various concentrations of magnesium (Figure 3-11a). To determine initial k_{obs} at Mg^{2+} concentrations less than 10 mM, data points between 0 min and 90 min were used, and data points between 0 min and 30 min were used to determine initial k_{obs} at Mg^{2+} concentrations greater than 10 mM. Shorter time period data sets were used at high Mg^{2+} concentrations, because the initial cleavage rate was significantly faster at these concentrations to obtain linear initial cleavage rate slopes. Figure 3-11b shows that the magnesium concentration in the reaction can affect the degree of the allosteric response. At Mg^{2+} concentrations less than 20 mM, the cleavage rate in the presence of closed BDHP-PEG continued to rise linearly. However, at greater than 20 mM Mg^{2+} concentrations, the cleavage rate in the presence of closed BDHP-PEG began to level off. Therefore, a decrease in the extent of the ribozyme activation at high magnesium concentrations was observed. The cleavage rate in the presence of open BCPD-PEG was determined only in 20 and 30 mM Mg^{2+} concentrations, because if the inhibition of catalytic RNA cleavage of the ribozyme in the presence of open BCPD-PEG was maintained at high Mg^{2+} concentrations, there was no need to determine the cleavage rate at low Mg^{2+} concentrations. Indeed, the cleavage rate

in the presence of open BCPD-PEG was determined to be negligible even at high Mg^{2+} concentrations compared to the cleavage rate in the presence of closed BDHP-PEG.

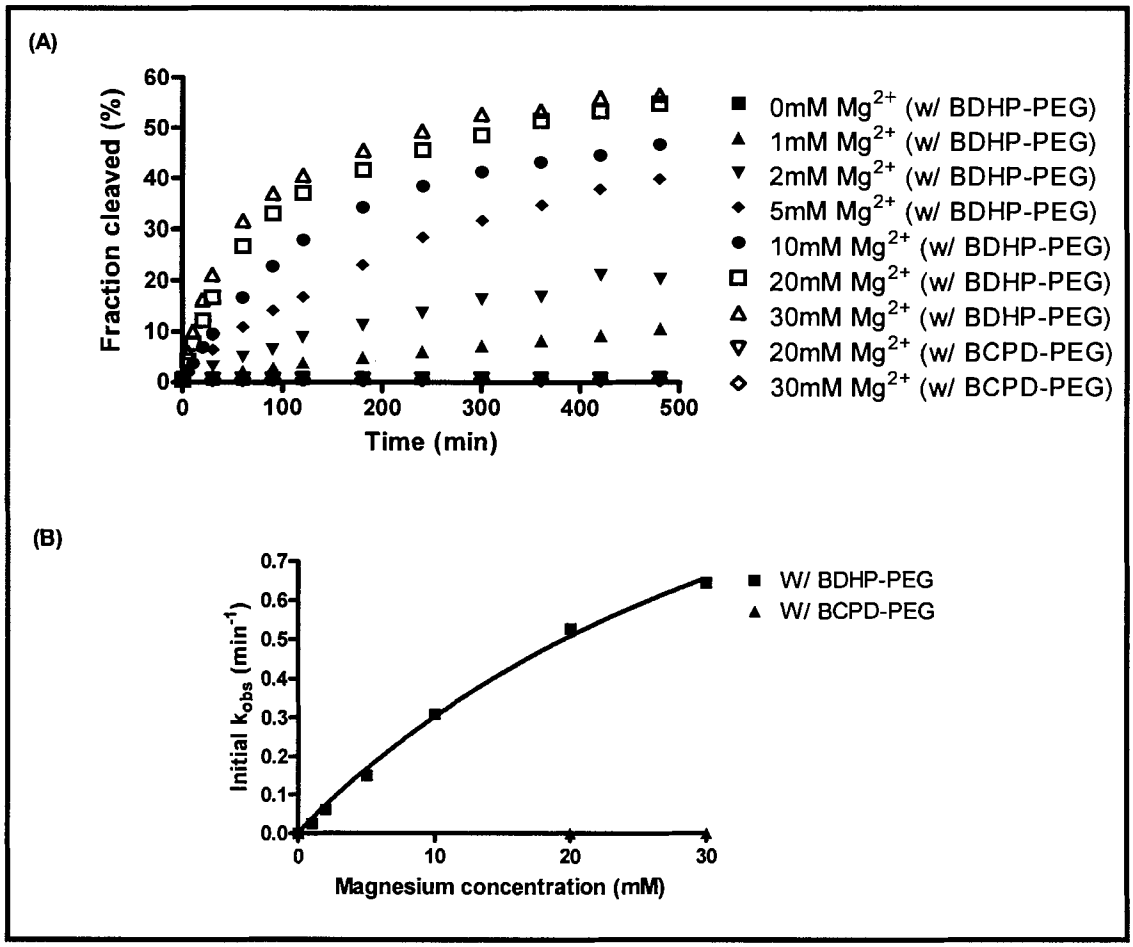

Figure 3-11 Magnesium dependence of UGLoop allosteric hammerhead ribozyme. Single turnover reactions were performed with various concentrations of Mg^{2+} at room temperature. (A) Time course of RNA cleavage activity of UGLoop construct in the presence of 10 μM BDHP-PEG or BCPD-PEG with various concentrations of Mg^{2+}. (B) Dependence of the k_{obs} on Mg^{2+} concentration in the presence of 10 μM BDHP-PEG or BCPD-PEG.

3.3.6 Change of Cleavage Rates by a Change in the Irradiation Wavelength

Figure 3-12 demonstrates the real-time light-responsive switching activity of the UGLoop allosteric hammerhead ribozyme by a change in the irradiation wavelength of light. The ribozyme and its ^{32}P-labeled substrate were incubated in the presence of 10 μM closed BDHP-PEG and 20 mM Mg^{2+} at room temperature with continuous irradiation of 280-375 nm wavelength of UV light. Light of 280-375 nm wavelength was provided by a 312 nm hand-held UV lamp. The 312 nm hand-held UV lamp was used, even though a short UV light exposure with a 254 nm hand-held UV lamp, which roughly provides 250-275 nm wavelength of UV light, was normally used to effectively and readily change the compound in closed form, because RNA is damaged with a long exposure of 260 nm wavelength of UV light. Aliquots were taken from the reaction mixture at various time points. At 60 minutes into the reaction, the irradiation wavelength was switched to greater than 400 nm of visible light to change the conformation of the compound from closed to open form, which took approximately 10 minutes for almost 100% switching (Figure 3-13). Irradiation at this wavelength was maintained for another 60 minutes, and then the irradiation was switched back to 280-375 nm to change the conformation of the compound from open to closed form, which took approximately 30 minutes for almost 100% switching (Figure 3-14). Irradiation at this wavelength was maintained for another 60 minutes. Figure 3-10 shows that through the changes in the irradiation wavelength, the ribozyme clearly demonstrated the real-time light-responsive switching activity as expected. The ribozyme was activated with UV light irradiation and almost completely inactivated with visible light. In addition, the catalytic rate constant of the ribozyme between 0 and 60 minutes was 0.32 min^{-1}, and the catalytic rate constant of the ribozyme between 160 and 220 minutes was 0.21 min^{-1}. The catalytic rate was approximately 1.5-

fold slower between 160 and 220 minutes than that between 0 and 60 minutes, probably due to the transformation of the compound from open to closed form state. Therefore, the light-responsive transformations of the compound initiated switchable catalysis of the ribozyme.

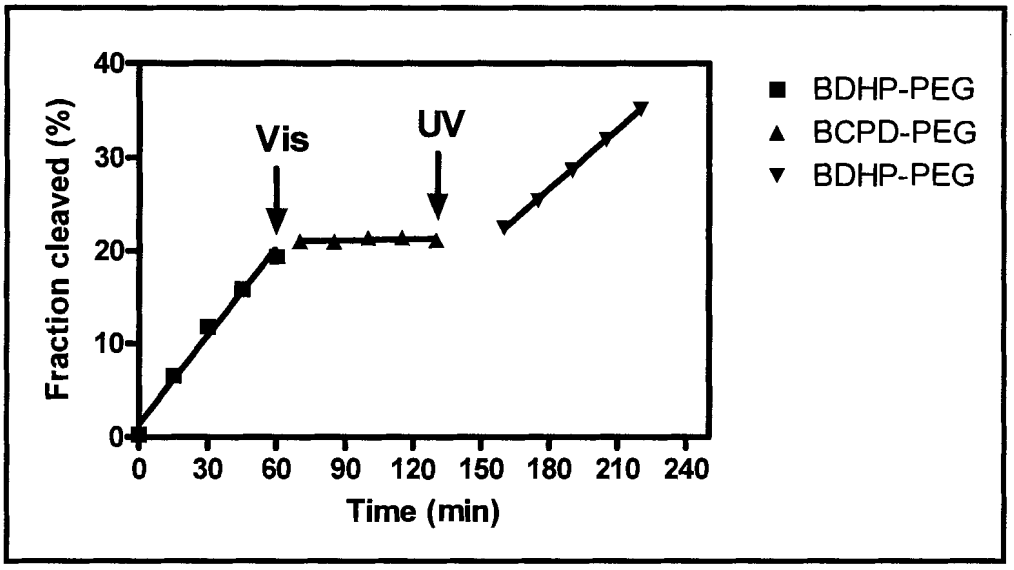

Figure 3-12 Real-time change of cleavage rates by a change in the irradiation wavelength to change initially from the closed form of the compound (10 μM) to the open form and finally back to the closed form again. Single turnover reactions were performed with 20 mM Mg^{2+} at room temperature. The arrows indicate the time points where a change in the irradiation wavelength occurs. The gaps between the lines represent the duration of the irradiation with chosen wavelength to convert one form of the compound to the other form.

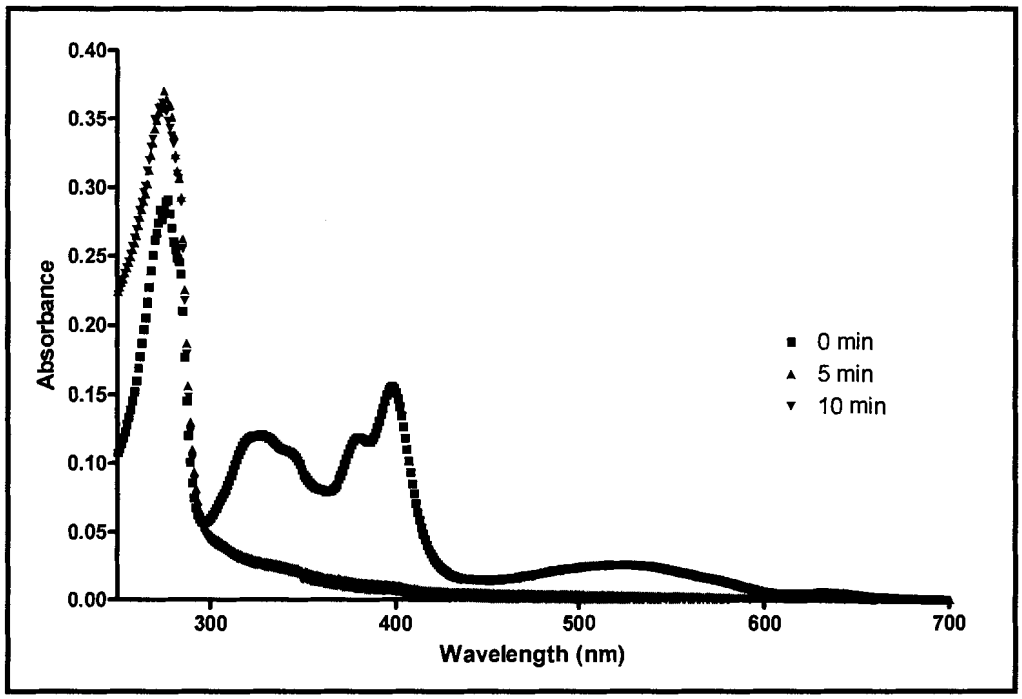

Figure 3-13 Spectroscopic monitoring of the transformations from BDHP-PEG to BCPD-PEG by measuring absorbance changes at 0, 5, and 10 minutes with irradiation of visible light. The concentration of the compound was 10 μM.

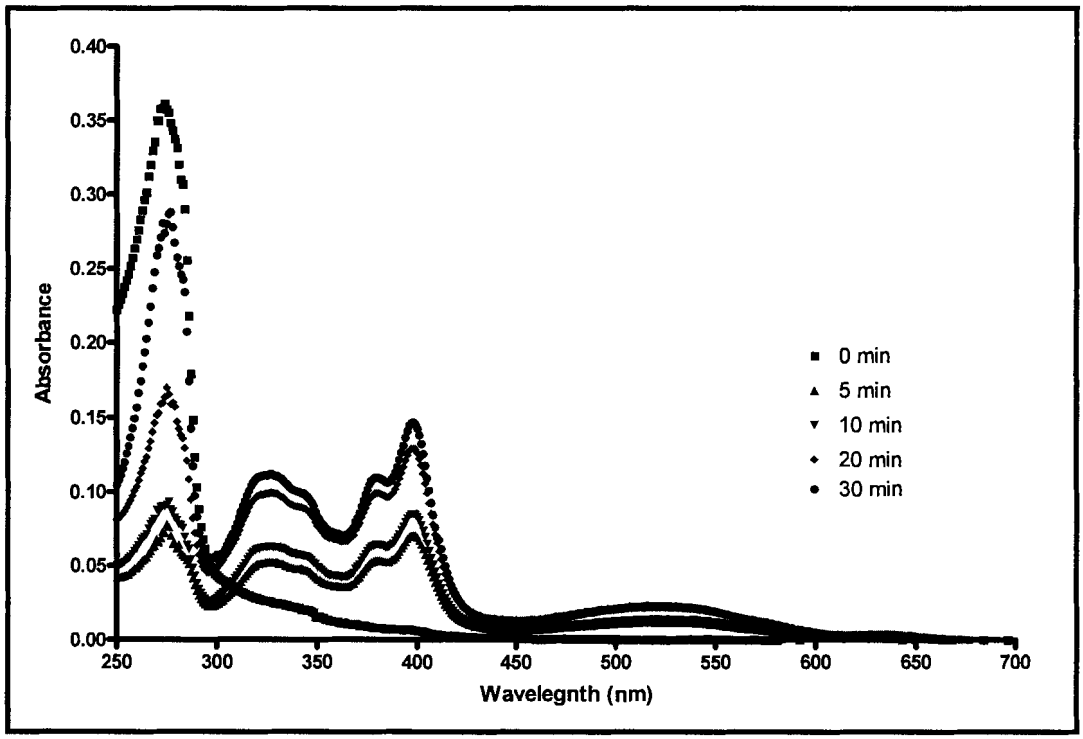

Figure 3-14 Spectroscopic monitoring of thetransformations from BCPD-PEG to BDHP-PEG by measuring absorbance changes at 0, 5, 10, 20, and 30 minutes with irradiation of UV light. The concentration of the compound was 10 μM.

3.4 Conclusion

Modular rational design of a light-responsive allosteric hammerhead ribozyme and the characterization of this ribozyme were described in this chapter. The rational designing of the allosteric ribozyme was performed by appending C8 aptamer sequences to *trans*-acting hammerhead ribozymes via previously studied communication module sequences. The UGLoop construct that had a loop-shape aptamer binding motif and a single G·U wobble base pair showed specific allosteric activation in the presence of closed BDHP-PEG and inactivation in the absence of closed BDHP-PEG with 13-fold increase in cleavage activity.

The functional dissociation constant for closed BDHP-PEG or open BCPD-PEG binding to the allosteric ribozyme was determined in the presence of 1 mM physiological

magnesium concentration by plotting a semi-log plot of the initial observed rate constants for the allosteric ribozyme obtained in the presence of various concentrations of the ligand. Sigmoidal curves were formed in both cases. The functional K_d values were estimated by determining the ligand concentration that produces a half maximal rate constant (½ k_{max}), and these concentrations were determined to be 12 μM for closed BDHP-PEG and 160 μM for open BCPD-PEG. These binding constants were approximately four- and eight-fold higher than the binding constants previously established for the C8 aptamer alone against closed BDHP-PEG and open BCPD-PEG respectively, because both the ribozyme and aptamer domains shared the weakened G·U wobble stem II.

The RNA-cleaving activities of the UGLoop allosteric hammerhead ribozyme were measured in the presence of 20 mM magnesium and either closed BDHP-PEG or open BCPD-PEG. The initial k_{obs} (0-45 min) for the ribozyme in the presence of closed BDHP-PEG was determined to be 0.53 min^{-1}, whereas k_{obs} for the ribozyme in the presence of open BCPD-PEG was determined to be 0.00059 min^{-1}. This represented a rate enhancement of about 900-fold upon the addition of closed BDHP-PEG. This high initial k_{obs} at in the presence of closed form of the compound was very surprising, because other similarly designed allosteric hammerhead ribozymes that had a U·G wobble base pair as a bridging sequence previously showed relatively low initial catalytic rate constants and low rate enhancements upon addition of effector molecules. Such high rate enhancements were generally observed from previous studies by the combination of modular rational design and *in vitro* selection for the creation of allosteric ribozymes that exhibited maximum catalytic activity for therapeutic application purposes (Soukup *et al.*

2000). Therefore, this study demonstrated for the first time to date that such a high rate enhancement was achievable only via modular rational design, if the stabilization of weakened bridging element was effectively modulated by adaptive binding of ligand to its binding site.

The effect of magnesium concentration on the UGLoop allosteric hammerhead ribozyme was also studied. At Mg^{2+} concentrations less than 20 mM, the cleavage rate in the presence of closed BDHP-PEG continued to rise linearly. However, at greater than 20 mM Mg^{2+} concentrations, the cleavage rate in the presence of closed BDHP-PEG began to level off. Therefore, a decrease in the extent of the ribozyme activation at high magnesium concentrations was observed. The cleavage rate in the presence of open BCPD-PEG to inactivate the cleavage activity was determined to be negligible, even at high Mg^{2+} concentrations compared to the cleavage rate in the presence of closed BDHP-PEG.

Finally, the light-responsive switching activity of the UGLoop allosteric hammerhead ribozyme by a change in the irradiation wavelength of light was determined to demonstrate how effectively the ribozyme was turned on and off by merely changing the irradiation wavelength of light. As expected, the ribozyme clearly demonstrated light-responsive switching activity by showing that the ribozyme was activated with UV light irradiation and almost completely inactivated with visible light. Therefore, the light-responsive transformations of the compound clearly induced switchable catalysis of the ribozyme.

The next chapter summaries all the key findings of this research, and describes its potential applications for the control of gene expression.

CHAPTER 4:
CONCLUSION

4.1 Summary of Results

The goal of my research was to demonstrate the light-responsive allosteric hammerhead ribozyme that was rationally designed by incorporating a RNA aptamer, which bound and distinguished different forms of the light-responsive dihydropyrene-cyclophanediene system, into the hammerhead ribozyme and its possible use as a light-induced gene expression controlling tool.

In vitro selection techniques and numerous discoveries and development of natural and synthetic ribozymes gave us ideas to develop the light-responsive allosteric hammerhead ribozyme. In the first part of the thesis, *in vitro* selection was performed to isolate RNA aptamers that recognized and bound either closed or open form of the compound. Subsequent characterization of the isolated RNA aptamers showed that these aptamers were able to discriminate different light-responsive forms of the compound in various degrees with irradiation of different wavelength of light. Among these isolated aptamers, the C8 aptamer, which bound to the closed form of the compound showed the best affinity and specificity with the low micromolar K_d, and was able to discriminate its isomeric open form of the compound with approximately a seven-fold lower binding affinity. This aptamer was the only aptamer that recognized light-responsive transformations of a photochromic compound to date and perhaps employs only base-stacking interactions to specifically recognize the compound instead of recognizing its

ligand by usual hydrogen bonding. The minimum ligand binding domain of C8 aptamer was also determined by boundary analysis and truncation experiments, and the minimum aptamer motif was able to discriminate two different isomers of the compound by showing high binding affinity to the closed form of the compound and low binding affinity to the open form of the compound. This isolated C8 aptamer that recognized and distinguished different conformational forms of the photochromic compound was incorporated into the hammerhead ribozyme to rationally design a light-responsive allosteric ribozyme. By testing several different rationally designed constructs for their activation in the presence of the closed form compound, the UGLoop construct that had a loop-shape aptamer binding motif and a single G·U wobble base-pair as a communication module showed the best specific allosteric activation in the presence of closed form of the compound and inactivation in the absence of closed form of the compound.

The study for determining the functional dissociation constants of the ribozyme binding to closed or open form of the compound showed that the functional K_d value was determined to be sixteen-fold smaller for the closed form of the compound compared to the apparent K_d value for the open form of the compound. These binding constants were approximately four- and eight-fold higher than the binding constants previously estabilished for the C8 aptamer alone against closed and open form of the compound respectively, because both the ribozyme and aptamer domains shared the weakened G·U wobble stem II.

The study of initial observed rate constants illustrated that the initial k_{obs} for the ribozyme in the presence of closed form of the compound and 20 mM Mg^{2+} was determined to be close to the maximum catalytic constant of the natural hammerhead

ribozyme at 1 mM physiological magnesium concentration with a rate of about 1 min^{-1}. However, k_{obs} for the ribozyme in the presence of open form of the compound was determined to be virtually negligible. This represented a rate enhancement of nearly thousand-fold upon the addition of the closed form of the compound. This initial high k_{obs} at active state was very surprising and unique, because other similarly designed allosteric hammerhead ribozymes that had a U·G wobble base pair as a bridging sequence previously showed relatively low initial catalytic rate constants and low rate enhancements upon addition of effector molecules. Such high rate enhancements were generally observed from previous studies by the combination of modular rational design and *in vitro* selection. Therefore, this study demonstrated for the first time that such a high rate enhancement was achievable only via modular rational design, if the stabilization of weakened bridging element was effectively modulated by adaptive binding of ligand to its binding site.

The study to illustrate how effectively the ribozyme was activated and inhibited by changing the irradiation wavelength of light in the presence of the compound clearly demonstrated light-responsive switching activity of the ribozyme with UV light-induced activation and almost complete visible light-induced inactivation. Therefore, the light-responsive transformations of the compound clearly induced switchable catalysis of the ribozyme.

4.2 Implications for the Control of Gene Expression

The ability to activate or inhibit the expression of a specific gene is the most important for the analysis of gene function and the manipulation of gene expression with precise temporal and spatial control is of great interest to control biological systems at the molecular level. It is now relatively easy to inhibit expression of a specific gene by using simple and precise knockout tools such as RNA interference (RNAi), RNA aptamer, and ribozyme technologies that function at the mRNA level (Akashi *et al.* 2005; Werstunk and Green 1998).

RNAi has been used as a powerful tool for gene silencing in recent years. RNAi is an RNA-dependent gene silencing mechanism that is mediated by the same cellular machinery that processes microRNA, known as the RNA-induced silencing complex (RISC) (Bernstein *et al.* 2001). The process is initiated by the ribonuclease protein Dicer, which binds and cleaves exogenous double-stranded RNA molecules to produce double-stranded fragments of 20-25 base pairs with few unpaired overhang nucleotides on each end. These short double-stranded fragments are called small interfering RNAs (siRNAs), and they are separated, and incorporated into the RISC (Vermeulen *et al.* 2005). The siRNA-RISC complex recognizes and cleaves the target mRNA in a sequence specific manner (Nykanen *et al.* 2001). RNAi has been applied as an experimental tool to study the unknown function of genes in organisms such as *C. elegans* and *D. melanogaster* (Dzitoyeva et al. 2003; Fortunato and Fraser 2005). Double-stranded RNA for a gene of interest is introduced into a cell or organism, and RNAi causes significant reduction in expression of the protein the gene codes for. Determining the effects of this reduction allows to identify the protein's role and function. Also, RNAi has potential for

therapeutic purposes according to recent studies that demonstrated the proposed clinical uses of RNAi to silence hepatitis A and B virus infection by siRNAs (Kusov *et al.* 2006; Jia *et al.* 2006). Therefore, RNAi can be used effectively to silence expression of a specific gene.

RNA aptamers and ribozymes have also been shown in previous studies to effectively inhibit expression of a specific gene at the mRNA level. Recently, it was shown that insertion of a small molecule aptamer into the 5′ untranslated region of a messenger RNA allowed its mRNA translation to be inhibited by addition of certain dye compounds, which were nontoxic and cell-permeable *in vitro* as well as in mammalian cells (Werstunk and Green 1998). Also, hairpin ribozymes were designed to disrupt hepatitis-B virus replication in a recent study by targeting the specific mRNAs encoding the polymerase, and transduction of vectors containing the ribozymes into liver cells inhibited the replication significantly (Welch *et al.* 1997). Similarly, allosteric ribozymes can be fused to mRNAs so that when corresponding effector molecule was added to the cell, the ribozyme domain initiates its catalytic activity. Therefore, allosteric ribozymes can be used to either activate or inhibit translation, and ultimately the expression of a target gene.

As previously mentioned, the hammerhead ribozyme has been engineered to cleave any chosen RNA by an intermolecular attack in *trans*-acting (Haseloff and Gerlach 1992; Uhlenbeck 1987). This has been accomplished by modifying the substrate-recognition arms of the ribozyme. The *trans*-acting ribozyme can bind to the substrate RNA molecule through recognition arms that are complementary the target sequence. The ability to change sequences of the substrate binding arms has allowed the extensive

use of hammerhead ribozymes as gene control tools and potential therapeutic agents. The advantages of using hammerhead ribozymes include easy modification and synthesis of the ribozymes, and regulating target mRNAs in a highly sequence specific manner (Rossi and Sarver 1990). However, the cleavage activities of ribozymes *in vitro* are generally more effective than that of ribozymes in the cellular environment. Therefore, many parameters must be considered and many modifications and improvements are required in the ribozyme expression system as well as methods for introducing ribozymes into cells. There are two main aspects of the ribozyme expression system that are crucial for optimal *in vivo* cleavage activities of hammerhead ribozymes. These are high expression levels of the ribozymes, efficient delivery of the ribozymes to the cell.

RNA polymerase III promoters are mainly used in the transcription of short RNAs, particularly for the expression of ribozymes (Geiduschek and Tocchini-Valentini 1988). RNA polymerase II promoters were also widely used for the expression of ribozymes. In RNA polymerase II expression system, the cap structure and the poly(A) tail are automatically added at the 5′ and 3′ ends of the transcripts respectively. Thus, transcripts are protected from degradation by exonucleases and exported from the nucleus to the cytoplasm, just like an mRNA (Rossi 1995). However, RNA polymerase II expression system is generally appropriate for transcribing several hundred or several thousand base long RNAs, and it may not be suitable for the transcription of short RNAs such as ribozymes. In addition, poly(A) extra sequences may decrease the activity of ribozymes by disrupting its highly ordered structures (Rossi 1995). Since polymerase III expression systems are mainly involved in the transcription of tRNA, and their level of transcription is 2 to 3 orders higher than that of polymerase II systems (Geiduschek and Tocchini-

Valentini 1988), the polymerase III system is ideal for the expression of ribozymes, as high levels of transcripts are required for strong activity. Indeed, pol III expression systems that contain the $tRNA^{Met}$, $tRNA^{Lys}$, or $tRNA^{Val}$ gene promoter have been used for the expression of hammerhead ribozymes in cells (Good *et al.* 1997). As the tRNA promoter is an internal promoter with the site of initiation of transcription is upstream of the promoter, the transcript contains tRNA sequence with the internal promoter sequence in its 5′ half and the ribozymes sequence in its 3′ half. The 5′ tRNA sequence does not disrupt the ribozyme's activity. Since 3′ tRNase cleaves the ribozyme part of the tRNA-ribozyme complex, and the cleaved ribozyme becomes a target against endogenous RNase, a linker sequence between the tRNA and ribozyme regions are required to form a stem-bulge structure to prevent the cleavage of the ribozyme from the complex. In addition, the linker sequence allows efficient transport of tRNA-ribozyme complex from nucleus to cytoplasm by protecting it from RNases and ultimately, improves the intracellular ribozyme activity.

There are two applications for ribozymes *in vivo*, and these are endogenous expression via plasmid vectors, and exogenous ribozyme transfection. Exogenous administration of ribozymes generally does not work efficiently, because nucleic acids are rapidly targeted and degraded by cellular nucleases. To improve this problem, some chemical modifications can be made on synthesized ribozymes such as thio modification or alkylation at the ribose 2′-hydroxyl group from the ribozymes to prevent the cleavage of phosphodiester bonds by RNases (Yang *et al.* 1992). However, the modifications can be impractical due to high costs for preparation, and decrease in the ribozyme activity. On the other hands, vector-based delivery is much more efficient, because the ribozyme

gene can be administered as stable DNA, which produces ribozymes inside target cells. Many viral vectors have shown as potential gene delivery tools including adenovirus, and retrovirus (Kovesdi *et al.* 1997; Wu and Ataai 2000). Furthermore, artificial non-viral vectors are being developed recently for oligonucleotide delivery, because they are safer to use and easier to produce than the viral vectors.

Therefore, UGLoop allosteric hammerhead ribozymes that contain C8 aptamer motifs for BDHP-PEG binding can be delivered efficiently according to the above examples for their intracellular catalytic cleavage activities. In addition, it should not be a problem of introducing BDHP-PEG into cells, since the compound is relatively hydrophilic due to the presence of a water-soluble polyethelene glycol group on the compound.

REFERENCE LIST

Akashi, H., Matsumoto, S., and Taira, K. (2005) Gene discovery by ribozyme and siRNA libraries. *Nat. Rev. Mol. Cell Biol.*, **6**, 413-422.

Ananvoranich, S., Lafontaine, D.A., and Perreault, J.P. (1999) Mutational analysis of the antigenomic trans-acting delta ribozyme: the alterations of the middle nucleotides located on the P1 stem. *Nucleic Acids Res.*, **27**, 1473-1479.

Araki, M., Okuno, Y., Hara, Y., and Sugiura, Y. (1998) Allosteric regulation of a ribozyme activity through ligand induced conformational change. *Nucleic Acids Res.*, **26**, 3379-3384.

Asanuma, H., Ito, T., and Komiyama, M. (1998) Photo-responsive oligonucleotides carrying azobenzene in the side-chains. *Tetrahedron Letters*, **39**, 9015-9018.

Bass, B.L., and Cech, T.R. (1984) Specific interaction between the self-splicing RNA of *Tetrahymena* and its guanosine substrate: implications for biological catalysis by RNA. *Nature*, **308**, 820-826.

Bergeron, L.J., and Perreault, J.P. (2002) Development and comparison of procedures for the selection of *delta* ribozyme cleavage sites within the hepatitis B virus. *Nucleic Acids Res.*, **30**, 4682-4691.

Bernstein, E., Caudy, A.A., Hammond, S.M., and Hannon, G.J. (2001) Role of bidentate ribonuclease in the initiation step of RNA interference. *Nature*, **409**, 363-366.

Blattmann, H.R., Meuche, D., Heilbronner, E., Molyneux, R.J., and Boekelheide, V. (1965) Photoisomerization of *trans*-15,16-dimethyldihydropyrene. *J. Am. Chem. Soc.*, **87**, 130-131.

Blount, K.F., and Uhlenbeck, O.C. (2002) The hammerhead ribozyme. *Biochem. Soc. Trans.*, **30**, 1119-1122.

Bock, L.C., Griffin, L.C., Latham, J.A., Vermass, E.H., and Toole, J.J. (1992) Selection of single-stranded DNA molecules that bind and inhibit human thrombin. *Nature*, **355**, 564-566.

Bouas-Laurent, H., and Dürr, H. (2001) Organic photochromism. *Pure Appl. Chem.*, **73**, 639-665.

Breaker, R.R., and Joyce, G.F. (1994) Inventing and improving ribozyme function: rational design versus iterative selection methods. *Trends Biotechnol.*, **12**, 268-275.

Breaker, R.R. (1997) *In vitro* Selection of Catalytic Polynucleotides. *Chem. Rev.*, **97**, 371-390.

Breaker, R.R. (2004) Natural and engineered nucleic acids as tool to explore biology. *Nature*, **432**, 838-845.

Cech, T.R. (1990) Self-splicing of group I introns. *Annu. Rev. Biochem.*, **59**, 543-568.

Chinnapen, D.J., and Sen, D. (2002) Hemin stimulated docking of cytochrome c to a hemin-DNA aptamer complex. *Biochemistry*, **41**, 5202-5212.

Ciesiolka, J., and Yarus, M. (1996) Small RNA-divalent domains. *RNA*, **2**, 785-793.

Collins, R.A. and Saville, B.J. (1990) Independent transfer of mitochondrial chromosomes and plasmids during unstable vegetative fusion in Neurospora. *Nature*, **345**, 177-179.

Collins, R.A. and Olive, J.E. (1993) Reaction conditions and kinetics of self-cleavage of a ribozyme derived from Neurospora VS RNA. *Biochemistry*, **32**, 2795-2799.

Doudna, J.A., and Cech, T.R. (2002) The chemical repertoire of natural ribozymes. *Nature*, **418**, 222-228.

Dzitoyeva, S., Dimitrijevic, N., and Manev, H. (2003) Gamma-aminobutyric acid B receptor 1 mediates behaviour-impairing actions of alcohol in Drosophila: adult RNA interference and pharmacological evidence. *Proc. Natl. Acad. Sci. USA*, **100**, 5485-5490.

Ellington, A.D., and Szostak, J.W. (1990) *In vitro* selection of RNA molecules that bind specific ligands. *Nature*, **346**, 818-822.

Ellington, A.D., and Szostak, J.W. (1992) Selection *in vitro* of single-stranded DNA molecules that fold into specific ligand-binding structures. *Nature*, **355**, 850-852.

Famulok, M., and Szostak, J.W. (1992) Stereospecific recognition of trytophan agarose by *in vitro* selected RNA. *J. Am. Chem. Soc.*, **114**, 3990-3991.

Famulok, M. (1999) Oligonucleotide aptamers that recognize small molecules. *Curr. Opin. Struct. Biol.*, **9**, 324-329.

Fan, P., Suri, A.K., Fiala, R., Live, D., and Patel, D.J. (1996) Molecular recognition in the FMN-RNA aptamer complex. *J. Mol. Biol.*, **258**, 480-500.

Fang, X.W., Yang, X.J., Littrell, K., Niranjanakumari, S., Thiyagarajan, P., Fierke, C.A., Sosnick, T.R., and Pan, T. (2001) The Bacillus subtilis RNase P holoenzyme contains two RNase P RNA and two RNase P protein subunits. *RNA*, **7**, 233-241.

Fedor, M.J., and Uhlenbeck, O.C. (1992) Kinetics of intermolecular cleavage by hammerhead ribozymes. *Biochemistry*, **31**, 12042-12054.

Ferre-D'Amaré, A.R., Zhou, K., and Doudna, J.A. (1998) Crystal structure of a hepatitis delta virus ribozyme *Nature*, **395**, 567-574.

Ferre-D'Amaré, A.R., and Rupert, P.B. (2002) The hairpin ribozyme: from crystal structure to function. *Biochem. Soc. Trans.*, **30**, 1105-1109.

Forster, A.C., and Altman, S. (1990) External guide sequences for an RNA enzyme. *Science*, **249**, 783-786.

Forster, A.C., and Symons, R.H. (1987) Self-cleavage of virusoid RNA is performed by the proposed 55-nucleotide active site. *Cell*, **50**, 9-16.

Fortunato, A., and Fraser, A.G. (2005) Uncover genetic interactions in Caenorhabditis elegans by RNA interference. *Biosci. Rep.*, **25**, 299-307.

Frank, D.N., and Pace, N.R. (1998) Ribonuclease P: unity and diversity in a tRNA processing ribozyme. *Annu. Rev. Biochem.*, **67**, 153-180.

Geiduschek, E.P., and Tocchini-Valentini, G.P. (1988) Transcription by RNA polymerase III. *Annu. Rev. Biochem.*, **57**, 873-914.

Gilbert, W. (1986) The RNA world. *Nature*, **319**, 618.

Good, P.D., Krikos, A.J., Li, X.L., Lee, N.S., Giver, L., Ellington, A., Zaia, J.A., Rossi, J.J., and Engelke, D.R. (1997) Expression of small, therapeutic RNAs in human cell nuclei. *Gene Ther.*, **4**, 45-54.

Guerrier-Takada, C., Gardiner, K., Marsh, T., Pace, N., and Altman, S. (1983) The RNA moiety of ribonuclease P is the catalytic subunit of the ribozyme. *Cell*, **35**, 849-857.

Guo, H.C. and Collins, R.A. (1995) Efficient trans-cleavage of a stem-loop RNA substrate by a ribozyme derived from *Neurospora* VS RNA. *EMBO J.*, **14**, 368-376.

Guo, H., Zimmerly, S., Perlman, P.S., and Lambowitz, A.M. (1997) Group II intron endonucleases use both RNA and protein subunits for recognition of specific sequences in double-stranded DNA. *EMBO J.*, **16**, 6835-6848.

Hamaguchi, N., Ellington, A., and Stanton, M. (2001) Aptamer beacons for the direct detection of proteins. *Anal. Biochem.*, **294**, 126-131.

Haseloff, J., and Gerlach, W.L. (1988) Simple RNA enzymes with new and highly specific endoribonuclease activities. *Nature*, **334**, 585-591.

Haseloff, J., and Gerlach, W.L. (1992) Simple RNA enzymes with new and highly specific endoribonuclease activities. *Biotechnology*, **24**, 264-269.

Hermann, T., and Patel, D.J. (2000) Adaptive recognition by nucleic acid aptamers. *Science*, **287**, 820-825.

Hicke, B.J., Christian, E.L., and Yarus, M. (1989) Stereoselective arginine binding is a phylogenetically conserved property of group I self-splicing RNAs. *EMBO J.*, **8**, 3843-3851.

Huizenga, D.E., and Szostak, J.W. (1995) A DNA aptamer that binds adenosine and ATP. *Biochemistry*, **34**, 656-665.

Ingram, G.J. (1957) Gene mutation in human hemoglobin: the chemical difference between normal and sickle cell hemoglobin. *Nature*, **180**, 326-328.

Jayasena, S.D. (1999) Aptamers: an emerging class of molecules that rival antibodies in diagnostics. *Clin. Chem.*, **9**, 1628-1650.

Jenison, R.D., Gill, S.C., Pardi, A., and Polisky, B. (1994) High-resolution molecular discrimination by RNA. *Science*, **263**, 1425-1429.

Jhaveri, S., Rajendran, M., and Ellington, A.D. (2000) *In vitro* selection of signaling aptamers. *Nature Biotechnol.*, **18**, 1293-1297.

Jia, F., Zhang, Y.Z., and Liu, C.M. (2006) A retrovirus-based system to stably silence hepatitis B virus genes by RNA interference. (2006) *Biotechnol. Lett.*, **28**, 1679-1685.

Jones, F.D., Ryder, S.P., and Strobel, S.A. (2001) An efficient ligation reaction promoted by a Varkud Satellite ribozyme with extended 5'- and 3'-termini. *Nucleic Acids Res.*, **29**, 5115-5120.

Joyce, G.F. (1996) Ribozymes: Building the RNA world. *Curr. Biol.*, **6**, 965-967.

Kertsburg, A., and Soukup, G.A. (2002) A versatile communication module for controlling RNA folding and catalysis. *Nucleic Acids Res.*, **30**, 4599-4606.

Kirsebom, L.A. (2002) RNase P RNA-mediated catalysis. *Biochem. Soc. Trans.*, **30**, 1153-1158.

Koizumi, M., Soukup, G.A., Kerr, J.N.Q., and Breaker, R.R. (1999) Allosteric selection of ribozymes that respond to the second messengers cGMP and cAMP. *Nat. Struct. Biol.*, **6**, 1062-1071.

Kore, A.R., Vaish, N.K., Kutzke, U., and Eckstein, F. (1998) Sequence specificity of the hammerhead ribozyme revisited; the NHH rule. *Nucleic Acids Res.*, **26**, 4116-4120.

Kovesdi, I., Brough, D.E., Brude, J.T., and Wickham, T.J. (1997) Adenoviral vectors for gene transfer. *Curr. Opin. Biotechnol.*, **8**, 583-589.

Kruger, K., Grabowski, P.J., Zang, A.J., Sands, J., Gottschling, D.E., and Cech, T.R. (1982) Self-splicing RNA: autoexcision and autocyclization of the ribosomal RNA intervening sequence of Tetrahymena. *Cell*, **31**, 147-157.

Kusov, Y., Kanda, T., Palmenberg, A., Sgro, J.Y., and Gauss-Muller, V. (2006) Silencing of hepatitis A virus infection by small interfering RNAs. *J. Virol.*, **80**, 5599-5610.

Kuwabara, T., Warashina, M., Tanabe, T., Tani, K., Asano, S., and Taira, K. (1998) A novel allosterically *trans*-activated ribozyme, the maxizyme, with exceptional specificity *in vitro* and *in vivo*. *Mol. Cell*, **2**, 617-627.

Lan, N., Howrey, R.P., Lee, S.W., Smith, C.A., and Sullenger, B.A. (1998) Ribozyme-mediated repair of sickle beta-globin mRNAs in erythrocyte precursors. *Science*, **280**, 1593-1596.

Lewin, A.S., and Hauswirth, W.W. (2001) Ribozyme gene therapy: applications for molecular medicine. *Trends Mol. Med.*, **7**, 221-228.

Li, Y. and Breaker, R.R. (1999) Kinetics of RNA degradation by specific base catalysis of transesterification involving the 2'-hydroxyl group. *J. Am. Chem. Soc.*, **121**, 5364-5372.

Liang, X., Asanuma, H., Kashida, H., Takasu, A., Sakamoto, T., Kawai, G., and Komiyama, M. (2003) NMR study on the photoresponsive DNA tethering an azobenzene. Assignment of the absolute configuration of two diastereomers and structure determination of their duplexes in the trans-form. *J. Am. Chem. Soc.*, **125**, 16408-16415.

Liu, Y., and Sen, D. (2004) Light-regulated catalysis by an RNA-cleaving deoxyribozyme. *J. Mol. Biol.*, **341**, 887-892.

Long, D.M., and Uhlenbeck, O.C. (1994) Kinetic characterization of intramolecular and intermolecular hammerhead RNAs with stem II deletions. *Proc. Natl. Acad. Sci. USA*, **91**, 6977-6981.

Macaya, R.F., Schultz, P., Smith, F.W., Roe, J.A., and Feigon, J. (1993) Thrombin-binding DNA aptamer forms a unimolecular quadruplex structure in solution. *Proc. Natl. Acad. Sci. USA*, **90**, 3745-3749.

Mandal, M., and Breaker, R.R. (2004a) Adenine riboswitches and gene activation by disruption of a transcription terminator. *Nat. Struct. Mol. Biol.*, **11**, 29-35.

Mandal, M., and Breaker, R.R. (2004b) Gene regulation by riboswitches. *Nature Reviews*, **5**, 451-463.

Mandal, M., Lee, M., Barrick, J.E., Weinberg, Z., Emilsson, G.M., Ruzzo, W.L., and Breaker, R.R. (2004c) A glycine-dependent riboswitch that uses cooperative binding to control gene expression. *Science*, **306**, 275-279.

Mathews, C.K., Holde, K.E., and Ahern, K.G. (2000) *Biochemistry* (3rd ed.). San Francisco: Heyden.

Michel, F., and Ferat, J.L. (1995) Structure and activities of group II introns. *Annu. Rev. Biochem.*, **64**, 435-461.

Mitchell, R.H., Ward, T.R., Yan, J.S.H., and Dingle, T.W. (1982) Toward the understanding of benzannelated annulenes: synthesis and properties of an [*e*]-ring monobenzannelated dihydropyrene. *J. Am. Chem. Soc.*, **104**, 2551-2559.

Mitchell, R.H., Ward, T.R., Chen, Y., Wang, Y., Weerawarna, S.A., Dibble, P.W., Marsella, M.J., Almutairi, A., and Wang, Z.Q. (2003) Synthesis and photochromic properties of molecules containing [*e*]-annelated dihydropyrenes. Two and three way π-switches based on the dimethyldihydropyrene-metacyclophanediene valence isomerization. *J. Am. Chem. Soc.*, **125**, 2974-2988.

Morris, K.N., Jensen, K.B., Julin, C.M., Weil, M., and Gold, L. (1998) High affinity ligands from *in vitro* selection: complex targets. *Proc. Natl. Acad. Sci. USA*, **95**, 2902-2907.

Nahvi, A., Sudarsan, N., Ebert, M.S., Zou, X., Brown, K.L., and Breaker, R.R. (2002) Genetic control by a metabolite binding mRNA. *Chem. Biol.*, **9**, 1043-1049.

Nieuwlandt, D., Wecker, M., and Gold, L. (1995) *In vitro* selection of RNA ligands to substance P. *Biochemistry*, **34**, 5651-5659.

Nissen, P., Hansen, J., Ban, N., Moore, P.B., and Steitz, T.A. (2000) The structural basis of ribosome activity in peptide bond synthesis. *Science*, **289**, 920-930.

Nykanen, A., Haley, B., and Zamore, P.D. (2001) ATP requirements and small interfering RNA structure in the RNA interference pathway. *Cell*, **107**, 309-321.

Orgel, L.E. (1968) Evolution of the genetic apparatus. *J. Mol. Biol.*, **38**, 381-393.

Osborne, S.E., and Ellingtion, A.D. (1997) Nucleic acid selection and the challenge of combinatorial chemistry. *Chem. Rev.*, **97**, 349-370.

Padmanabhan, K., Padmanabhan, K.P., Ferrara, J.D., Sadler, J.E., and Tulinsky, A. (1993) The structure of alpha-thrombin inhibited by a 15-mer single-stranded DNA aptamer. *J. Biol. Chem.*, **268**, 17651-17654.

Pan, W., Craven, R.C., Qiu, Q., Wilson, C.B., Wills, J.W., Golovine, S., and Wang, J.F. (1995) Isolation of virus-neutralizing RNAs from a large pool of random sequences. *Proc. Natl. Acad. Sci. USA*, **92**, 11509-11513.

Patel, D.J., Suri, A.K., Jiang, F., Jiang, L., Fan, P., Kumar, R.A., and Nonis, S. (1997) Structure, recognition and adaptive binding in RNA aptamer complexes. *J. Mol. Biol.*, **272**, 645-664.

Porta, H., and Lizardi, P.M. (1995) An allosteric hammerhead ribozyme. *Biotechnology*, **13**, 161-164.

Puglisi, J.D., Tan, R., Calnan, B.J., Frankel, A.D., and Williamson, J.R. (1992) Conformation of the TAR RNA-arginine complex by NMR spectroscopy. *Science*, **257**, 76-80.

Ringquist, S., Jones, T., Snyder, E.E., Gibson, T., Boni, I., and Gold, L. (1995) High-affinity RNA ligands to Escherichia coli ribosomes and ribosomal protein S1: comparison of natural and unnatural binding sites. *Biochemistry*, **34**, 3640-3648.

Robertson, M.P., and Ellington, A.D. (1999) *In vitro* selection of an allosteric ribozyme that transduces analytes to amplicons. *Nat. Biotechnol.*, **17**, 62-66.

Romig, T.S., Bell, C., and Crolet, D.W. (1999) Aptamer affinity chromatography: combinatorial chemistry applied to protein purification. *J. Chromatogr. B. Biomed. Sci. Appl.*, **731**, 275-284.

Rossi, J.J. (1995) Controlled, targeted, intracellular expression of ribozymes: progress and problems. *Trends Biotechnol.*, **13**, 301-306.

Rossi, J.J., and Sarver, N. (1990) RNA enzymes (ribozymes) as antiviral therapeutic agents. *Trends Biotechnol.*, **8**, 179-183.

Roy, G., Ananvoranich, S., and Perreault, J.P. (1999) Delta ribozyme has the ability to cleave in transan mRNA. *Nucleic Acids Res.*, **27**, 942-948.

Rupert, P.B., Massey, A.P., Sigurdsson, S.T., and Ferre-D'Amaré, A.R. (2002) Transition state stabilization by a catalytic RNA. *Science*, **298**, 1421-1424.

Saville, B.J. and Collins, R.A. (1991) RNA-mediated ligation of self-cleavage products of a Neurospora mitochondrial plasmid transcript. *Proc. Natl. Acad. Sci. U.S.A.*, **88**, 8826-8830.

Sassanfar, M., and Szostak, J.W. (1993) An RNA motif that binds ATP. *Nature* **364**, 550-553.

Seetharaman, S., Zivarts, M., Sudarsan, N., and Breaker, R.R. (2001) Immobilized RNA switches for the analysis of complex chemical and biological mixtures. *Nat. Biotechnol.*, **19**, 336-341.

Serra, M.J., and Turner, D.H. (1995) Predicting thermodynamic properties of RNA. *Meth. Enzymol.*, **259**, 242-261.

Soukup, G.A., and Breaker, R.R. (1999a) Design of allosteric hammerhead ribozymes activated by ligand-induced structure stabilization. *Structure*, **7**, 783-791.

Soukup, G.A., and Breaker, R.R. (1999b) Engineering precision RNA molecular switches. *Proc. Natl. Acad. Sci. USA*, **96**, 3584-3589.

Soukup, G.A., Emilsson, G.A.M., and Breaker, R.R. (2000) Altering molecular recognition of RNA aptamers by allosteric selection. *J. Mol. Biol.*, **298**, 623-632.

Suess, B., Hanson, S., Berens, C., Fink, B., Schroeder, R., and Hillen, W. (2003) Conditional gene expression by controlling translation with tetracycline-binding aptamers. *Nucleic Acids Res.*, **31**, 1853-1858.

Sullenger, B.A., and Cech, T.R. (1994) Ribozyme-mediated repair of defective mRNA by targeted, trans-splicing. *Nature*, **371**, 619-622.

Sudarsan, N., Wickiser, J.K., Nakamura, S., Ebert, M.S., and Breaker, R.R. (2003) An mRNA structure in bacteria that controls gene expression by binding lysine. *Genes Dev.*, **17**, 2688-2697.

Sunshine, H.R., Hofrichter, J., and Eaton, W.A. (1978) Requirement for therapeutic inhibition of sickle hemoglobin gelation. *Nature*, **275**, 238-240.

Symons, R.H. (1992) A small catalytic RNAs. *Annu. Rev. Biochem.*, **61**, 641-671.

Tang, J., and Breaker, R.R. (1997a) Rational design of allosteric ribozymes. *Chem. Biol.*, **4**, 453-459.

Tang, J., and Breaker, R.R. (1997b) Examination of the catalytic fitness of the hammerhead ribozyme by *in vitro* selection. *RNA*, **3**, 914-925.

Tang, J., and Breaker, R.R. (1998) Mechanism for allosteric inhibition of an ATP-sensitive ribozyme. *Nucleic Acids Res.*, **26**, 4222-4229.

Tanner, N.K. (1999) Ribozymes: the characteristics and properties of catalytic RNAs. *FEMS Microbiol. Rev.*, **23**, 257-275.

Travascio, P., Li, Y., and Sen, D. (1998) DNA-enhanced peroxidase activity of a DNA aptamer-hemin complex. *Chem. Biol.*, **5**, 505-517.

Tuerk, L., and Gold, L. (1990) Systematic evolution of ligands by exponential enrichment: RNA ligands to bacteriophage T4 DNA polymerase. *Science*, **249**, 505-510.

Tuerk, L., MacDougal, S., and Gold, L. (1992) RNA pseudoknots that inhibit human immunodeficiency virus type I reverse transcriptase. *Proc. Natl. Acad. Sci. USA*, **89**, 6988-6992.

Tuschl, T., and Eckstein, F. (1993) Hammerhead ribozymes: importance of stem-loop II for activity. *Proc. Natl. Acad. Sci. USA*, **90**, 6991-6994.

Uhlenbeck, O.C. (1987) A small catalytic oligoribonucleotide. *Nature*, **328**, 596-600.

Vermeulen, A., Behlen, L., Reynolds, A., Wolfson, A., Marshall, W.S., Karpilow, J., and Khvorova, A. (2005) The contributions of dsRNA structure to Dicer specificity and efficiency. *RNA*, **11**, 674-682.

Vioque, A., Arnez, J., and Altman, S. (1988) Protein-RNA interactions in the RNase P holoenzyme from *Escherichia coli*. *J. Mol. Biol.*, **202**, 835-848.

Wang, D.Y., and Sen, D. (2002) Rationally designed allosteric variants of hammerhead ribozymes responsive to the HIV-1 Tat protein. *Comb. Chem. High Throughput Screen*, **5**, 301-312.

Wang, K.Y., McCardy, S., Shea, R.G., Swaminathan, S., Bolton, P.H. (1993) The tertiary structure of a DNA aptamer which binds to and inhibits thrombin determines activity. *Biochemistry*, **32**, 1899-904.

Welch, P.J., Tritz, R., Yei, S., Barber, J., and Yu, M. (1997) Intracellular application of hairpin ribozyme genes against hepatitis B virus. *Gene Ther.*, **4**, 736-743.

Werstuck, G., and Green, M. (1998) Controlling gene expression in living cells through small molecule-RNA interactions. *Science*, **282**, 296-298.

Williams, K.P., and Bartel, D.P. (1996) *In vitro* selection of catalytic RNA. *Nucleic Acids Mol. Biol.*, **10**, 367-381.

Wilson, D.S., and Szostak, J.W. (1999) In vitro selection of functional nucleic acids. *Annu. Rev. Biochem.*, **68**, 611-647.

Winkler, W.C., Nahvi, A., and Breaker, R.R. (2002a) Thiamine derivatives bind messenger RNAs directly to regulate bacterial gene expression. *Nature*, **419**, 952-956.

Winkler, W.C., Cohen-Chalamish, S., and Breaker, R.R. (2002b) An mRNA structure that controls gene expression by binding FMN. *Proc. Natl. Acad. Sci. USA*, **99**, 15908-15913.

Winkler, W.C., and Breaker, R.R. (2003a) Genetic control by metabolite-binding riboswitches. *Chem. Bio. Chem.*, **4**, 1024-1032.

Winkler, W.C., Nahvi, A., Sudarsan, N., Barrick, J.E., and Breaker, R.R. (2003b) An mRNA structure that controls gene expression by binding S-adenosylmethionine. *Nat. Struct. Biol.*, **10**, 701-707.

Winkler, W.C., Nahvi, A., Roth, A., Collins, J.A., and Breaker, R.R. (2004) Control of gene expression by a natural metabolite-responsive ribozyme. *Nature*, **428**, 281-286.

Woese, C.R., Dugre, D.H., Saxinger, W.C., and Dugre, S.A. (1966) The molecular basis for the genetic code. *Proc. Natl. Acad. Sci. USA*, **55**, 966-974.

Wu, H.N., Lin, Y.J., Lin, F.P., Makino, S., Chang, M.F., and Lai, M.M. (1989) Human hepatitis δ virus RNA subfragments contain an autocleavage activity. *Proc. Natl. Acad. Sci. USA*, **86**, 1831-1835.

Wu, N., and Ataai, M.M. (2000) Production of viral vectors for gene therapy applications. *Curr. Opin. Biotechnol.*, **11**, 205-208.

Yang, J.H., Usman, N., Chartrand, P., and Cedergreen, R. (1992) Minimum ribonucleotide requirement for catalysis by the RNA hammerhead domain. *Biochemistry*, **31**, 5005-5009.

Zhong, J., and Lambowitz, A.M. (2003) Group II intron mobility using nacent strands at DNA replication fork to prime reverse transcription. *EMBO J.*, **22**, 4555-4565.

Zimmerly, S., Guo, H., Perlman, P.S., and Lambowitz, A.M. (1995) Group II intron mobility occurs by target DNA-primed reverse transcription. *Cell*, **82**, 545-554.

Zimmerly, S., Guo, H., Eskes, R., Yang, J., Perlman, P.S., and Lambowitz, A.M. (1995) A group II intron RNA is a catalytic component of a DNA endonuclease involved in intron mobility. *Cell*, **83**, 529-538.

Zimmerly, S., and Lambowitz, A.M. (2004) Mobile group II introns. *Annu. Rev. Genet.*, **38**, 1-35.

Zimmermann, G.R., Jenison, R.D., Wick, C.L., Simorre, J.P., and Pardi, A. (1997) Interlocking structural motifs mediate molecular discrimination by a theophylline-binding RNA. *Nat. Struct. Biol.*, **4**, 644-649.